

Contract No:

This document was prepared in conjunction with work accomplished under Contract No. DE-AC09-08SR22470 with the U.S. Department of Energy (DOE) Office of Environmental Management (EM).

Disclaimer:

This work was prepared under an agreement with and funded by the U.S. Government. Neither the U. S. Government or its employees, nor any of its contractors, subcontractors or their employees, makes any express or implied:

- 1) warranty or assumes any legal liability for the accuracy, completeness, or for the use or results of such use of any information, product, or process disclosed; or
- 2) representation that such use or results of such use would not infringe privately owned rights; or
- 3) endorsement or recommendation of any specifically identified commercial product, process, or service.

Any views and opinions of authors expressed in this work do not necessarily state or reflect those of the United States Government, or its contractors, or subcontractors.

We put science to work.™



**Savannah River
National Laboratory™**

OPERATED BY SAVANNAH RIVER NUCLEAR SOLUTIONS

A U.S. DEPARTMENT OF ENERGY NATIONAL LABORATORY • SAVANNAH RIVER SITE • AIKEN, SC

WTP Pretreatment Facility Potential Design Deficiencies - Sliding Bed and Sliding Bed Erosion Assessment

E. K. Hansen

May 2015

SRNL-STI-2015-00014, Revision 0

SRNL.DOE.GOV

DISCLAIMER

This work was prepared under an agreement with and funded by the U.S. Government. Neither the U.S. Government or its employees, nor any of its contractors, subcontractors or their employees, makes any express or implied:

1. warranty or assumes any legal liability for the accuracy, completeness, or for the use or results of such use of any information, product, or process disclosed; or
2. representation that such use or results of such use would not infringe privately owned rights; or
3. endorsement or recommendation of any specifically identified commercial product, process, or service.

Any views and opinions of authors expressed in this work do not necessarily state or reflect those of the United States Government, or its contractors, or subcontractors.

Printed in the United States of America

**Prepared for
U.S. Department of Energy**

Keywords: *Hanford, critical velocity, sliding bed, erosion, Pretreatment Facility*

Retention: *Permanent*

WTP Pretreatment Facility Potential Design Deficiencies - Sliding Bed and Sliding Bed Erosion Assessment

E. K. Hansen

May 2015

Prepared for the U.S. Department of Energy under
contract number DE-AC09-08SR22470.



OPERATED BY SAVANNAH RIVER NUCLEAR SOLUTIONS

REVIEWS AND APPROVALS

AUTHOR:

E. K. Hansen, Engineering Process Development Date

TECHNICAL REVIEW:

M. R. Poirier, Advanced Characterization and Processing Date

APPROVAL:

S. D. Fink, Senior Advisory Engineer Date
Environmental & Chemical Process Technology Research Programs

E.N. Hoffman, Manager Date
Engineering Process Development

S.L. Marra, Manager Date
Environmental & Chemical Process Technology Research Programs

EXECUTIVE SUMMARY

This report was requested by the Department of Energy (DOE) - Office of River Protection (ORP) to address concerns raised by the Defense Nuclear Facilities Safety Board (DNFSB) in their August 8, 2012, letter to the DOE regarding the Waste Treatment and Immobilization Plant (WTP). In this letter, the DNFSB discussed the behavior of both Newtonian and non-Newtonian slurries having the following design deficiencies: (1) Formation of Sliding Beds and (2) Erosion/Corrosion from sliding bed. In the first deficiency, there is a need to avoid the formation of a bed of sliding solids on the pipe invert and to design a flushing system. The second deficiency raises the issue of the solids from the sliding bed leading to increased wear pipe invert and uneven pipe wear.

This assessment is based on readily available literature and discusses both Newtonian and non-Newtonian slurries with respect to sliding beds and erosion due to sliding beds. This report does not quantify the size of the sliding beds or erosion rates due to sliding beds, but only assesses if they could be present. This assessment addresses process pipelines in the Pretreatment (PT) facility and the high level waste (HLW) transfer lines leaving the PT facility to the HLW vitrification facility concentrate receipt vessel.

For the case of Newtonian based slurries that will be processed in the WTP-PT facility, it is not expected that sliding beds of solids will be present given the constraints provided by the applicable interface control document (ICD-19), the safety margin in the WTP design for Newtonian slurries, the projected HLW streams that will be processed (Wilkins²²), the transport velocity of 6 ft/s in the PT facility, and testing performed by WRPS and PNNL. This finding is for systems where centrifugal pumps are utilized to transfer or recirculate waste in a 3 inch transfer line.

For the non-Newtonian case, there is insufficient data available to determine if sliding beds will cause more erosion compared to turbulent flow and the mechanism of sliding bed erosion is different than that experienced in turbulent flow. Experience at SRS processing only HLW slurries in the tank farm showed essentially no erosion over a 10 year span. Processing HLW slurries containing large and abrasive frit in DWPF showed an erosion rate of 4 mils per year over a 10 year span without any observation of erosion due to sliding bed. Testing with non-Newtonian slurries shows that a sliding bed can be present below the critical transition velocity and such conditions could exist in WTP for the higher combinations of yield stress and plastic viscosity given a 6 ft/s flowrate in 3 inch pipe. For a 30 Pa, 30 cP Bingham plastic fluid, the transition velocity in a 3 inch pipe is 9.3 ft/s. Observations of the sliding beds could be due to the flocculation of colloidal particles, at high non-Newtonian conditions. Literature does not provide sufficient information on the size (depth) of the sliding bed for non-Newtonian slurries. The following recommendations are provided to assess for sliding bed erosion.

- 1: Perform a technical review of characterized Tank Farm and processed (Al-dissolution/washing) Hanford HLW waste where mass fraction versus Bingham Plastic rheological and physical properties have been ascertained in the regions shown in Table 3-1. Characterization of the solids speciation is also a requirement, such as chemical composition, density, hardness, and particle size distribution. Assess this data to determine if a sliding bed could be present for pipeline velocity of 6 ft/s using the methods specified by Poloski et al^{66,49} and Goosen and Paterson⁶⁸ to assess for sliding bed. An additional assessment should also determine the fraction of HLW streams that could have a sliding bed based on using a process model (such as G2) and existing characterization data. Based on the latter assessment, if the fraction of non-Newtonian HLW for sliding beds is reasonably low, Recommendation 2 below should be reassessed to determine if it necessary to be performed for the non-Newtonian sliding bed erosion testing. Such a

reassessment for instance could include evaluating the average hardness of the calculated sliding bed materials as compared to the piping material in reaching this determination.

- 2: Perform pipe loop testing to determine the size (height/width) of the sliding bed, composition of the sliding bed, and erosion at steady state conditions and potentially the erosion rate for start/stop conditions. Elbow and vertical piping should also be assessed if testing is required and captured in this testing. If start/stop testing is to be performed, an assessment of WTP-PT operations should be performed to determine the fraction of operating time stop/start activities occur for HLW vessels. If start/stop operations are a small percentage of the overall transfer operations, then such testing may not be necessary. Flushing activities should be consistent with WTP protocol to verify flushing methodology is adequate. Both Poloski et al.⁶⁶ and Goosen and Paterson⁶⁸ (two-layer model) methods should be used to assess the collected data.
- 3: Assess RFD operations for systems in WTP-PT that are utilized in transporting HLW. Assessment is to review how the RFD will be operated; flowrate, number of cycles per nominal transfer and flushing capabilities. Assessment should include open literature on the operation and erosion issues related to RFD operations. Issues raised in this review should determine if additional testing is required to assess the overall issue of erosion due to a cyclic pumping system given the streams it will process.
- 4: UFP-VSL-00002A/B are the primary HLW processing vessels in PT. These vessels utilize a 10 inch transfer line for crossflow filter activities. There is insufficient data to determine if this transfer line has been properly assessed for both Newtonian and non-Newtonian operations, including flushing in maintaining the line for long term operations. An independent assessment of this transfer system is recommended.

TABLE OF CONTENTS

LIST OF TABLES	ix
LIST OF FIGURES	x
LIST OF ABBREVIATIONS.....	xii
1.0 Introduction.....	1
2.0 Properties, Sliding Bed and Erosion	6
2.1 WTP Pretreatment Slurries Properties	6
2.1.1 RPP-9805, (2002)	6
2.1.2 External Flowsheet Review Team Issue M1 Closure (2009)	6
2.1.3 Process Inputs Basis of Design (PIBOD), (2011).....	7
2.1.4 24590-WTP-RPT-PE-12-005, (2013).....	8
2.1.5 WTP Design and Safety Margin (2014)	10
2.1.6 ICD-19, (2014)	11
2.2 Regions of Flow for Newtonian Slurries.....	12
2.2.1 Newitt et al., 1955.....	12
2.2.2 Carleton and Cheng, 1977	15
2.2.3 Turian et al. – Critical Velocity 1987	16
2.2.4 Cho et al. Minimum Transport Velocity –Multiple Solids Components and Solids Densities ..	17
2.2.5 Critical Velocity – Small Particles and Their Effect	19
2.2.5.1 Parzonka et al.- 1981	19
2.2.5.2 Hisamitsu et al.- 1978	20
2.2.5.3 Warren, 1981.....	21
2.2.5.4 Cairns and Turner, 1958.....	21
2.2.5.5 Thomas, 1979 – Viscous Sublayer Effect	22
2.2.6 Pinto et al., Critical Velocity, 2014	23
2.2.7 Poloski et al., 2009(development of Stability Map)	26
2.2.8 Pressure-Drop and Velocity Regions for Heterogeneous Flow	26
2.3 Regions of Solids Flow for non-Newtonian Slurries	28
2.3.1 Thomas, 1978	28
2.3.2 Shah and Lord, 1991	30
2.3.3 Song and Chiew, 1991	30
2.3.4 Thomas, 1961	32
2.3.5 Thomas et al., 2004.....	34
2.3.6 Poloski et al., 2009 (development of Stability Map)	36

2.3.7 Poloski et al., 2009.....	38
2.3.8 Goosen and Paterson, 2014.....	40
2.3.9 Washington River Protection Solution (WRPS) Data	43
2.3.10 Savannah River Site Data	45
2.4 Erosion	48
2.4.1 Wilson et al., 1997, Erosive Mechanism	48
2.4.2 Baker and Jacobs, 1979, Sliding Bed Erosion	49
2.4.3 Wu et al., 2011, Visual Means.....	49
2.4.4 Savannah River Site – Experience.....	50
3.0 Discussion and Conclusion	51
3.1 Newtonian Slurries	51
3.2 non-Newtonian Slurries.....	52
4.0 Recommendations.....	53
5.0 References.....	55

LIST OF TABLES

Table 1-1 Newtonian Slurry Flow Regimes (Author’s Position).....	5
Table 2-1 RPP-9805 Waste Feed Properties ¹⁷	6
Table 2-2 EFRT M1 Closure Criteria and Resolution ¹⁸	7
Table 2-3 Summary of Weighted Particle Properties for Each Feed - Stream FRP14 ²²	8
Table 2-4 Summary of Weighted Particle Properties for Composite Feed - Stream FEP19 ²²	9
Table 2-5 Summary of Weighted Particle Properties for Each Feed - Stream UFP07 & FEP19 ²²	9
Table 2-6 d95 Particle Size, Critical Velocity, and Settling Velocity - Stream FRP14 ²²	9
Table 2-7 WTP Design Basis for Slurry Transport ²³	10
Table 2-8 Sensitivity Evaluation Around WTP Design Basis Slurry ²³	10
Table 2-9 Safety Margin Conclusion on Critical Velocity for WTP Newtonian Slurry ²³	11
Table 2-10 HLW Feed – Waste Feed Acceptance Criteria ICD-19 to WTP ⁷	11
Table 2-11 Newitt et al. Description of Solids Behavior in Pipe Flow ²⁴	13
Table 2-12 Design Velocities as Specified by Carleton and Cheng ²⁸	15
Table 2-13 Design Velocities for Iron Oxide in 53 mm Pipe ²⁸	16
Table 2-14 Data Used to Fit the Turian et al. and Oroskar-Turian Critical Velocity Correlations ³¹	16
Table 2-15. Comparison of Correlations to Experimental Critical Velocity Data	17
Table 2-16 Materials Used in Cho’s Experiments ³⁴	18
Table 2-17 Materials Used in Cairns Testing ^{40, 41}	22
Table 2-18 Materials Used in Pinto’s Testing ⁴⁴	24
Table 2-19 Correlation Used to Calculate Deposition Velocity ⁴⁴	25
Table 2-20 Correlation Used to Calculate Deposition Velocity	26
Table 2-21 Properties of Material Used in non-Newtonian Slurries ⁶¹	32
Table 2-22 Steps to Calculate the Critical Deposition Boundary by Thomas ⁶¹	34
Table 2-23 Steps to Calculate the Critical Deposition Boundary ⁴⁹	37
Table 2-24 Steps to Calculate the Transition Deposition Boundary ⁴⁹	37
Table 2-25 Steps to Calculate the Laminar Deposition Boundary ⁴⁹	37
Table 2-26 Physical Properties of Slurries Used to Determine Sliding Bed Region ⁶⁶	38

Table 2-27 Averaged Volumetric Particle Size Distribution of Slurries Used to Determine Sliding Region ⁶⁶	39
Table 2-28 WRPS Solids Components Used in Typical and High Solids ⁸⁰	44
Table 2-29 Physical Properties of Supernates Used in WRPS Testing at 20°C	44
Table 2-30 WRPS Sliding Bed and Critical Velocity Results ⁷⁹	45
Table 2-31 Frit Particle Size Specification	46
Table 2-32 Physical Properties Tested By GIW 1979 and 1982 Tests ⁸⁶	47
Table 2-33 DWPF Slurry Mix Evaporator (SME) and Melter Feed Tank (MFT) Design Basis	47
Table 2-34 1982 GIW Test Slurry Properties ⁸⁷	47
Table 2-35 Particle Size Distribution of Frit Used in 1982 GIW Tests ⁸⁷	48
Table 2-36 Magnetic Iron Ore Particle Size Distribution ⁹⁰	49
Table 3-1 Critical Transition Velocity for Bingham Plastic Fluid	53

LIST OF FIGURES

Figure 1-1. Recent Informal DRAFT Pretreatment Flowsheet (Prior to Single HLW Vessel Design)	3
Figure 1-2. Schematic of Reverse Flow Diverter Pumping System	4
Figure 1-3. Regions of Newtonian Slurry Flow	5
Figure 2-1. Newitt et al. Description of the Impact of Solids Concentration on Bed Formation and Pluggage ²⁴	12
Figure 2-2. Miedema Describing Flow Regime By Newitt Description ²⁷	14
Figure 2-3. Durand's Function, F_L ²⁷	14
Figure 2-4. Critical Velocity versus Concentration of Large and Small Sand Blends ³⁴	18
Figure 2-5. Minimum Transport Velocity versus Concentration of Heavy Sand and Cast Iron Blends ³⁴ ..	19
Figure 2-6. Overall Variation of the Dimensionless Deposition Velocity, F_L , with Solids Concentration and Particle Size for Slurries of Sand and Gravel in Water ³⁶	20
Figure 2-7 Predicted Deposition Velocity for Various Particle Sizes Below 0.5 mm for Silica Sand in 20°C Water ⁴³	23
Figure 2-8 Comparison of the Predictive Critical Deposition Velocities with the Observed V_c ⁴⁴	25
Figure 2-9 Representative Pressure Drop versus Flow Condition for Heterogeneous Slurry ³⁹	27
Figure 2-10 Settling Slurry Flow Regime ⁵⁷	28

Figure 2-11 Settled Bed in Laminar Flow (China Clay and Sand) - Thomas ⁵⁸	29
Figure 2-12 Settled Bed in Laminar Flow (China Clay and Coal) - Thomas ⁵⁸	29
Figure 2-13 Thickness Relationships between Thickness of Coarse Particle Deposition h and Cross-sectional Velocity V for Various Solids Concentration and Fixed Fluid ⁶⁰	31
Figure 2-14. Effect of Suspension concentration on minimum transport and initial sliding velocities on Kaolin-water suspensions ⁶¹	33
Figure 2-15. Effect of Yield Stress on Minimum Transport Velocity ⁶¹	33
Figure 2-16 Stills Taken from Video of Settling in a non-Newtonian Fluid	35
Figure 2-17 Fluid Axial Profile Image Showing a Sliding Bed ⁶⁴	35
Figure 2-18. Slurry Stability Map ⁴⁹	36
Figure 2-19 Deposition Velocity 150mm Glass Bead + Kaolin Slurry (Top) and AZ-101 HLW Pretreated Simulant (Bottom) ⁶⁶	39
Figure 2-20 Gold Tailing Particle Size Distribution ⁶⁸	40
Figure 2-21 Gold Tailing Bingham Plastic Rheological Properties ⁶⁸	40
Figure 2-22 Stationary Deposition Velocity Data, 100 mm I.D. Pipe ⁶⁸	41
Figure 2-23 Definition Sketch for Force-Balance Analysis ⁶⁸	41
Figure 2-24 Sliding Bed Observed During WRPS Testing ⁸⁰	45
Figure 2-25 Shape of Crushed Frit Used at DWPF – Frit 418.....	46
Figure 2-26 Erosive Mechanisms ⁸⁹	48
Figure 2-27 Flow Erosion Pattern in Horizontal Pipe ⁹¹	50

LIST OF ABBREVIATIONS

DNFSB	Defense Nuclear Facilities Safety Board
DOE	Department of Energy
HLW	High Level Waste
HTF	Hanford Tank Farm
ICD	Interface Control Document
LAW	Low Activity Waste
OPR	Office of River Protection
O-T	Oroskar and Turian
PIBOD	Process Inputs Basis of Design
PT	Pretreatment (Facility)
SRNL	Savannah River National Laboratory
SG	Specific gravity
UDS	Undissolved Solids
WTP	Waste Treatment and Immobilization Facility

1.0 Introduction

This report was requested by the Department of Energy (DOE) - Office of River Protection (ORP) to address concerns raised by the Defense Nuclear Facilities Safety Board (DNFSB) in their August 8, 2012, letter to the DOE regarding the Waste Treatment and Immobilization Plant (WTP).¹ In this letter, the DNFSB discussed the behavior of both Newtonian and Non-Newtonian slurries having the following design deficiencies: (1) Formation of Sliding Beds and (2) Erosion/Corrosion from sliding bed. In the first deficiency, there is a need to avoid the formation of a bed of sliding solids on the pipe invert and to design a flushing system. The second deficiency raises the issue of the solids from the sliding bed leading to increased wear pipe invert and uneven pipe wear. The DOE response letter states:² “It is conceivable that sliding beds could be present for short-time intervals of initial start-up of pumps, near the end of a waste transfer, or where the target transport velocity cannot be achieved due to competing design requirements. Hence, BNI will perform additional analysis of sliding beds to determine whether sliding bed erosion is more aggressive than turbulent erosion in small-diameter pipelines.”

The scope defined by ORP is³:

“To support closure of DNFSB concerns, ORP is requesting Savannah River National Laboratory (SRNL) to provide recommendations for the testing or analyses that need to be completed to close these outstanding DNFSB issues. SRNL should **perform the necessary literature review and consultation** with ORP and BNI to provide these recommendations. **SRNL should recommend any testing required to close the piping and component erosion issues** identified by BNI”

This assessment is based on readily available literature and discusses both Newtonian and non-Newtonian slurries with respect to sliding beds and erosion due to sliding beds. This report does not quantify the size of the sliding beds or erosion rates due to sliding beds, but only assesses if they could be present. This assessment addresses process pipelines in the PT facility and the HLW transfer lines leaving the PT facility to the HLW vitrification facility concentrate receipt vessel.

The WTP presently has three design guides for handling slurries within WTP. 24590-WTP-GPG-M-0058⁴ deals with Newtonian fluid as the carrier fluid transporting undissolved solids. This design guide uses a modified Oroskar and Turian (O-T) critical velocity correlation (equation (14))⁴. The fraction of UDS that are less than 74 μ m are considered part of the carrier fluid and the O-T is modified by reducing the fraction of UDS to those greater than or equal to 74 μ m, with the density and viscosity of the fluid corrected for the UDS less than 74 μ m. For particles smaller than 74 μ m, Thomas’s correlation (equation (15))⁴ is used and if the velocity is less than the calculated value, the particles that are less than 0.3 times the thickness of the laminar sub-layer are transported in a sliding bed. A 30% design margin is applied and the larger value of the two methods is the minimum critical velocity. This critical velocity is defined as the point where solids deposit to form a stationary bed. The other design guides, 24590-WTP-GPG-M-016⁵ and 24590-WTP-GPG-M-039⁶ deal with non-Newtonian fluids which can be modeled using either a Bingham Plastic or Power Law fluid respectively to determine the pressure drop for piping and fittings. These guides do not provide any guidance for determining the critical velocity for non-Newtonian fluids. There are no WTP design guides that provide a means to know when flow conditions exist that result in sliding beds.

In August 2014 the DOE² responded to the August 8, 2012, DNFSB letter¹. In this response, DOE provided a new in-depth strategy to address the issues raised by the DNFSB. DOE proposed a new minimum transfer velocity of 6 ft/s as compared to 4 ft/s to mitigate plugging based on literature review provided in their letter. The response did not address if a sliding bed is present in either Newtonian or

non-Newtonian slurries, though the letter noted that such behavior could potentially exist with non-Newtonian slurries. The same flushing and transfer strategy of using a minimum pipeline velocity of 6 ft/s is planned in the WTP – PT HLW transfer lines with at least 3 volume transfer line volumes of flush water to clean the lines and remove solids.*

The present interface control document (ICD) - 19⁷ describes the required physical and administrative interactions to allow for transfer of Hanford Tank Farm (HTF) tank waste by the Tank Operations Contractor to the WTP – PT facility. The present waste feed acceptance criteria for transfer (see Table 7)⁷ of interest is the maximum insoluble particle size, which is 310 μ m. Additionally, the HLW slurry will be transferred at a minimum of 6 ft/s (section 2.5.2)⁷ to the PT facility. The transfer line will be flushed between 6 and 10 ft/s (section 2.4.2)⁷ with a volume of water that, combined with any pre-transfer flush, is not more than three times the transfer pipeline capacity⁸ for a total flush volume of not more than 7,500 gallons. Given HLP-22 (the HLW receipt vessel in PT facility) will be a Standard High Solids Vessel Design (SHSVD), this total flush volume could be problematic given the batch volume is only 10,400 gallons⁹ and this 7,500 gallon flush volume was based on the previous working volume of 145,000 gallons.

The present configuration of vessels in the PT is considered to contain Newtonian slurries in HLP-22, FEP-17, and UFP-01, where Newtonian “Slurry” means the behavior of the slurry is predominately Newtonian. UFP-02 is considered to contain both Newtonian and non-Newtonian slurries. Vessels HLP-27 and HLP-28 are expected to contain non-Newtonian slurries, where non-Newtonian “slurry” means the rheological behavior of the slurry is not Newtonian and the solids affect the rheological properties. The typical pipeline transfer paths for the HLW containing vessels within the PT facility are, as shown in Figure 1-1, except for HLP-28 which sends its feed to the HLW facility. The SHSVD vessels UFP-VSL-00001A/B, UFP-VSL-00002A/B, HLP-VSL-00022A,B,C, HLP-VSL-00028, and HPV-VSL-00027A/B have 3-inch schedule 40 transfer piping and plans are to use centrifugal pumps for the transfer. Recirculation pumps used for heat exchanger purposes for the SHSVD vessels, other than UFP-VSL-00002A/B, will also utilize the same size transfer lines and centrifugal pumps. UFP-VSL-00002A/B ultrafiltration loop utilizes a 10 inch pipe and centrifugal pumps with a nominal recirculation flowrate of 2200 gallon per minute (GPM)¹⁰. PWD-VSL-00044A/B obtains waste from PWD-VSL-00033/44 and transfers the waste to FEP-VSL-00017A/B. The transfer lines between the PWD vessels and from the PWD vessel to the FEP vessel are 4-inch schedule 40 piping and reverse flow diverters (RFD) are used to pump the fluids. An RFD is a machined tee piece with an inlet (connected to a charge vessel) and outlet (connected to the transfer line) nozzle opposing each other and an entrainment port. Figure 1-2 provides a systems schematic of a RFD process, but in the case of WTP, the buffer tank is replaced with a pump pair to provide the pneumatics. There are no break pots used with these RFD transfer lines. The flow rates in these systems range from 89.5 to 111 GPM.

* Per discussion with Doug Vo, WTP, 1-9-2015

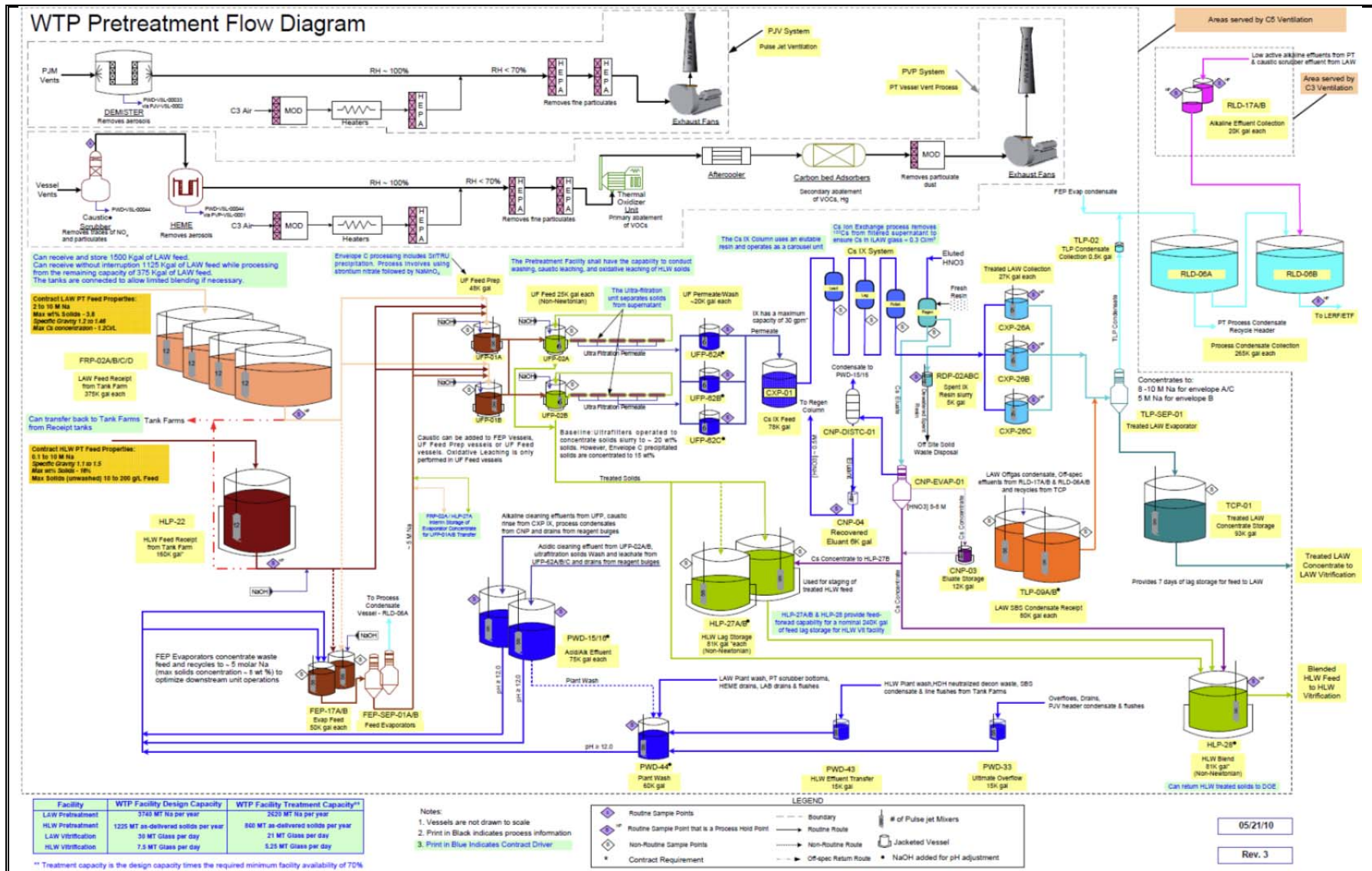


Figure 1-1. Recent Informal DRAFT Pretreatment Flow sheet (Prior to Single HLW Vessel Design)

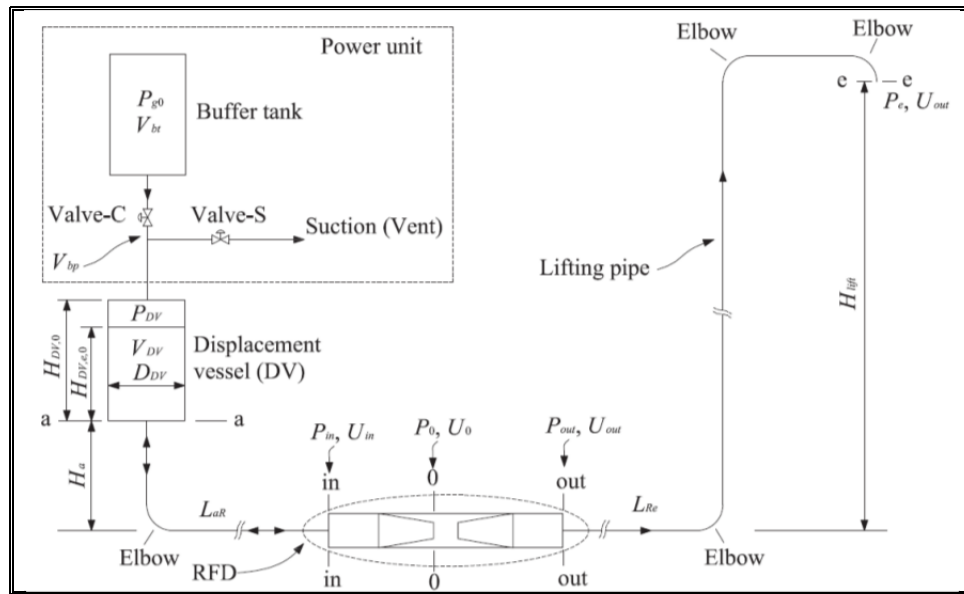


Figure 1-2. Schematic of Reverse Flow Diverter Pumping System¹¹

As previously stated, this report is a review of existing literature to assess if a sliding bed and its wear can exist in the WTP PT. If a sliding bed exists in WTP, there is a probability that a sliding bed will exist in the HTF given similar operating conditions of the transfer line. Both the HTF and WTP transfer lines are 3" schedule 40 piping. WTP also uses 3" piping for pump suction piping.*

Table 1-1 is a description of what the author believes are the various flow regimes for Newtonian slurry pipe transport, starting at the lowest velocity where solids depositions occurs to the highest velocity where the flow is homogeneous. This change in flow regime is due to the level of turbulence, as the flow increases, the level of turbulence increases, further supporting the suspension of solids. Figure 1-3 provides a visual interpretation, excluding a settled bed condition. These velocities are based on reducing the velocity from a "pseudo-homogeneous/homogenous" state to a settled bed state. For non-Newtonian slurries, literature is limited concerning sliding beds, but the transition point between laminar and turbulent flow has been denoted as the critical velocity or critical transitional velocity.^{12,13,14,15} This notion is consistent in most literature, and is typically the minimum point at which to operate the slurry transport line. This position is provided given the lack of clarity that at times is presented in the reviewed literature.

This report does not assess the following:

- synergetic wear effects due to corrosion/erosion from a sliding bed;
- the different HLW waste stream compositions (densities and particle size distributions) by models such as HTWOs or G2 and if such streams could be considered candidates in generating a sliding bed;
- the transport methods used by WTP to assess critical velocity;
- the size and composition of the sliding beds that could be present; and
- a quantified effect of the sliding bed on erosion.

* Per discussions with Doug Vu, WTP, 12-12-8-2014

Table 1-1 Newtonian Slurry Flow Regimes (Author's Position)

Velocity	Flow Regime	Condition
	Settled bed	This is the velocity at which a stationary bed has formed on the bottom of the pipe. This value is typically stated by most authors as the “critical”, “minimum”, “deposit”, or “deposition” velocity. This is the critical velocity based on the author’s view of literature.
	Sliding bed	This is the minimum velocity at which a sliding bed is present. The velocity range for sliding bed can be large.
	Saltation	This behavior can be hard to distinguish from that of sliding bed. Solids can flow in dunes.
	Heterogeneous	This behavior occurs at a velocity where all solids are in suspension. There exists both a velocity and solids concentration gradient in the cross-section of piping.
	Pseudo-Homo / Homogeneous	This behavior occurs at a velocity at which the solids concentration is fairly uniform across the pipe cross-section. It is not “truly” homogeneous.

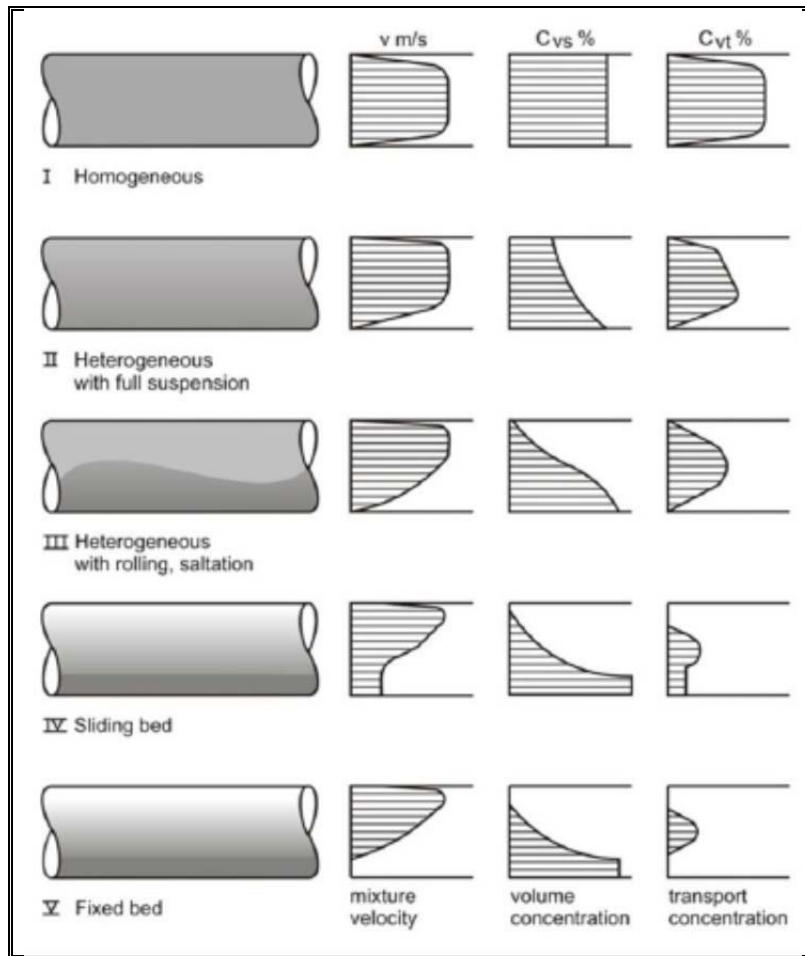


Figure 1-3. Regions of Newtonian Slurry Flow¹⁶

2.0 Properties, Sliding Bed and Erosion

This section is divided into four parts and provides a review of open literature. The first section discusses requirements for and/or estimates of the physical properties of the slurries to be transported in WTP. The second section discusses the various flow regions for Newtonian fluids. The third section discusses non-Newtonian fluid flow regions. The last section covers erosion due to sliding beds.

2.1 WTP Pretreatment Slurries Properties

The following documents were selected to provide input for this assessment. This is not an assessment of those documents, but rather a utilization of the data.

2.1.1 RPP-9805, (2002)

RPP-9805¹⁷ provided one of the earlier sets of recommended values for waste properties for the waste feed delivery transfer system and included particle size distribution (PSD), particle density and slurry viscosity. Table 2-1 is a summary from this report. To determine viscosity, RPP-9805 recommends using the equation shown in Table 2-1. The document further goes on to state that agglomerates and flocculants tend to make up a lot of the larger particles and contain interstitial liquid that would reduce the agglomerated/flocculated densities.

Table 2-1 RPP-9805 Waste Feed Properties¹⁷

Property		Values					
Solids concentration (g-solids/L-slurry)		200 (max)					
Solids density (g/ml)							
Average solids density		2.9					
95% confidence interval		2.6 to 3.2					
95/95 tolerance limit		3.9					
Particle Size Distribution (µm)							
Percentile	1	5	25	50	75	95	99
Mean	0.7	1.2	3.7	7.5	31	140	210
Standard Deviation	0.4	0.6	1.8	4.2	38	94	145
95% confidence limit	1	1.6	5	11	58	210	310
95/95 tolerance limit	2	3.1	10	22	160	460	700
Viscosity (cP)							
$\mu_M = 2.0 \cdot [1 + 2.5 \cdot C_V + 10.05 \cdot C_V^2 + 1.3\{exp(17 \cdot C_V) - 1\}] \cdot \gamma^{-0.06}$							
Where: μ_M = viscosity of sludge C_V = solids volume fraction γ = shear rate (1/s), typically obtained between 100 to 200 s ⁻¹							

2.1.2 External Flowsheet Review Team Issue M1 Closure (2009)

CCN214961¹⁸ summarizes the four closure criteria that addressed the External Flowsheet Review Team (EFRT) question that any line containing both solids and liquids can be expected to plug and should be designed to prevent plugging for both rapidly settling and hindered-settling slurries. In summary, the

EFRT recommended a thorough review of all slurry containing process lines to ensure the line-plugging potential is minimized. CCN214961¹⁸ addressed the EFRT M1 issue by closing the four closure criteria identified in the Issue Response Plan¹⁹. The four closure criteria and resolution for closure are provided in Table 2-2.

Table 2-2 EFRT M1 Closure Criteria and Resolution¹⁸

#	Criteria	Resolution
1	A report is issued documenting design basis particulate size and density with support by Hanford waste characteristics experts.	Reports referenced for this closure were RPP-9805 and WTP-RPT-153 that identified the particle size and density for the d95 and d98 particles. 24590-WTP-GPG-M-0058 was used to determine the critical velocities.
2	A bounding interim Design Guide (DG-1) is issued that specifies minimum slurry flow velocity, pipe flushing velocity, and preferred piping configuration.	Design guide 24590-WTP-GPG-M-0058 Rev. 0 was issued to provide guidance in determining the minimum pipe flow velocity for transfer of Newtonian Fluids, including margin. Pipeline flushing requirements are specified in 24590-WTP-GPG-M-0058. 24590-WTP-GPG-M-0058 also addresses the special considerations for vertical lines, elbows, traps and dead legs, valves, jumpers and pumps.
3	The design of WTP piping is evaluated against the interim Design Guide to identify the set of modifications required to correct deficiencies.	24590-WTP-GPG-M-0058 was used to complete the piping system design assessment calculations for plugging in the case of Newtonian and low-yield stress non-Newtonian fluids. Approximately 300 transfer routes were assessed to define normal-process and flush-flow velocity requirements, evaluate available flow margins, and establish the potential of mechanical plugging due to solids settling. Based on this assessment, seven design changes proposals were made.
4	The final design guide is expected to be confirmatory based on final particulate characterization and R&T results. Nevertheless, closure of M-1 is contingent upon the final design guide.	24590-WTP-GPG-M-0058 has been confirmed experimentally by a series of fluid flow tests (CCN: 137169, Use of MI Test Data Provided by Pacific Northwest National Laboratory (PNNL)) for Newtonian fluids. For fluids not defined in 24590-WTP-GPG-M-0058 other design guides have been implemented: <ul style="list-style-type: none"> (1) 24590-WTP-GPG-M-059 -Avoiding Chemical Line Plugging-Plant Design Considerations. This design guides provides a basis understanding of chemical plugging mechanisms and plant design considerations for plug removal. (2) 24590-WTP-GPG-M-016 -Pipe Sizing for Lines with Liquids Containing Solids - Bingham Plastic Model. This design guide is applicable to Bingham plastic fluids in laminar and turbulent flow conditions. This design guide can be used to determine if the slurry is homogenous, the pressure drop per length of pipe and the pressure drop for valves and fittings. (3) 24590-WTP-GPG-M-027 - Recommended Slopes for Piping Systems. This design guide provides piping slope recommendations for pressure and gravity transfer process systems. Pressure and gravity transfer piping is further divided into recommendations for black cell piping, hot cell piping, and piping outside these areas such as between facilities. (4) 24590-WTP-GPG-M-032 - Vessel Overflow and Gravity Line Sizing. This design guide provides guidance for sizing vessel overflow nozzles and gravity overflow lines that are subject to unsteady flow and surges due to periodic siphons and venting of air from piping.

2.1.3 Process Inputs Basis of Design (PIBOD), (2011)

The PIBOD²⁰ documents the physical properties of WTP process streams based on a mass balance calculation using tank waste feed classes and processing scenarios representing the entire WTP process. The physical properties of interest that are provided for the process streams are: liquid and slurry density, mass fraction total solids, mass fraction suspended solids, and rheology. For the non-Newtonian streams in PT, the plastic viscosity ranges from 6 to 30 centipoise and the Bingham Plastic yield stress ranges from 6 to 30 Pa. The Newtonian viscosity is limited by that stated in ICD-19.⁷ The results from the PIBOD are to be used in conjunction with data from other sources for design confirmation. For instance,

neither the particle size distributions or particle densities are provided by PIBOD, but the average particle density can be deduced from the data provided. PIBOD states that RPP-9805¹⁷ and WTP-RPT-153²¹ are available resources to determine the particle properties. PIBOD also recommends considering adding additional contingency consistent with standard engineering practice.

2.1.4 24590-WTP-RPT-PE-12-005, (2013)

24590-WTP-RPT-PE-12-005²² serves the purpose of proving a supporting argument for the current basis for crystalline particle properties to be processed through the WTP. This study checks that the design basis limits on particles are reasonably bounded based on engineering interpretation of the available data and analysis. A total of six process nodes were assessed in WTP and only four of the nodes are of relevance to this study and are located within the PT facility. These nodes are identified as Stream FRP14 (HLW feed to the PT facility), Stream FEP19 (concentrate from the waste feed evaporation process system (FEP)), Stream UFP07 (concentrate from the ultrafiltration process system (UFP)), and Stream HLP09 (feed to the HLW vitrification facility). UFP07 and HLP09 are the same, given one feeds the other without any processing. Six groups of waste feed types were analyzed and provided. The results of that assessment for those various streams are provided in Table 2-3 through Table 2-5. In summary, for all waste feed group types, the hardness and density increased after solids treatment and the particle size decreased, implying that after leachable solids are removed, the remaining particles are harder, smaller and denser. Stream FEP19 includes recycle streams from both HLW and LAW. The document clearly states that the particle sizes utilized in this document do not account for agglomeration and/or fused particles, hence should not be considered conservative. The values provided in Table 2-3 through Table 2-5 are weighted values as defined in Appendix D of 24590-WTP-RPT-PE-12-005 and some of these mean values exceed the design basis limits stated in the document. It is not the intent of this document to assess the methodologies, data, calculations, or results stated in 24590-WTP-RPT-PE-12-005, but rather use the results in this report. Mean weighted average values are such that there will be compounds that exceed the values stated in these tables and their impact is unknown. For instance, the weight based value for moh hardness does not take into consideration the particle size distribution, which could be an important parameter in erosion. Such unknowns will not be considered.

Table 2-3 Summary of Weighted Particle Properties for Each Feed - Stream FRP14²²

Waste Feed Group Type	Weighted Mean Hardness (moh)	Weighted Mean Density (kg/m ³)	Weighted Min mean Particle Size (µm)	Weighted Mean or Median Particle size (µm)	Weighted Max Particle Size (µm)
Composite	4.6	2938	0.6	2.5	66.7
Chromium	4.7	2831	0.7	3.0	91.4
Bismuth	4.8	3082	0.6	2.4	43.7
Zirconium-Aluminum	4.2	2693	0.8	3.7	128.9
Aluminum-high leachability	4.7	2842	0.7	2.7	75.5
Iron	4.7	3298	0.6	2.5	75.3
DESIGN BASIS LIMIT	≤ 4.4	2180	NA	11	210

Table 2-4 Summary of Weighted Particle Properties for Composite Feed - Stream FEP19²²

Waste Feed Group Type	Weighted Mean Hardness (moh)	Weighted Mean Density (kg/m ³)	Weighted Min mean Particle Size (µm)	Weighted Mean or Median Particle size (µm)	Weighted Max Particle Size (µm)
Composite	4.5	2741	0.7	3.2	76.9
Chromium	4.3	2590	0.6	3.3	61.7
Bismuth	4.4	2796	0.7	2.9	55.4
Zirconium-Aluminum	5.0	2992	0.7	2.5	28.6
Aluminum-high leachability	4.5	2623	0.7	3.1	57.9
Iron	4.8	3106	0.6	2.5	52.9
DESIGN BASIS LIMIT	NA	NA	NA	NA	NA

Table 2-5 Summary of Weighted Particle Properties for Each Feed - Stream UFP07 & FEP19²²

Waste Feed Group Type	Weighted Mean Hardness (moh)	Weighted Mean Density (kg/m ³)	Weighted Min mean Particle Size (µm)	Weighted Mean or Median Particle size (µm)	Weighted Max Particle Size (µm)
Composite	4.8	3443	0.5	1.1	11.5
Chromium	4.9	3405	0.4	1.0	9.4
Bismuth	4.9	3870	0.4	1.1	7.3
Zirconium-Aluminum	5.2	3332	0.7	1.8	11.2
Aluminum-high leachability	5.0	3228	0.6	1.5	10.5
Iron	5.1	4013	0.2	1.0	8.7
DESIGN BASIS LIMIT	NA	3800	NA	NA	300

For the HLW incoming stream FRP14, the maximum weighted particles were treated as the d95 particles and the mean average densities were used to calculate the critical transport and settling velocities provided in Table 2-6. The critical velocity was determined using the WTP design procedure⁴ for Newtonian slurries and includes the 30% design margin.

Table 2-6 d95 Particle Size, Critical Velocity, and Settling Velocity - Stream FRP14²²

Waste Feed Group Type	d95 Particle Size (µm)	Solids Density (kg/m ³)	Critical Velocity (ft/s)	Settling Velocity (ft/s)
Baseline	210	2180	3.7	0.036
Composite	67	2938	4.0	0.007
Cr	91	2831	4.1	0.012
Bi	44	3082	3.9	0.003
Zr-Al	129	2693	4.2	0.022
Al-HL	76	2842	4.0	0.009
Fe	75	3298	4.5	0.011

2.1.5 WTP Design and Safety Margin (2014)

CCN229195²³ applies the design and safety margin to the WTP design for the current (at that time, the 95th confidence level particle size distribution stated in RPP-9805¹⁷) particle size distribution. Baseline calculations were based on the WTP design basis input for slurry transport, Table 2-7. The critical velocity calculated⁴ for the design basis with the 30% margin was 3.72 ft/s and 2.86 ft/s without margin. A sensitivity evaluation using the O-T critical velocity correlations specified in 24590-WTP-GPG-M-0058⁴ was performed without using margin and the values stated in Table 2-7 were used as the baseline condition. The results from this evaluation are provided in Table 2-8 and summarized in Table 2-9.

Table 2-7 WTP Design Basis for Slurry Transport²³

Parameter	Value	Units
d_p	210	Micron
ρ_s	2.18	g/mL
P_L	1.1	g/mL
μ_L	2	cP
C_s	200	g/L
η_{homo}	50	%
D	3	Inch (Sch. 40)

Table 2-8 Sensitivity Evaluation Around WTP Design Basis Slurry²³

Critical Velocity (ft/s)	Variable Change					Response			
	d_p (μm)	C_s (g/L)	η_{homo} (%)	ρ_s (g/cm^3)	30% Design Margin	ρ_s (g/cm^3)	d_p (μm)	Critical Velocity (ft/s)	
	Baseline Table 2-7					Yes			3.72
	Baseline Table 2-7					No			2.86
4					No	3.2			
	310				No				3.05
		50			No				2.49
			0		No				3.41
4	310				No	2.94			
	700			2.9	No				4.53
	1100			2.9	No				4.89
6					No		17,500		
6					No	6.1			

Table 2-9 Safety Margin Conclusion on Critical Velocity for WTP Newtonian Slurry²³

1	Based on the estimated required particle size or particle density required to achieve a critical velocity of 6 ft/s, the recommended use of a 6 ft/s transfer velocity in the WTP design provides considerable margin.
2	A particle size limit of 310 microns results in a required density of ~ 2.9 g/mL in order to achieve a critical velocity of 4 ft/s. The 2.9 g/mL value is the design basis density used for mixing.
3	A factor of 4 change to the solids concentration results in a 15-20% increase to the critical velocity. Thus, even with the potential for solids stratification in the WTP PJM mixed vessels, the required critical velocity will not exceed 6 ft/s with a feed delivery limit of 4 ft/s.
4	The use of the homogenous fraction accounts for the presence of the smaller particles which aid in the movement of the larger particles. However, the use of the d95 particle size effectively states that the remainder of the solid particles are at the d95 size. Therefore, while the use of a non-zero homogeneous fraction results in a lower critical velocity, the use of the d95 particle size is conservative.

2.1.6 ICD-19, (2014)

ICD-19⁷ is the interface control document for waste feed between the HTF and the WTP PT facility. The HLW feed data of interest is listed in Table 2-10. The critical velocity listed in Table 2-10 is based on bulk slurry parameters, not that of subsets of compounds with specific size and density values that could exceed this limit. The upper particle size limit will be controlled via process or procedure (to be determined) and is the D99 particle size at the 95% confidence level stated in Table 2-3. Given a 310µm size particle and using the upper critical velocity of 4 ft/s, the maximum density of the particle is 2.9 g/cm³ without any margin using the WTP design procedure.⁴ Particle density limits or particle size distributions are not provided. Additional information of interest are the slurry transport velocity between the HTF at a minimum of 6 ft/s followed by flush water velocity between 6 and 10 ft/s.

Table 2-10 HLW Feed – Waste Feed Acceptance Criteria ICD-19 to WTP⁷

Property	Limits
Solids concentration	≤ 200 g/L for transfer (maximum) <u>In WTP receipt vessel after blending the contents of unwashed solids, the linear range of</u> $107 \leq$ g/L at 0.1M sodium to $144 \leq$ g/L at 7M sodium
Slurry bulk density	< 1.5 kg/L
Critical velocity	≤ 4 ft/s
Maximum particle size	310 µm
Slurry rheology at 25 °C	
Plastic viscosity	< 10 cP
Yield Stress	< 1.0 Pa

2.2 Regions of Flow for Newtonian Slurries

The description of the various regions of solids transport has been described by many authors in various articles.

2.2.1 Newitt et al., 1955

This article discusses sliding beds. One of the original descriptions of flow regimes for Newtonian slurries was provided by Newitt et al.²⁴. Newitt et al. performed preliminary tests using 3/4 inch glass tube, water, and 60 micron glass beads having a density of 2.8 g/cm³. The results from this test are provided in Figure 2-1, showing various regions of both sliding/settle beds. Notice the large region (difference in velocity) where the sliding bed is present prior to becoming fully suspended.

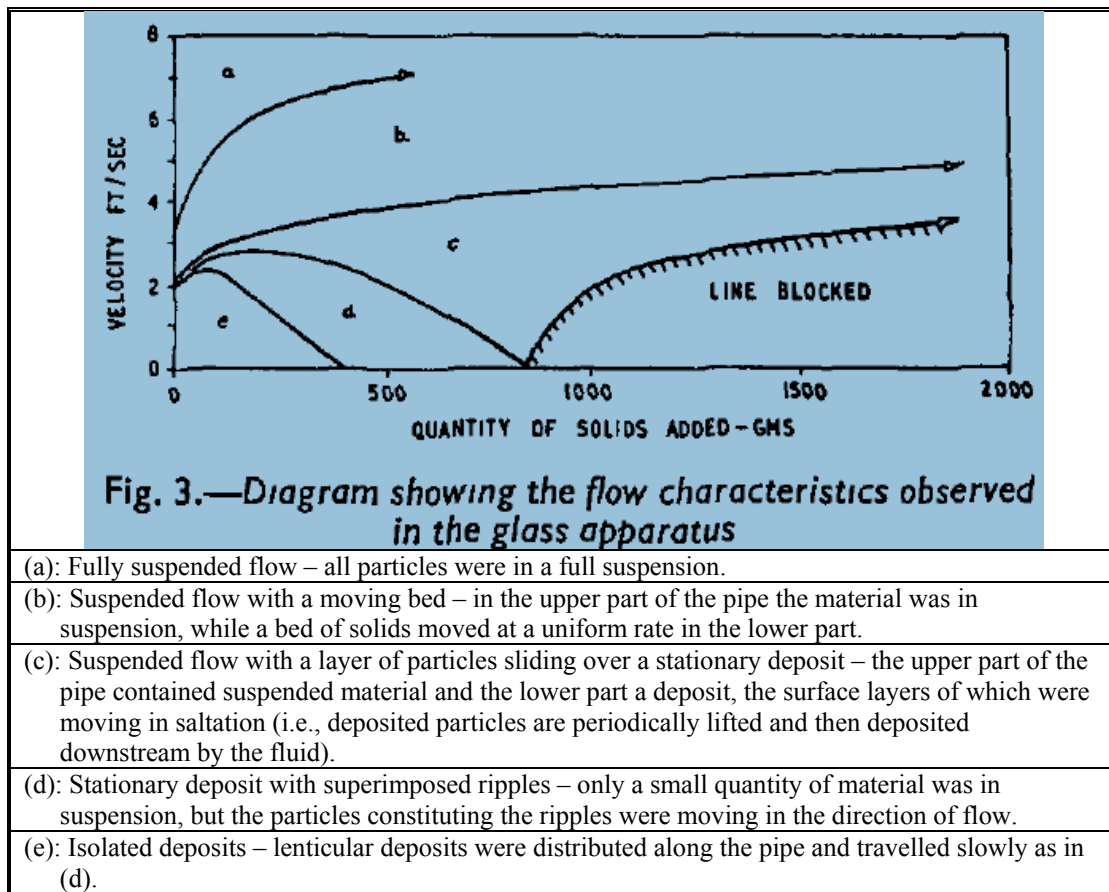
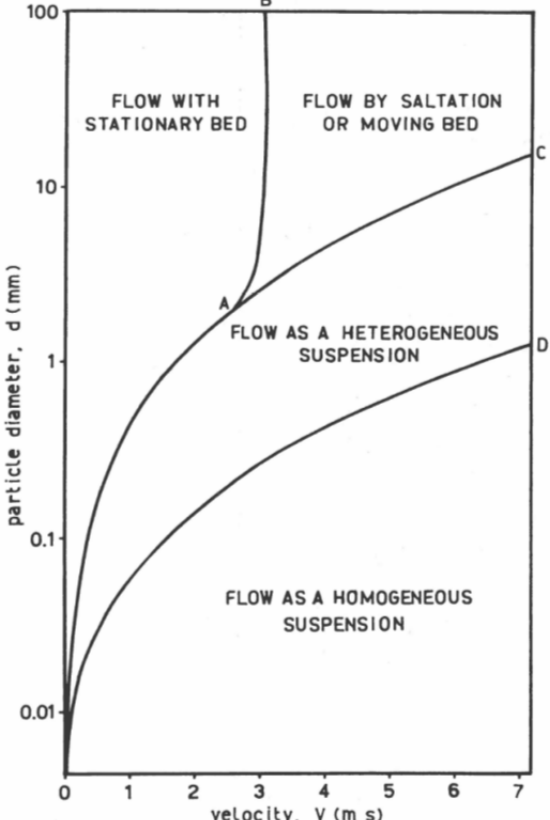


Figure 2-1. Newitt et al. Description of the Impact of Solids Concentration on Bed Formation and Pluggage²⁴

In this article, Newitt et al. described the various transitions in velocities from his tests, starting with the lowest velocity to the highest as shown in Table 2-11. The lowest velocity is denoted the critical deposition velocity (V_C), which is the point where a stationary bed of solid first forms, the next is the saltation or sliding bed velocity (V_B), which is the point where the flow turns into a heterogeneous flow, and finally to homogeneous velocity (V_H) where the solids concentration is fairly constant across the pipeline cross-section. This analysis was based on the energy (work) required to convey material between two points at a specific rate and can be assessed by

measuring the difference in the hydraulic gradient between the liquid and suspension. In this study, water was the only carrier fluid used. The solids used in assessing the pressure/flow curves were Perspex (i.e., poly(methyl methacrylate)), coal, sand, gravel, manganese dioxide, and zircon sand with narrow particle size distributions between 110 to 6000 microns, and solid volume fraction between 0.05 and 0.35. No uncertainties of the velocities correlations were provided. The critical velocity was based on Durand's²⁵ work and is the velocity where a stationary bed has formed. Above this velocity, there is flow with a moving bed of solids. The curve OAB shown in Table 2-11 was as defined²⁶ the accepted definition for critical velocity, which is the mean velocity of mixture at which the stationary bed begins to appear at the bottom of the pipe as the velocity is decreasing. Additional details of the work performed by Newitt et al. for the various flow regimes are provided by Miedema²⁷. Miedema provides an example of the various flow regimes as described by Newitt for a 1" and 6" pipe conveying sand in water as shown in Figure 2-2. Figure 2-3 shows Durand's function (F_L) as function of particle size and concentration. Note that as the particle size increases, so does F_L , up to about 1000-1500 μm , at which point there is little change in F_L .

Table 2-11 Newitt et al. Description of Solids Behavior in Pipe Flow²⁴

Provided Curve	Velocity	Definition
 <p>The graph plots particle diameter d (mm) on a logarithmic y-axis (0.01 to 100) against velocity V (m/s) on a linear x-axis (0 to 7). Four curves originate from the origin (0,0). The uppermost curve is labeled 'FLOW WITH STATIONARY BED' and has a point 'B' at approximately $V=3$, $d=100$. The middle curve is labeled 'FLOW BY SALTATION OR MOVING BED' and has a point 'C' at approximately $V=7$, $d=15$. The lower curve is labeled 'FLOW AS A HETEROGENEOUS SUSPENSION' and has a point 'A' at approximately $V=2.5$, $d=2$. The bottom curve is labeled 'FLOW AS A HOMOGENEOUS SUSPENSION' and has a point 'D' at approximately $V=7$, $d=1.2$. A vertical line segment connects point 'B' to point 'A'.</p>	$V_C = F_L \sqrt{2gD(S - 1)}$	V_C = Critical Velocity, below which a stationary bed exists. (Line OAB) F_L = Durand's Function, see Figure 2-3 g = Acceleration due to gravity D = Pipe inside diameter $S = \frac{\rho_s}{\rho_L}$ ρ_s = Density of solid ρ_L = Density of liquid
	$V_B = 17W$	V_B = transition flow between saltation or sliding bed and a heterogeneous suspension (Line AC) W = particle terminal falling Velocity.
	$V_H = \sqrt[3]{1800gDW}$	V_H = transition between flow as a heterogeneous suspension and homogeneous flow

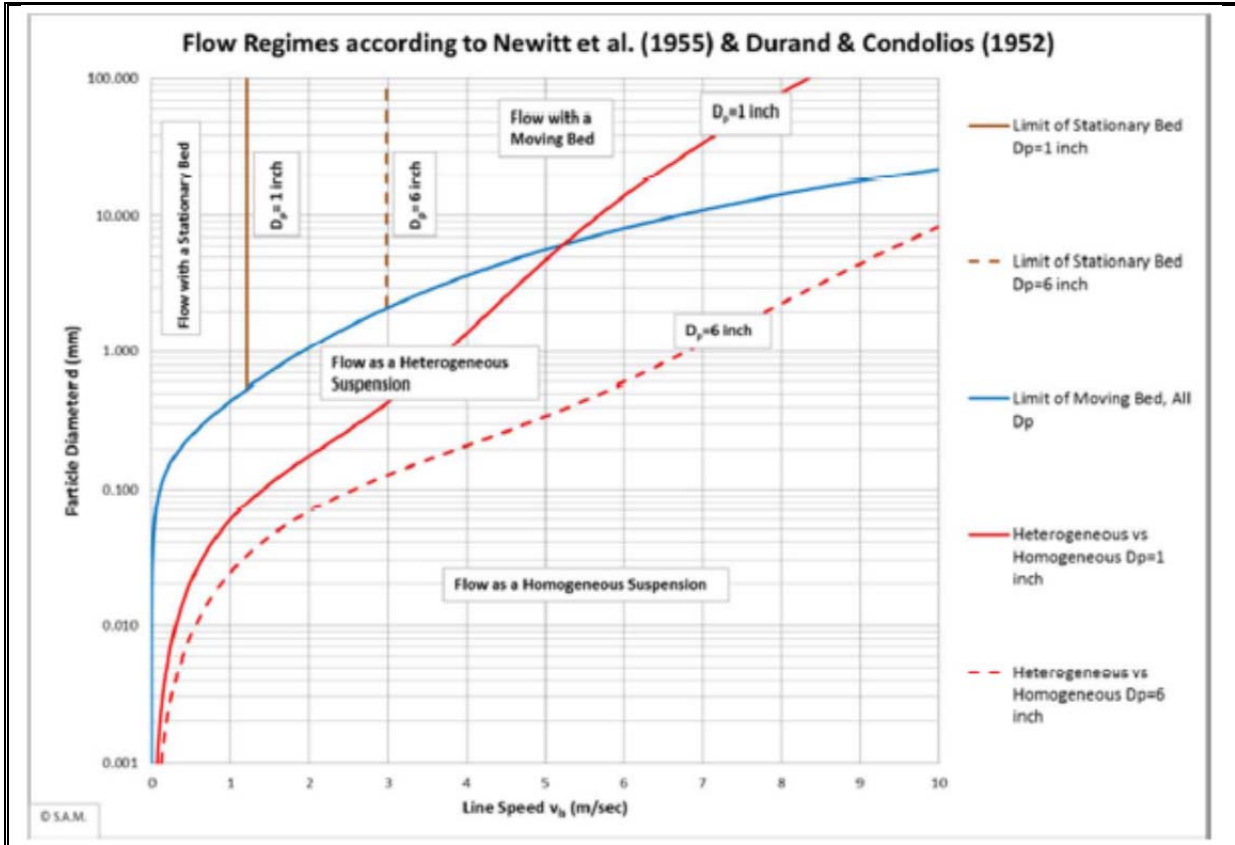


Figure 2-2. Miedema Describing Flow Regime By Newitt Description²⁷

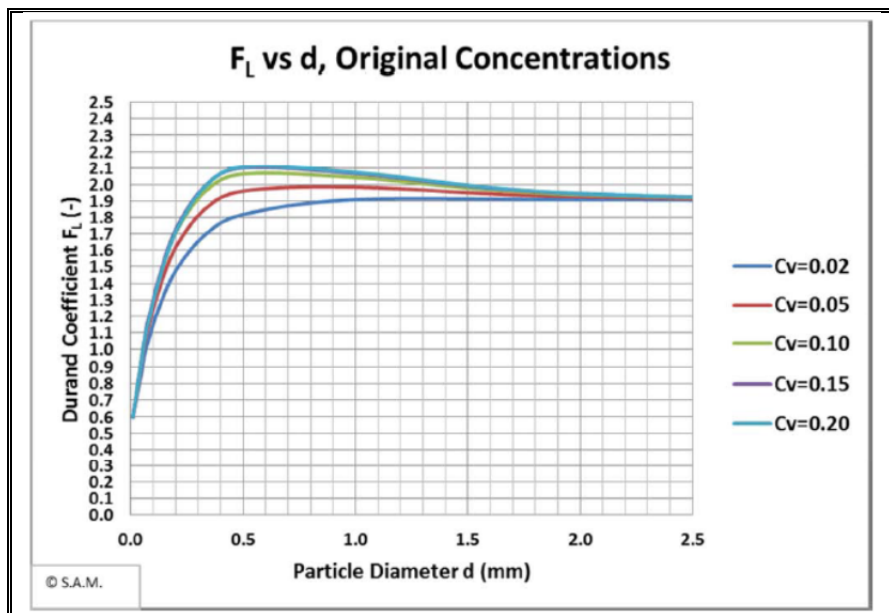


Figure 2-3. Durand's Function, F_L ²⁷

2.2.2 Carleton and Cheng, 1977

This article discusses critical velocity. Carleton and Cheng²⁸ provided definitions of design velocities for correlations developed to that point in time. The design velocities and definitions are provided in Table 2-12 and can lead to confusion. For instance, one would expect that the sliding bed velocity would be below that of deposition or critical velocities, given the description provided by Carleton and Cheng. Carleton and Cheng used some 50 or so correlations and made a comparison between predicted and measured values for a 25 weight percent (wt. %) suspension of 50 micron iron oxide (with density not provided, but expected to be between 5.2 to 5.7 g/cm³)²⁹ in a 53 mm (2-in.) pipe. The results, provided in Table 2-13 clearly show that the correlations do not agree with measured values and note that the sliding bed predictions exceed those of all the other predictions other than the heterogeneous/homogeneous transition. The standard deviations of the correlations used are quite large and for the sliding bed, it exceeds the mean. The article³⁰ in which these data were analyzed could not be obtained to determine which correlations were used to support these calculations.

Table 2-12 Design Velocities as Specified by Carleton and Cheng²⁸

Velocity in increasing order	Description
Deposit	The velocity at which particles start to settle out as the flow is lowered. The particles may settle to a static or a sliding bed. This velocity is not necessarily the same as the suspending velocity.
Sliding bed	This is the velocity at which the shearing forces in the liquid are just sufficient to move particles that lie on the floor of the pipe. This is normally an inefficient method of transporting the solids, but it may well be the mechanism by which solids are carried in high-concentration conveying.
Saltating	At this velocity, particles are repeatedly picked up by the liquid and deposited further along the pipe. This form of transport is not used for long-distance lines carrying fine particles, but for short lines carrying coarse particles, it may be necessary to operate with saltating flow.
Suspending	This is the lowest velocity at which all the particles are picked up and remain in suspension. This velocity is used for designing most pipelines but it is difficult to determine with precision, particularly when the particles have a wide size distribution and when fine particles suspended in the liquid make it opaque.
Minimum in the pressure gradient versus velocity curve (Critical)	This is often known as the critical velocity . Its determination does not require observations of the flow regime but the minimum point is difficult to locate with precision because the curve is often shallow and not necessarily continuous. Thus, correlations in which the position of the minimum has been derived by differentiation of an analytical expression derived from experimental points must be used with great caution. It is usually assumed that the critical velocity is higher than the suspending velocity so that its use leads to a safe design. Although this is usually true, there can be no guarantee that it is always so.
Homogeneous flow	In theory, this is the velocity at which the particles become evenly distributed throughout the pipe. In practice, it is defined as the velocity at which the concentration profile across the pipe attains some arbitrary degree of uniformity. Alternative definitions for homogeneous flow are based either on the assumption of the pressure gradient in the pipeline being equal to (1) that for a fluid having the same density as that of the suspension and the viscosity of water (the standard velocity), or (2) that predicted from viscometer measurements on the homogeneous suspension. However, velocities corresponding to homogeneous flow will normally lead to a design that is too conservative.

Table 2-13 Design Velocities for Iron Oxide in 53 mm Pipe²⁸

Design Velocity	Number of Correlations	Mean of predictions (m/s)	Standard deviation (m/s)	Measured value (m/s)
Laminar/turbulent transition	2	0.41	-	1.01 (calculated from viscometric data)
Sliding-bed velocity	7	1.47	1.51	-
Suspending velocity	11	0.58	0.5	1.10 – 1.80 (not sharply defined)
Deposition velocity	11	0.83	.31	(as for suspending velocity)
Critical velocity	10	0.66	0.10	0.29 (not sharply defined)
Heterogeneous/homogeneous transition	5	1.74	1.37	1.46

2.2.3 Turian et al. – Critical Velocity 1987

This article does not discuss sliding bed. Turian et al.³¹ performed a detailed examination of the critical velocity of non-colloidal slurries in pipeline flow and provided an improved critical velocity correlation using a large data base as compared to other correlations developed at that time. In this article, they define the critical velocity as the minimum velocity demarcating flows in which the solids form a bed at the bottom of the pipe from fully suspended flow. The authors go on to state it is also referred to as the minimum carrying or the limiting deposition velocity, which is the point where a stationary bed of solids initially form. The number of data sources and points used and ranges of physical properties used in his correlation are provided in Table 2-14. In 1980, Oroskar and Turian³² (O-T) provided a critical velocity correlation and the same critical velocity definition was used as in this article. Table 2-14 also provides the number of data sources and points used and ranges of physical properties used in his correlation. Turian et al. 1987 data includes most of Oroskar’s data.

Table 2-14 Data Used to Fit the Turian et al. and Oroskar-Turian Critical Velocity Correlations³¹

Value	Turian ^{xvi}	O-T ^{xvii}
Sources	41	5
Number of critical velocity Data Points	864	357
Solids Density (g/cm ³)	1.15 – 8.9	1.3 – 5.24
Fluid Density (g/cm ³)	0.77 – 1.35	0.9 – 1.35
Fluid Viscosity (cP)	0.5 – 190	0.47 – 1300
Particle Size (microns)	20 – 19,000	100 – 2040
Pipe Diameter (cm)	1.27 – 31.5	1.905 – 31.5
Volumetric Concentration (vol %)	0.1 – 56.1	1 – 50

The correlations developed by Turian et al. and O-T are shown as equations (1) and (2) respectively. The stated relative root mean square standard (RMS) deviation for the Turian et al. correlation is 0.3416 and for the O-T it is 0.2182, given their data sets. It is not clear upon reviewing these articles that the reported O-T RMS is correct, given what is stated in the Turian et al. article. O-T assessed their data using their generic critical velocity relationship (eq. 41)³² for n = 2 (this is the power relation for hindered settling velocity due to solids concentration on the unhindered velocity) and reported an RMS of 0.2594, the same value reported by Turian et al., but in this case Turian (see Table 1)³¹ reported this as the absolute average percent deviation (\bar{D}) with an RMS of 0.4331. Turian et al. does not include the O-T equation (2) in their assessment, which is the equation WTP utilizes to determine the critical velocity. The \bar{D} for Turian et al. equation (1) is 20.53%, lower than equation (2). It is unclear to this author which uncertainty data is

correct for the O-T equation (2). Table 2-15 provides a distribution of percent deviation for each critical velocity data point using equation (2) and O-T (eq. 41)³². The results show the calculated critical velocity can be quite different than what was measured. The reported RMS is one standard deviation. Based on Oroskar's thesis³³, the d_{50} volume basis particle size was used.

$$V_D = 1.7951 \cdot C_V^{0.1087} \cdot (1 - C_V)^{0.2501} \cdot \left(\frac{D \cdot \rho_f \cdot \sqrt{g \cdot D \cdot (S - 1)}}{\mu_f} \right)^{0.00179} \cdot \left(\frac{d}{D} \right)^{0.06623} \cdot \sqrt{2 \cdot g \cdot D \cdot (S - 1)} \quad (1)$$

$$V_D = 1.85 \cdot C_V^{0.1536} \cdot (1 - C_V)^{0.3564} \cdot \left(\frac{D \cdot \rho_f \cdot \sqrt{g \cdot d \cdot (S - 1)}}{\mu_f} \right)^{0.09} \cdot \left(\frac{d}{D} \right)^{-0.378} \cdot \chi^{0.30} \cdot \sqrt{g \cdot d \cdot (S - 1)} \quad (2)$$

Where: C_V = Volumetric concentration (fraction)

d = particle diameter (m)

ρ_f = carrier liquid density (kg/m³)

g = gravitational constant (9.81 m/s²)

S = density ratio of solids to fluid

μ_f = carrier liquid viscosity (Pa-s)

D = inside pipe diameter (m)

χ = fraction of eddies with velocities exceeding the hindered settling velocity of solids

Table 2-15. Comparison of Correlations to Experimental Critical Velocity Data

Correlation	Number of points in deviation band				Maximum % deviation
	< 20%	20 – 50 %	50 -100%	> 100%	
Oroskar*	437	302	118	7	164
Turian	535	260	65	4	123

* Based on equation (41) in Oroskar³²

2.2.4 Cho et al. Minimum Transport Velocity – Multiple Solids Components and Solids Densities

This article does not discuss sliding bed but is insightful for understanding the impact of particle size or density on behavior. There is very limited literature available on this subject matter. Cho et al.³⁴ (written in Korean) tested both different particle sizes and densities. The materials they used and their properties are provided in Table 2-16. The particles were fairly uniform for a given particle size and density. In one test, he blended the large and small sand at a volumetric ratio of 2 to 1 and the controlling parameter for critical velocity was the larger sand and was similar to the minimum transport velocity curve of the heavy sand itself (Figure 2-4). As the volumetric concentration increased, there was a slight reduction in the minimum transport velocity of the blend as compared to the large sand. Cho et al. then blended the two largest heavy sands with the smallest cast iron, where the case iron contained a large volume of the solids, and these results are shown in Figure 2-5. This data clearly shows that more dense cast iron material dictated the critical velocity in all cases. In the final blend, a 1 to 1 volumetric ratio of the 137 micron large sand and 137 micron cast iron was performed and the results are shown in Table 2-16. In this case, the equal volume blend of solids resulted in having a lower critical velocity as compared to the case of iron by itself and this difference increased as the concentration of the slurry increased. The correlation/method they utilized in calculating the minimum transport velocity seemed to work quite well based on how the calculated curves fit the experimental data. Detailed explanation cannot be provided, given the article is written in Korean and a translation was not readily available for this author. In 1991, Bea et al.³⁵ (a co-author on Cho et al. article) provided methods for determining the minimum critical velocity of blended solids based on the method utilized by Cho et al., but with an exception where the turbulent intensity is determined differently and can be calculated for pipe size ranging between 1.6 to 5.0

cm. Detailed knowledge of the blended material, such as density, particle size distribution, and concentration must be known to obtain average values. Three different methods were presented, where two of the methods emphasized the least transportable material; hence the largest critical velocities were calculated. The 3rd method is cumbersome, due to it being an iterative process. The interesting result from these articles is that a controlling variable seems to be the particle with one of the highest settling velocity. From a conservative point, one could treat each particle separately (assuming each has the same concentration) and the one that yields the greatest minimum velocity determines the operating conditions.

Table 2-16 Materials Used in Cho's Experiments³⁴

Material	Mean particle size (μm)	Size (Mesh and μm)	Density	Terminal Falling velocity (cm/s)
Heavy sand	230	-60 / +70 > 210 - < 250	2.634	2.41
	163	-80 / +100 > 149 - < 177		1.92
	137	-100 / +120 > 125 - < 149		1.37
	115	-120 / +150 > 105 - < 125		0.98
Cast Iron	163	-80 / +100 > 149 - < 177	5.233	3.49
	137	-100 / +120 > 125 - < 149	5.138	3.10
	96	-140 / +170 > 88 - < 105	5.185	1.95

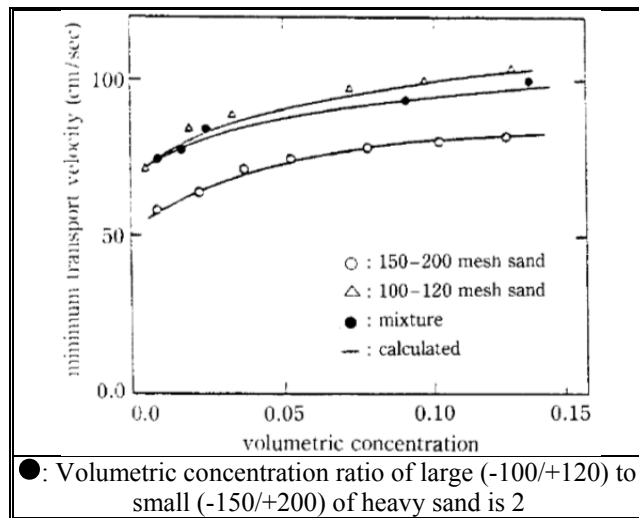


Figure 2-4. Critical Velocity versus Concentration of Large and Small Sand Blends³⁴

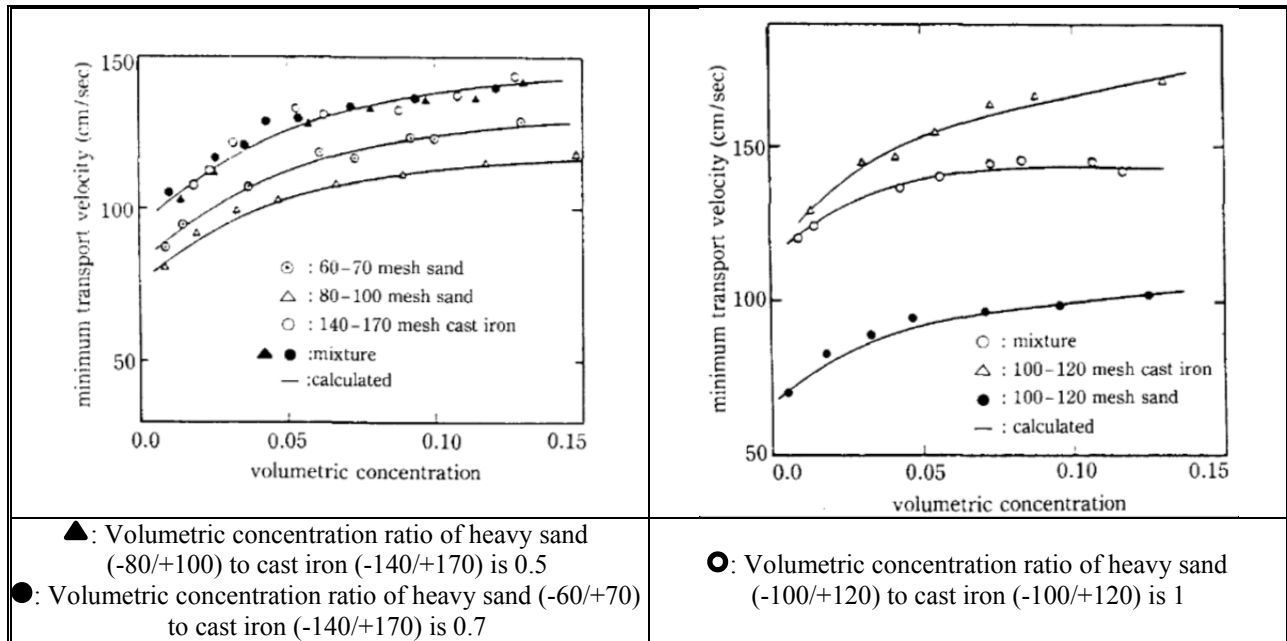


Figure 2-5. Minimum Transport Velocity versus Concentration of Heavy Sand and Cast Iron Blends³⁴

2.2.5 Critical Velocity – Small Particles and Their Effect

2.2.5.1 Parzonka et al.- 1981

Parzonka et al.³⁶ reviewed approximately 50 data sets of deposition velocity data. They defined the deposit velocity as the transition velocity between a heterogeneous suspension and heterogeneous suspension with a sliding bed and/or heterogeneous suspension with a stationary bed, given the difficulty at times to distinguish between the two by the various researchers. They divided their collated experimental data into five categories according to the type of solid and particle size range shown:

1. small size sand particles ($0.1 \text{ mm} < d < 0.28 \text{ mm}$),
2. medium size sand particles ($0.4 \text{ mm} < d < 0.85 \text{ mm}$),
3. coarse size sand and gravel ($1.15 \text{ mm} < d < 19 \text{ mm}$),
4. small size high density ($2.7 \text{ to } 5.3 \text{ g/cm}^3$) materials ($50 \text{ }\mu\text{m} < d < 300 \text{ }\mu\text{m}$), and
5. coal particles ($1 \text{ mm} < d < 2.26 \text{ mm}$).

The effects of solids concentration on the Durand and Condolios³⁷ dimensionless deposition velocity F_L at different mean particle diameters for a sand-water system with varying proportions of fine material is shown in Figure 2-6. This figure shows that without fines, F_L reaches a maximum when the volumetric fraction is in the range 0.1 to 0.15 and then remains almost constant. The presence of fine material (defined as $d < 75 \text{ microns}$ or 0.075 mm) causes F_L to decrease once it has passed its maximum value for a given concentration. Depending on the proportion of fine material present, the greater F_L falls with a greater proportion of fines and their effect is more pronounced as the large particle size decreases (see change in F_L ranging from the largest particle ($D_p=1.5\text{mm}$) to the smallest ($D_p=0.25\text{mm}$)). Parzonka et al. also include figures which provide guidelines for estimating F_L for very fine materials (such as iron ore) and coal. Parzonka et al. makes a statement that as the concentration approaches zero, F_L approaches 0.2 – 0.5. The impact of small micron size particles such as clays is not included in Figure 2-6 and they can cause the slurry to become non-Newtonian.

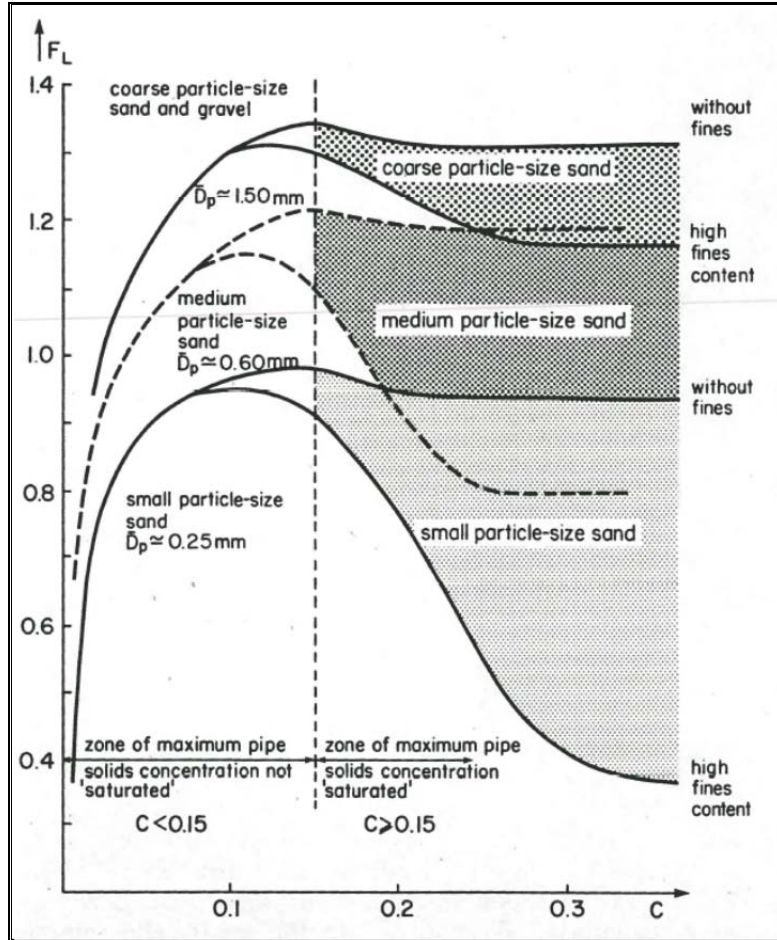


Figure 2-6. Overall Variation of the Dimensionless Deposition Velocity, F_L , with Solids Concentration and Particle Size for Slurries of Sand and Gravel in Water³⁶

2.2.5.2 Hisamitsu et al.- 1978

This article does not discuss sliding beds. Hisamitsu et al.³⁸ investigated the impact for concentrations of clay (mean particle size less than $1\mu\text{m}$) and limestone powder (mean particle size $7\mu\text{m}$) on the critical velocity of deposition and pressure loss of various sands of different particles sizes (200 to $800\mu\text{m}$). The clay volumetric percent ranged from 1.0 to 4.6 in the sand + clay and this mixture ranged from 9.5 to 25 volume percent, indicating a large fraction is sand. For the limestone powder, its volume percent ranged between 2.0 to 7.5 in the sand + limestone mixture ranged from 18 to 22 volume percent. The results showed that the clay reduced the critical velocity of deposition and pressure drop compared to processing just sand. This was not the case for limestone where the limestone did not impact the rheology in the same manner. The limestone slurry itself was Newtonian in behavior for all concentrations. It was shown that small particles do not necessarily affect the critical velocity of deposition in the same manner. This data supports Parzonka et al.³⁶ small fines assessment.

2.2.5.3 Warren, 1981

This article does not discuss sliding beds. Warren³⁹ investigated the critical velocity for fine glass particles with both narrow and broad particle size distribution of fine slurries ($d_{50} < 75 \mu\text{m}$). Warren defined the deposit velocity as the point of minimum pressure drop determined from a pressure drop versus flow curve. For the narrow particle size distribution, Warren utilized the 12 experiments with glass beads ($d_{50} = 12.5$ and $44.5 \mu\text{m}$) in water and pipes with pipe diameters ranging between 1.5 and 2.5 inches and obtained equation (3). Warren fitted 24 deposition velocities from Saskatchewan Research Council slurry flow data containing a broad particle size distribution of fine solids ($D = 2.056 - 12$ inch, $\rho_s = 1.441 - 5.245$, $d_{50} = 35 - 40 \mu\text{m}$, volume percent $C_v = 4.6 - 39.6$) resulting in equation (4). Warren compared both the narrow and broad particle size distribution deposit velocity with O-T equation (2) predictions and the O-T over-predicted the deposit velocity by 59%. It must be clear that the O-T equation (2) was not correlated using fine particles (less than $100 \mu\text{m}$); hence the use by Warren is outside of its fitted range, but does yield conservative values. Warren recommends using these equations with caution and the volume fraction of solids should be greater than 0.10.

$$V_{D,Narrow} = 1.90 \cdot \left(\frac{d}{D}\right)^{0.194} \cdot \sqrt{2 \cdot g \cdot D \cdot (S - 1)} \quad (3)$$

$$V_{D,Broad} = 0.694 \cdot \left(\frac{d}{D}\right)^{0.227} \cdot C_v^{-0.805} \cdot \sqrt{2 \cdot g \cdot D \cdot (S - 1)} \quad (4)$$

2.2.5.4 Cairns and Turner, 1958

Cairns and Turner^{40, 41} investigated the transport of submicron particles that were dense and where the volume percent was typically less than several percent. The density and particle size distribution (weight basis, equivalent to volume basis for a single type of material) of the solids are provided in Table 2-17. Water was used as the carrier fluid. Cairns and Turner measured transition velocities at the point where sliding beds first appear and when stationary beds appear for pipe diameter sizes $\frac{3}{4}$, 1, $1\frac{1}{2}$, and 2 inches. The data was regressed for both transition velocities. Equation (5) is for the sliding bed and equation (6) is for the stationary bed. Cairns and Turner⁴¹ then compared the deposition velocity for the UO_2 - NaK slurry data obtained by Abraham et al.⁴² and the results are comparable, even though the pipe diameter was outside of Cairns and Turner data set. The UO_2 - NaK test was performed using a 0.44 inch diameter tube with a UO_2 volume percent of 4.3 (equivalent to 36 wt. % in the slurry). Low volume fractions of solids seem to have little to no effect on the critical velocity and this is consistent with Parzonka et al.³⁶. Extrapolating this correlation to larger size pipe is questionable. Viscosity was not considered as a variable in developing the correlations but the deposition velocity works well with Abraham et al. results, where the carrier fluid was not water, but a molten salt. One of the solids that Cairns and Turner studied was tungsten, having a density of 19.3 g/cm^3 , something comparable to the small and most dense solids that could be in the Hanford waste streams, though the tested solid content is much higher. Cairns and Turner were very challenged in maintaining the tungsten in suspension in the mixing vessel.

Table 2-17 Materials Used in Cairns Testing^{40, 41}

Property		Material			
		Tungsten	Barium Sulfate	Red Lead	Talc
Density (g/cm ³)		19.3	4.5	9.1	2.7
		Particle Size - Microns			
Percent Under by Weight	100	15	20	29	52
	95	10	8.4	7.8	31
	85	7.9	6.1	4.4	24
	70	6.1	4.8	3.3	19
	50	4.8	3.7	2.3	15
	30	3.7	2.9	1.8	11
	15	2.8	2.3	1.4	8.4
	5	1.8	1.8	1.1	5.7
	0	1.0	1.4	0.96	2.4
wt. % in slurry		5.8 – 8.5	5.0 – 15.7	7.8 – 15.0	9.3 – 9.9
vol % in slurry		0.32 - 0.48	1.16 - 3.97	0.92 - 1.90	3.66 - 3.83
Moving Bed Velocity Range (ft/s)		3.06 – 3.17	1.55 – 1.97	2.04 - 2.57	1.37 – 1.62
Settled Bed Velocity Range (ft/s)		2.54 – 3.09	1.43 – 1.73	1.74 – 2.43	1.17 – 1.37

$$V_M = 1.9 \cdot (D)^{0.2}(S - 1)^{0.3} \quad (5)$$

$$V_T^{0.85} = 1.6 \cdot (D)^{0.2}(S - 1)^{0.3} \quad (6)$$

where V_M = Moving bed velocities (ft/s)
 V_T = Deposition bed velocities (ft/s)
 D = inside diameter (ft)
 S = Density ratio of solids to carrier fluid (unit less)

2.2.5.5 Thomas, 1979 – Viscous Sublayer Effect

Thomas⁴³ was concerned that the method used to determine the Durand's²⁵ function F_L in their sliding bed model was under-predicting F_L for particles smaller than 100 μm , resulting in a lower predicted critical deposition velocity in turbulent flow conditions. Thomas defined the critical deposition velocity as the velocity at which a stationary bed will appear at the bottom of the pipe. To correct for this deficiency in determining F_L , Thomas determined that the viscous sub-layer at the wall was the issue, where the turbulence was not present to support particle suspension. Hence the particles were sliding along the wall of the pipe in this viscous sub-layer. Thomas determined, from testing of 17 and 26 micron size sand in water and up to 12 volume percent solids, that if the maximum particles size was less than 0.3 times the thickness of the sub-layer and the particles are not flocculated, equation (7) is applicable. Thomas also assessed flocculated data where the particle size distribution were analyzed in quiescent conditions and determined that the conditions of turbulence in the pipe reduced the flocs to the individual particles that made up the floc. Thomas also provides a general equation to determine the critical deposition velocity for all particle sizes and this relationship is shown in Figure 2-7 for the case of silica sand in water. Figure 2-7 shows that larger particles require a larger critical velocity than smaller particles, given they are the same material. It also shows that as the pipe diameter gets larger, the larger particles critical velocity increase more than the smaller particles for a given pipe diameter. Finally, Thomas compared his critical deposition velocity predictions of the small and dense particles reported by Cairns⁴¹ and he states there is good agreement in determining the critical deposition velocity when using the d_{50} . If the friction factor is assumed to follow a power law approximation, Thomas provided equation (8), which is the same

as that provided in 24590-WTP-GPG-M-0058⁴. These equations are for particles sizes less than 100 μm and the particles smaller than 0.3 times the thickness of the laminar sub-layer

$$V_D = 1.1 \cdot \left(\frac{g \cdot \mu_f \cdot (\rho_s - \rho_f)}{\rho_f^2} \right)^{\frac{1}{3}} \quad (7)$$

$$V_D = 9.0 \cdot \left(\frac{g \cdot \mu_f \cdot \left(\frac{\rho_s}{\rho_f} - 1 \right)}{\rho_f} \right)^{0.37} \cdot \left(\frac{\rho_f \cdot D}{\mu_f} \right)^{0.11} \quad (8)$$

where: f = the pipe friction factor for the equivalent discharge of clear fluid

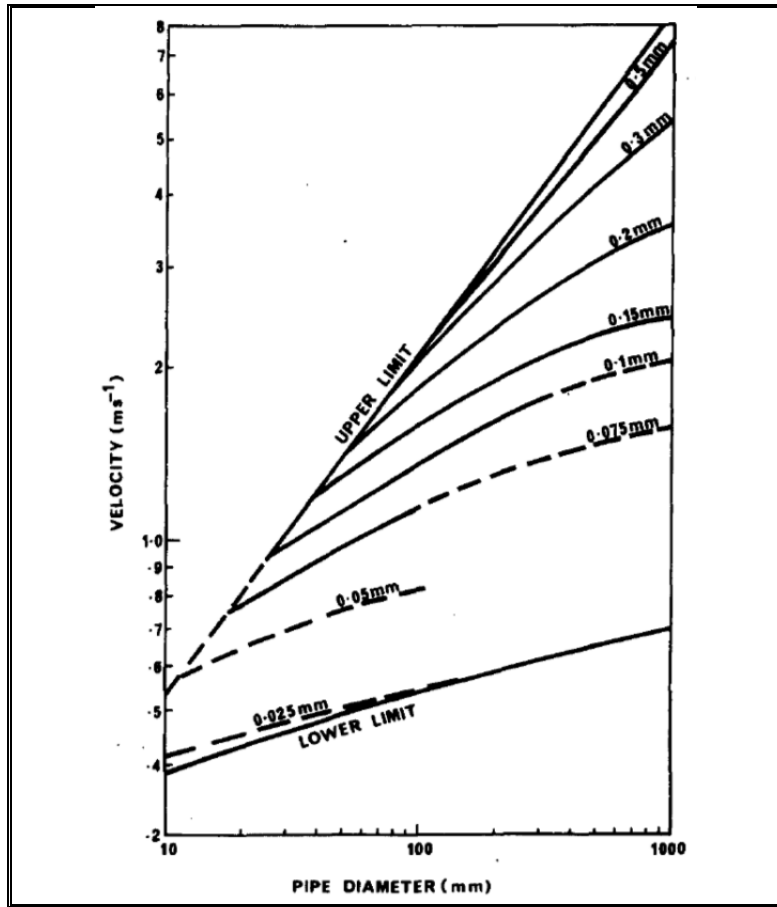


Figure 2-7 Predicted Deposition Velocity for Various Particle Sizes Below 0.5 mm for Silica Sand in 20°C Water⁴³

2.2.6 Pinto et al., Critical Velocity, 2014

This recent effort by Pinto et al.⁴⁴ addressed the issue of critical velocity for heterogeneous flow. The terms deposition velocity (V_D) and critical velocity of deposition (V_C) were noted in this article as terms

used rather loosely in literature due to a lack of a common agreed upon basis by the community. Pinto defined V_D and V_C as the same and as the velocity at which a moving bed of particles started to form (visually) on the bottom of the pipe and it was also the point of minimum pressure loss based on decreasing the velocity. The solid materials that were used and their properties and concentrations are shown in Table 2-18 and were tested using water in 25 and 50 mm diameter piping. Three different solid materials were used and two different narrow particle size of each material, denoted as Class-1 and Class-2 were used. The sphericity (shape) of the particles were reported and used to develop their correlation.

Table 2-18 Materials Used in Pinto's Testing⁴⁴

Solid Material	Sauter Mean diameter (microns)		Specific Gravity	Sphericity (Ψ)		Tested C_V (volumetric fraction)		
	Class-1	Class-2		Class-1	Class-2			
Quartz	265	132	2.62	0.80	0.81	0.14	0.20	0.27
Apatite	295	151	3.13	0.63	0.64	0.12	0.18	0.24
Hematite	336	163	4.9	0.39	0.37	0.08	0.12	0.17

In this article, the authors provide a new correlation for critical velocity given the results from their testing, equation (9). In this correlation, particle shape is considered but has a very low exponent, indicating it does little in contributing to the critical velocity. A decrease in particle sphericity will slightly increase the critical velocity.

$$V_C = 0.124 \cdot (S_S - 1)^{0.5} \cdot \left(\frac{d_S \cdot \rho_m \cdot \sqrt{g \cdot D}}{\mu_f} \right)^{0.37} \cdot \left(\frac{d_S \cdot \Psi}{D} \right)^{-0.007} \cdot e^{3.1 \cdot C_V} \quad (9)$$

where: S_S = relative density of the solid and slurry $\left(\frac{\rho_S}{\rho_m} \right)$

ρ_S = density of solid (kg/m³)

ρ_m = density of slurry (kg/m³)

d_S = particle Sauter mean diameter (m)

μ_f = fluid viscosity (Pa-s)

D = pipe inside diameter (m)

g = gravitational constant (m/s²)

Ψ = Particle sphericity

C_V = volumetric fraction concentration

Pinto et al. then compared the critical velocity measurements with other deposition velocity correlations provided in Table 2-19 and the results are shown in Figure 2-8. The results show that the deposition velocity correlations under predict the observed critical velocity. The Turian et al. equation (eq. 1) under predicts the critical velocity more than 25% in most cases. Note that Pinto et al. critical velocity was when a sliding bed first forms, different than Turian's or O-T definition. Attempts to duplicate the results using Turian et al.'s and O-T's equations (1) and (2) respectively with the data provided by Pinto et al., could not duplicate the results shown in Figure 2-8. This offset could be due to how Pinto et al. used their data in the critical velocity correlations listed in Table 2-19; they might not be the same values as reported in his paper. The other explanation is that Turian's and OT correlations are based on the critical velocity defined as that in which solids are deposited, which should predict a lower critical velocity than Pinto given that Pinto defined critical velocity as that when a sliding bed first occurs. Calculations using Turian's and O-T's equations (1) and (2) are provided in Table 2-20 using Pinot et al.'s data. All the predicted critical velocities were lower than the measured values, but not as low as Pinto et al. states.

Table 2-19 Correlation Used to Calculate Deposition Velocity⁴⁴

Researcher	Correlation
Durand ⁴⁵	$V_D = F_L \cdot \sqrt{2 \cdot g \cdot D \cdot (S - 1)}$
Wasp et al. ⁴⁶	$V_D = 4 \cdot \left(\frac{d}{D}\right)^{\frac{1}{6}} \cdot C_V^{0.2} \cdot \sqrt{2 \cdot g \cdot D \cdot (S - 1)}$
Turian et al. ³¹	$V_D = 1.7951 \cdot C_V^{0.1087} \cdot (1 - C_V)^{0.2401} \cdot \left(\frac{d_{95} \cdot \rho_f \cdot \sqrt{g \cdot D \cdot (S - 1)}}{\mu_f}\right)^{0.00179} \cdot \left(\frac{d}{D}\right)^{0.06623} \cdot \sqrt{2 \cdot g \cdot D \cdot (S - 1)}$
Schiller and Herbich ⁴⁷	$V_D = 1.3 \cdot C_V^{0.125} \cdot (1 - e^{-6.9 \cdot d}) \cdot \sqrt{2 \cdot g \cdot D \cdot (S - 1)}$
Wilson and Judge ⁴⁸	$V_D = 2.0 + 0.3 \log\left(\frac{d}{D \cdot C_D}\right) \cdot \sqrt{2 \cdot g \cdot D \cdot (S - 1)}$

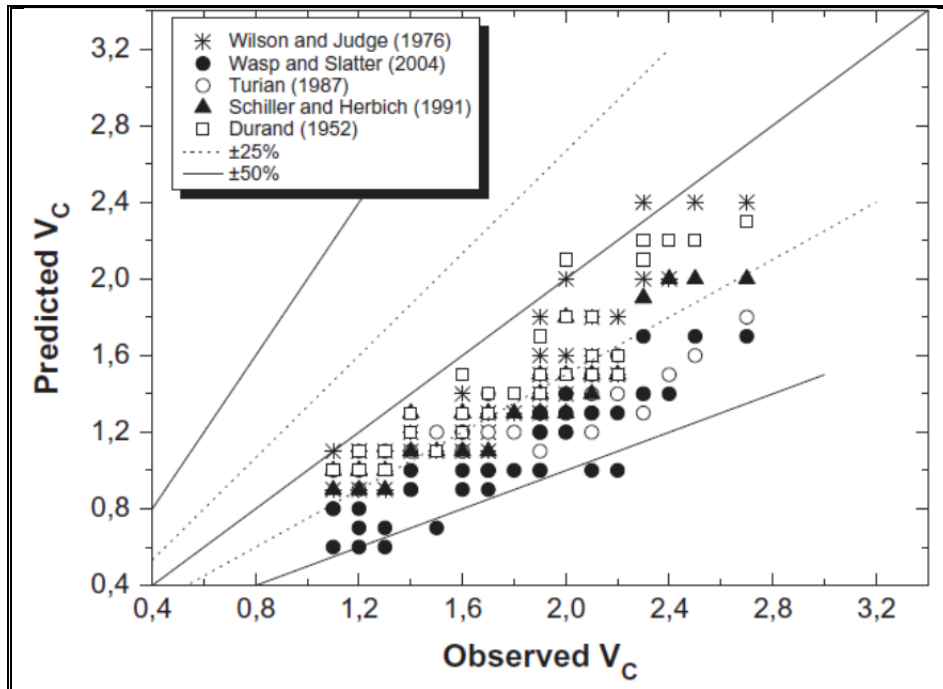


Figure 2-8 Comparison of the Predictive Critical Deposition Velocities with the Observed V_c⁴⁴

Table 2-20 Correlation Used to Calculate Deposition Velocity

Material	Density (g/cm ³)	Sauter Mean diameter μm	C_v (%)	Deposition Velocity (m/s)			Error in Prediction	
				Measured	Turian (eq. (1))	O-T (eq. (2))	Turian (eq. (1))	O-T (eq. (2))
Quartz	2.62	265	14	1.70	1.26	1.26	-26%	-26%
			20	1.90	1.29	1.29	-32%	-32%
			27	2.00	1.30	1.31	-35%	-34%
		132	14	1.30	1.20	1.12	-8%	-14%
			20	1.50	1.23	1.15	-18%	-23%
			27	1.70	1.24	1.17	-27%	-31%
Apatite	3.13	295	12	1.80	1.44	1.46	-20%	-19%
			18	2.00	1.48	1.52	-26%	-24%
			24	2.20	1.50	1.54	-32%	-30%
		151	12	1.50	1.37	1.31	-8%	-13%
			18	1.70	1.41	1.36	-17%	-20%
			24	1.90	1.43	1.38	-25%	-27%
Hematite	4.9	336	8	2.30	1.90	1.98	-17%	-14%
			12	2.30	1.96	2.08	-15%	-10%
			17	2.70	2.01	2.15	-26%	-21%
		163	8	1.90	1.81	1.76	-5%	-8%
			12	2.10	1.87	1.84	-11%	-12%
			17	2.30	1.91	1.90	-17%	-17%

2.2.7 Poloski et al., 2009(development of Stability Map)

Poloski et al.⁴⁹ performed tests to determine the critical deposition velocity, which is defined in this reference as the point where a fixed bed first starts to form for either the Newtonian and non-Newtonian slurries. Three types of solids were used and considered as course particles: (1) low: soda glass, 2.5 g/cm³, < 10 μm , (2) medium: aluminum oxide, 3.77 g/cm³, < 50 μm , and (3) high: 316L stainless steel (S/S), 7.95 g/cm³, 10 and 100 μm particles. Concentration of solids tested ranged between 16 and 45 wt %. Water was used for all tests. Results from this test indicate that the WTP method for estimating critical velocity (equation (2)) is conservative, but can be improved. All the measured critical deposition velocities, other than for the large 316L S/S particles, were below 6 ft/s. In all tests, a sliding bed or solids stratification towards the bottom of the pipe prior to achieving critical velocity were noted, but no details about when they occurred were provided. Poloski et al. recommend using the original basis of the Newtonian correlations (equation (2) that WTP utilizes in the design guide.⁴). Modification to the O-T equation without testing the underlying assumptions is not recommended, since no vetting with actual data has been performed. The O-T correlation is based on using the fluid properties, not the slurry properties for density and viscosity. Discussion about the non-Newtonian slurry studies by Poloski et al. are provided in section 2.3.6.

2.2.8 Pressure-Drop and Velocity Regions for Heterogeneous Flow

The terms deposition velocity and critical velocity at times are confusing, especially when data taken from one source is integrated with another and such definitive terms as deposition is replaced with critical or other terms. Much of the deposition velocity and critical velocity data has been obtained by visual observation of when the solids form a solid bed at the bottom of the pipe or by interpreting the pressure drop versus velocity curves for a heterogeneous flow and determining the minimum pressure drop.^{24,26,31,33,34,35,50,51,52} These two values are typically close to each other as shown in Figure 2-9, V_D is

when deposition occurs and V_{\min} is the minimum velocity in the pressure drop/flow curve. Some researchers have stated that the critical velocity is the point where the pressure drop is the minimum and past the point where sliding beds are present.^{28,53,44,54} Others⁵⁵ have stated the critical velocity is the point where either a sliding or stationary bed is present. It is the opinion of the author of this report that the deposition velocity or critical velocity is the point where solids form a settled bed at the bottom of the pipe based on the various correlations that have been reviewed, unless otherwise clearly stated (e.g., Pinto et al.⁴⁴). Prior to reaching the deposition velocity, a sliding bed could be present, given the properties of the solids and liquid. Cairns and Turner⁴¹ provided data that such conditions exist and the largest difference was approximately 0.2 m/s between the sliding bed and deposited bed velocities. Newitt et al.²⁴ state that a sliding or saltation bed exists above the deposition velocity and the difference in the velocity for onset (i.e., the delay, or higher velocity, before onset of sliding bed behavior) becomes larger as the critical velocity increases (Figure 2-1 and Table 2-11). Verkerk⁵⁶ performed testing using fly ash and gold slime where he noted a sliding bed prior to a settled bed. Crowe⁵⁷ provides a picture (Figure 2-10) showing the different solids concentration profile in the pipe between homogenous, heterogeneous, sliding bed, and settled bed conditions.⁵⁷

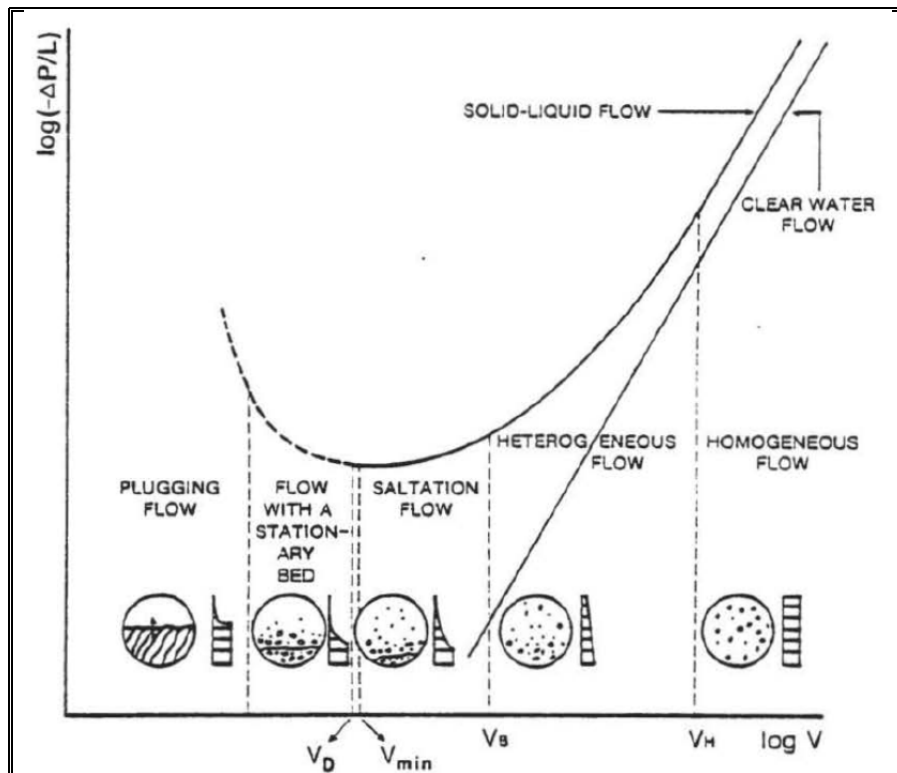


Figure 2-9 Representative Pressure Drop versus Flow Condition for Heterogeneous Slurry³⁹

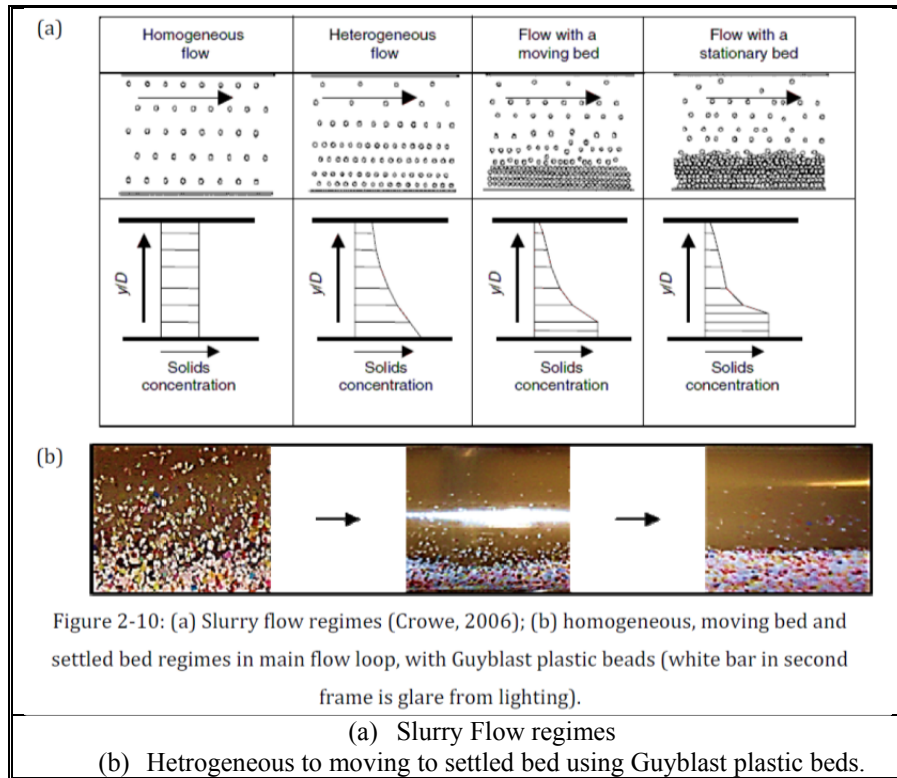


Figure 2-10 Settling Slurry Flow Regime⁵⁷

2.3 Regions of Solids Flow for non-Newtonian Slurries

2.3.1 *Thomas, 1978*

This article does not discuss sliding bed. Thomas⁵⁸ performed testing using china clay as the non-Newtonian carrier slurry with sand and coal as the coarse particles in a 105 mm pipe. One of the objectives was to better quantify the deposition of coarse particles during laminar flow for Bingham Plastic fluids. Figure 2-11 shows the results of using a fine sand (0.18 mm) and coarse sand (0.82 mm). The starting total percent volumetric concentration of solids for the fine sand + clay was 16.8% and coarse sand + clay was 18.5%. The variable C_m shown in Figure 2-11 is the clay concentration; hence when C_m decreases, the volume fraction of sand increases. For the fine sand, the addition of sand (note this is a large quantity) increases the pressure drop of the slurry, indicating an increase in the yield stress (that was not quantified). Additionally, a stationary bed was present for all the clays concentrations other than when clay concentration (C_m) was at its maximum concentration. The deposition velocity tends to decrease as the concentration of clay increases. For the coarse sand, only one concentration was examined and its pressure versus velocity response is similar to a Newtonian slurry response; after a minimum velocity is obtained, the pressure drop starts to increase as the velocity is reduced. Figure 2-12 shows the impact of adding the coal to the china clay. The size of the fine coal is 430 μm and the coarse coal is 2300 μm . Unlike the sand, the fine coal apparently reduced the yield stress of the slurry and slightly increased the yield stress for the coarse coal. Additionally, the impact on the deposition velocity of coal versus the rheological properties of the clay is not as significant. Thomas provides the rheological properties of the clay and some of the clay + sand blends in his report. The Bingham Plastic yield stress and plastic viscosity ranged between 1.25 and 6.5 Pa and 2.8 and 5.2 cP respectively for the clay only.

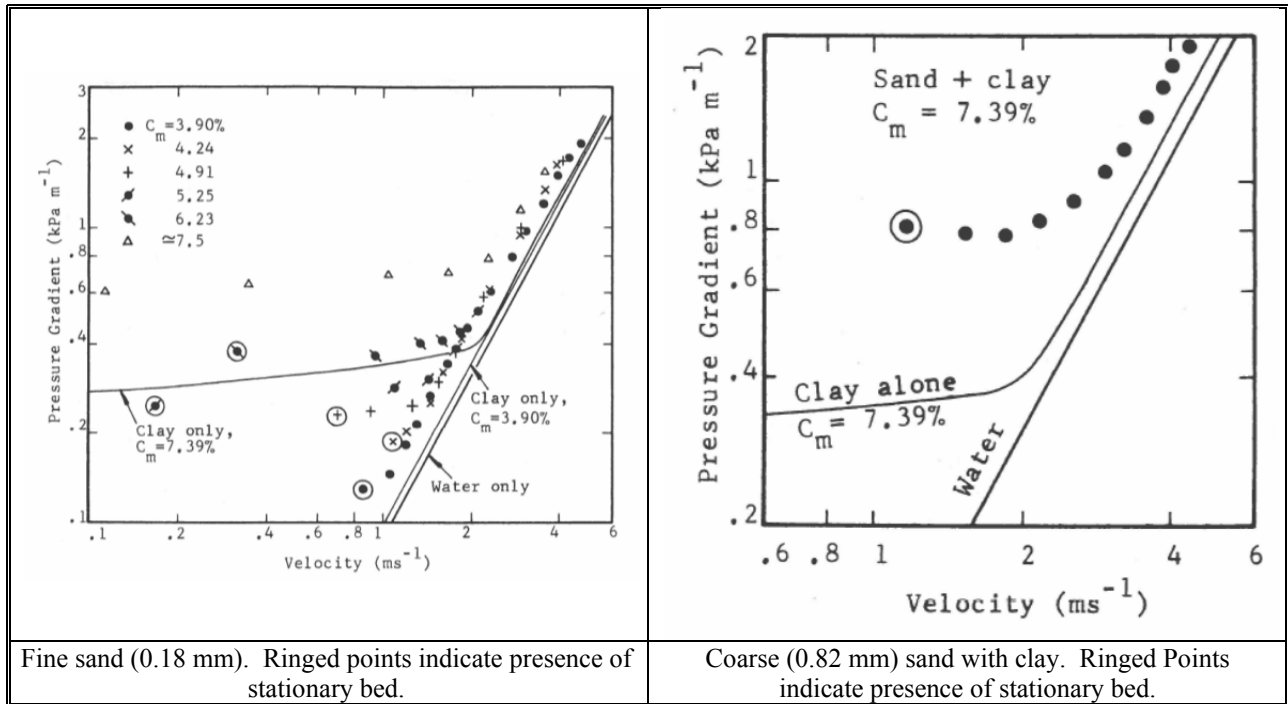


Figure 2-11 Settled Bed in Laminar Flow (China Clay and Sand) - Thomas⁵⁸

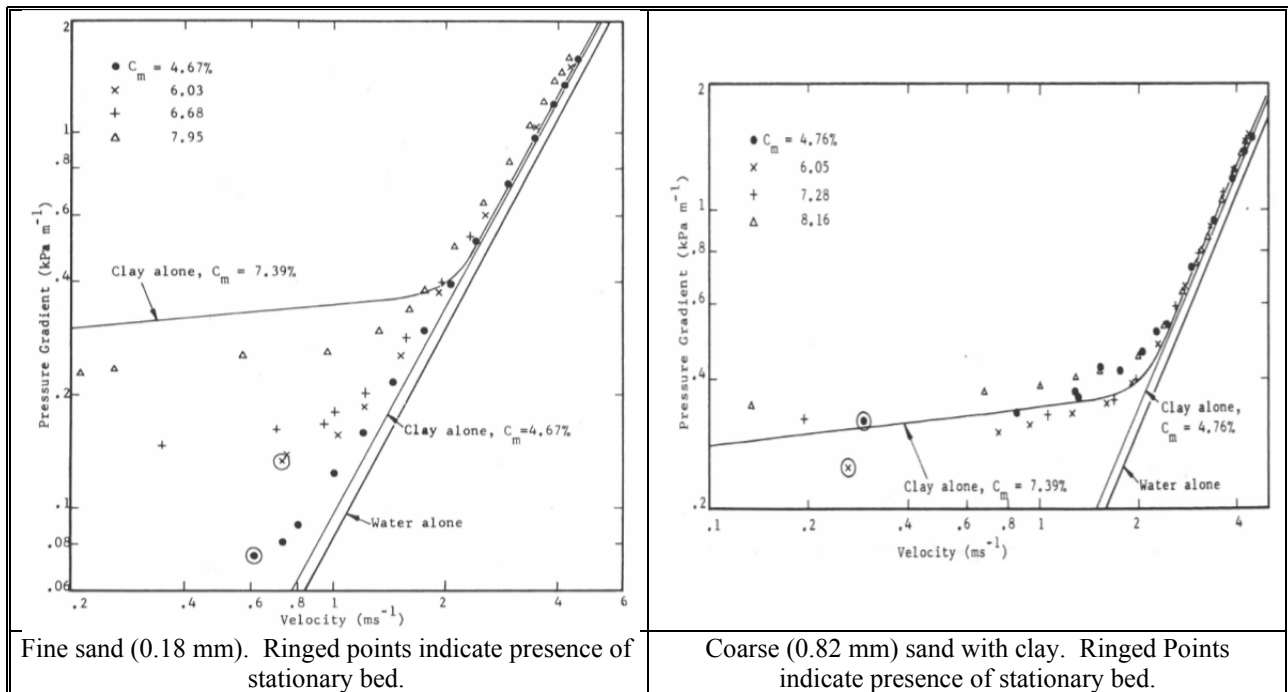


Figure 2-12 Settled Bed in Laminar Flow (China Clay and Coal) - Thomas⁵⁸

Thomas performed dimensional analysis for the deposition of solids and concluded it should be a function of concentration, density of the particle (ρ_p) and of the slurry (ρ_m), gravity (g), d_{50} (d) of the particle, inside diameter of the pipe (D), plastic viscosity (η_m), Bingham Plastic yield stress (τ_{om}), and wall shear

stress(τ_m), equation (10). He noted that velocity was not included because it is a function of multiple variables. He concluded that deposition was not affected by the dimensionless ratio D/d . His assessment showed that if the difference in the wall and Bingham Plastic yield stress was large, the last two variables in equation (10) can be plotted to provide a concentration for which solids would not settle in laminar flow. The results shown in Figure 2-11 and Figure 2-12 indicate that if the critical velocity (transition between laminar and turbulent flow) of the non-Newtonian properties is exceeded, settled beds were not observed.

$$f\left(\frac{D}{d}, C, \frac{\tau_m - \tau_{om}}{gd(\rho_p - \rho_m)}, \frac{d\sqrt{\rho_m(\tau_m - \tau_{om})}}{\eta_m}\right) = 0 \quad (10)$$

2.3.2 Shah and Lord, 1991

This article does not discuss sliding bed velocity. Shah and Lord⁵⁹ investigated the impact of using polymeric non-Newtonian solutions in determining both the critical deposition (V_D) and resuspension (V_S) velocities. In this study, critical deposition velocity is the velocity where solids are stationary at the bottom of the pipe and was determined by reducing the velocity until this behavior was achieved. The resuspension velocity was determined when the solids were picked up when increasing the flow. He utilized 20-40 mesh (630 μm) sand and 16-20 mesh (1016 μm) heavy weight ceramic (HWC) with a $SG = 3.25$ ranging from 0.15 to 0.31 volume fractions in 1.5 to 2.75 inch diameter pipe. Seven polymeric solutions were characterized as power-law fluids. Some have power law coefficient close to one, indicating they are similar to a Newtonian fluid while others were less than 0.5 and more non-Newtonian. Shah then took O-T's equation (2) and generalized it to equation (11). The turbulence function was eliminated because it contributes little and he added power law constants that were obtained via regression. For each fluid type, the fit was different, indicating a dependency on rheology.

$$\frac{[V_D] \text{ or } [V_S]}{\sqrt{g \cdot d \cdot (S - 1)}} = Y \cdot C_V^{0.1536} \cdot (1 - C_V)^{0.3564} \cdot \left(\frac{D \cdot \rho_f \cdot \sqrt{g \cdot d \cdot (S - 1)}}{\mu_a}\right)^Z \cdot \left(\frac{d}{D}\right)^{-W} \quad (11)$$

where: μ_a = the apparent viscosity at the point of deposition or re-suspension
 $Y, Z,$ and W = constants determined for each fluid via regression

The results from his tests showed that the re-suspension velocity was always greater than the critical velocity and this was also found for the case where he used only water and sand. The critical deposition velocities for all the polymeric solutions were less than that of the water only. Shaw concludes that the critical deposition velocity is dependent on pipe size, especially for the less viscous fluids. As the rheological properties increase the effect of pipe size is less. The range of particle concentration tested seemed to have little effect on the critical velocity and the particle size had no effect on the critical velocity. Finally Shaw stated that critical deposition velocities corresponded to the laminar or near-laminar flow condition based on a critical Reynolds number of 2100.

2.3.3 Song and Chiew, 1991

This article does not discuss sliding bed velocity. Song and Chiew⁶⁰ used a non-Newtonian clay carrier fluid with d_{50} of 150 μm sand in a rectangular duct (18 cm wide by 10 cm high). Seven different concentrations (0.018 to 0.088 volume fraction) of clay slurries (mean particle size 4.5 μm) were used, where the Bingham Plastic yield stresses ranged between 0.022 and 2.743 Pa and corresponding plastic viscosities of 1.27 to 3.95 cP. The volumetric solids concentration fraction of the sand ranged between

0.13 and 0.22. Results showed that as the velocity, V , increased from a no flow condition, solids start to migrate to the bottom of the duct due to the shearing at the surface of the duct (and eventually the interface of the settled bed and slurry) is the greatest. The solids continued to drop out of the slurry until they reached a maximum solids deposition height, at which time the velocity has sufficient turbulence to maintain the solids in suspension. Further increases in flow rate increase the level, h , of turbulence and fluid starts to pick up the solids that have settled. This can be seen in Figure 2-13 for a given fluid rheology and three different solids concentration. This was not the case for fluids which did not have sufficient Bingham Plastic yield stress to mitigate the sand from settling at no flow conditions, hence settling was observed prior to starting the test. This data shows that solids settle as the shear rate increases, but there is a point where they start to become resuspended, completely. Song and Chiew do not describe the condition of flow in this article during the settling and resuspension (e.g., flow laminar, turbulent, transitional velocity, etc.) transition points. They make no mention of a sliding bed prior to deposition or resuspension of solids on the rectangular duct used in the experiments.

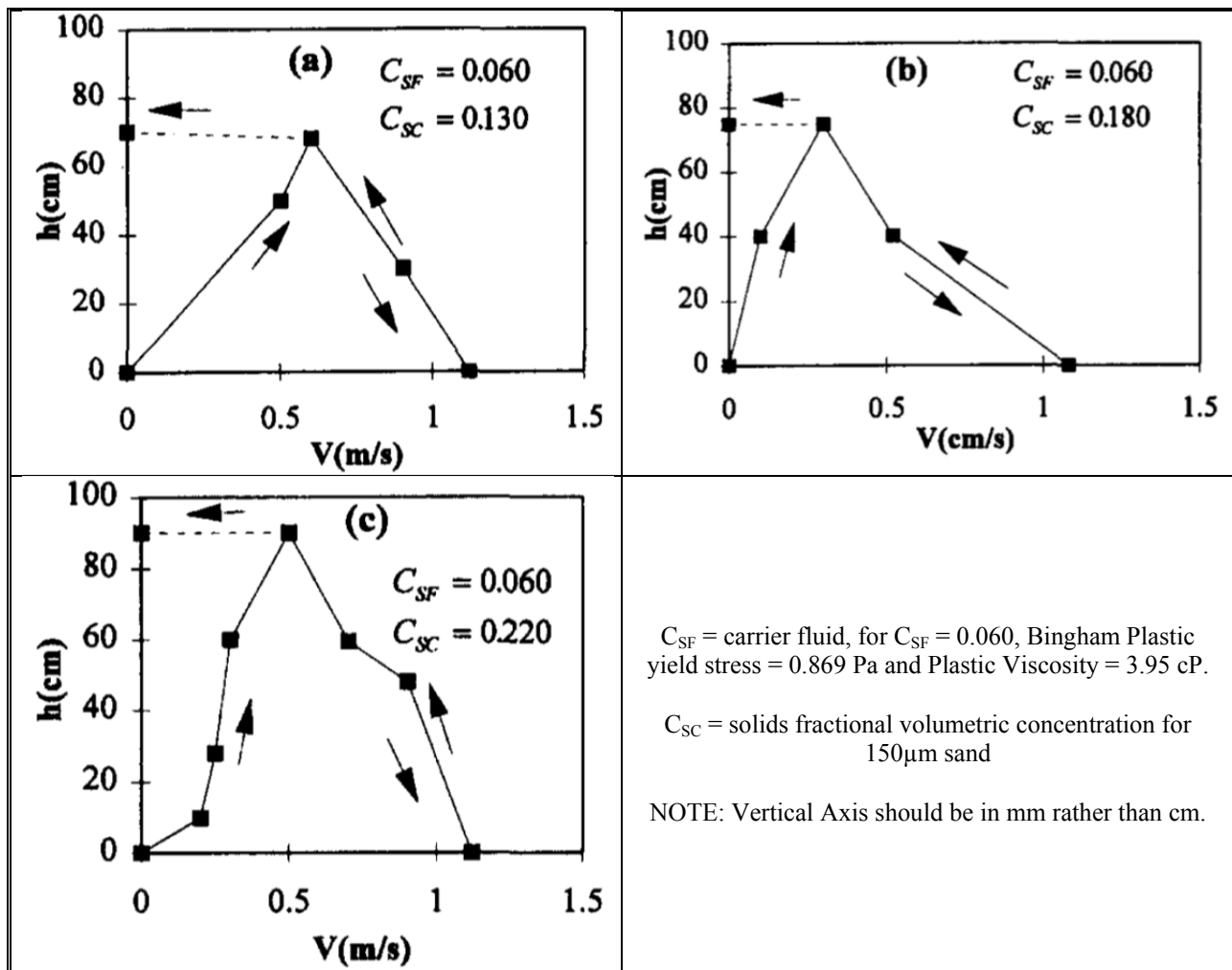


Figure 2-13 Thickness Relationships between Thickness of Coarse Particle Deposition h and Cross-sectional Velocity V for Various Solids Concentration and Fixed Fluid⁶⁰

2.3.4 Thomas, 1961

Thomas⁶¹ investigated the minimum transport velocity for flocculated suspensions or in other words, non-Newtonian slurries. In this study he used kaolin and two different sources of thorium oxide and their properties are provided in Table 2-21. Thomas⁶¹ does not provide the rheological properties of the kaolin and ThO₂ used in this study, but notes that their rheological data was obtained from a tube rheometer and modeled as a Bingham Plastic fluid for 0.01 to 0.17 volume fraction solids.

Table 2-21 Properties of Material Used in non-Newtonian Slurries⁶¹

Material	Particle Mean Diameter, D _p , (μm)	Density (g/cc)	Nitrogen Surface area, (m ² /g)	Settling Rate in water, (ft/s)
ThO ₂ – I	2.0	10.0	14.0	6.6 x 10 ⁻⁵
ThO ₂ – II	0.74	10.0	18.0	9.0 x 10 ⁻⁶
Kaolin	2.85	2.65	7.6	1.3 x 10 ⁻⁴

During the experiments, Thomas⁶¹ determined the minimum transport velocity, which is the transition velocity between laminar and turbulent flow, and was where the suspension was being transported by saltation. The sliding bed velocity was determined when a continuous filament of sliding bed was observed. Testing was performed using 1", 2" and 4" piping and these observations were made in the clear glass sections of piping. The results for the kaolin are provided in Figure 2-14. As the kaolin concentration increases, it parallels the minimum transport velocity and then tapers away. Thomas⁶¹ then goes on to state what other researchers have observed, the yield stress is the primary factor affecting the transition velocity between laminar and turbulent flow as the fluid become more non-Newtonian, such that the minimum transport velocity and transition velocity are the same (see Figure 2-15) and is somewhat insensitive to either pipe size or plastic viscosity as shown. For the very low yield stress values, Thomas⁶¹ provides another method to determine the critical velocity and relates these slurries to that of Newtonian slurries. To convert the units of yield stress in Figure 2-15 from lbf/ft² to Pa, multiply by 47.88. Finally, Thomas⁶¹ states the method proposed by Durand²⁵ to determine the minimum transport velocity under-estimates the velocity. Thomas⁶¹ provides his method to determine the minimum transport velocity, which also under-estimates the measured values and recommends using a multiplier of 1.6 (based on his data) to 4.0 (based on heat transfer relation). Both methods are provided in Table 2-22.

Thomas⁶¹ further explains the reasoning for the formation of the sliding bed in laminar flow is due to particles of near colloidal dimensions sticking together to form loose and irregular clumps of flocculated particles. For slurries that settle under hindered settling conditions, the flocs appear to settle as more or less discrete clumps, under compaction. Highly flocculated suspensions may be in compaction for volume solids fractions as low as 0.05, unlike that of non-interacting slurries having a solids volume fraction of 0.6. Thomas⁶¹ performed settling tests using various diameter settling tubes and determined that for sufficiently dilute concentrations of colloidal solids, the settling rate was independent of tube size. In the case where compaction occurred (hindered settling), the setting rate decreased sharply to a value one-tenth to one-fiftieth for a given critical concentration. Thomas⁶¹ was able to correlate the compaction concentration to that of the minimum transport velocity. This was observed in all solids tested.

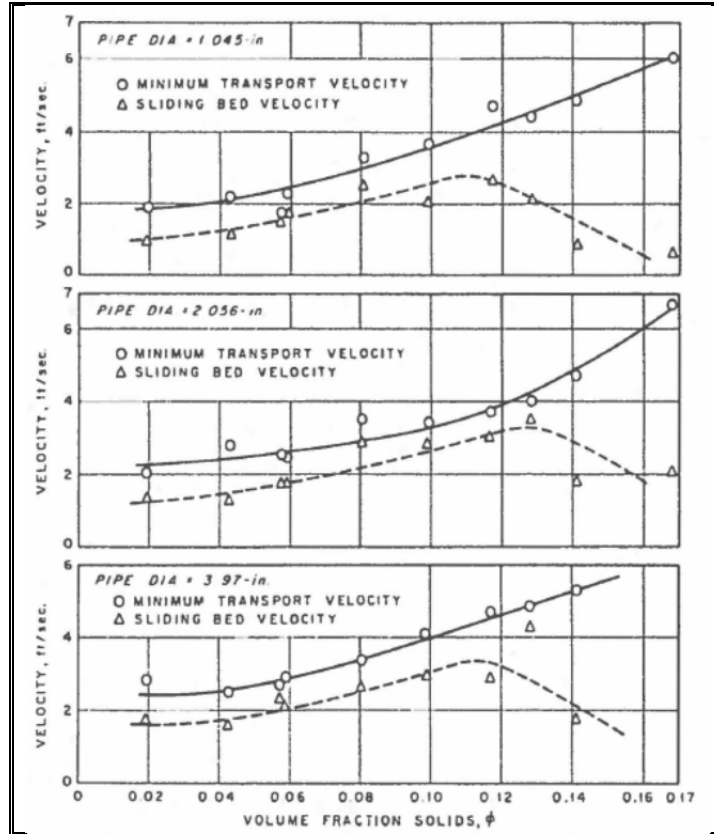


Figure 2-14. Effect of Suspension concentration on minimum transport and initial sliding velocities on Kaolin-water suspensions⁶¹

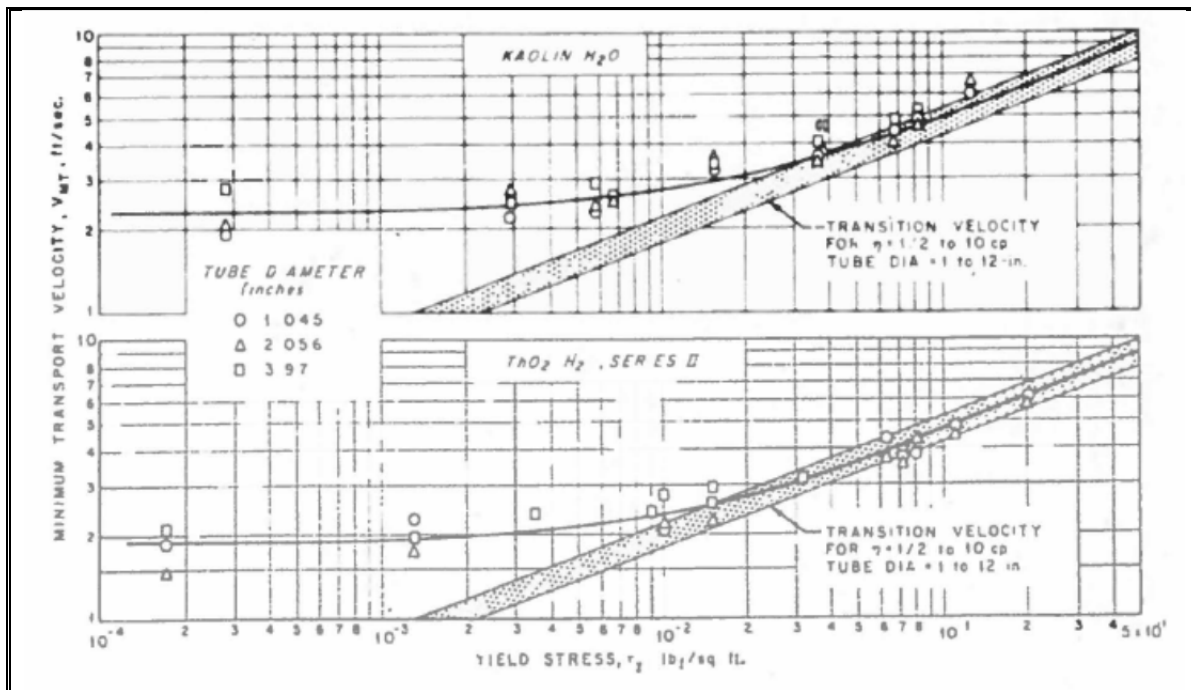


Figure 2-15. Effect of Yield Stress on Minimum Transport Velocity⁶¹

Table 2-22 Steps to Calculate the Critical Deposition Boundary by Thomas⁶¹

Durand's Method	Thomas's Method
$\frac{DV_{MT}\rho}{\mu_e} = \frac{DV_{MT}\rho}{\eta \left[1 + \frac{g_c D \tau_y}{6\eta V_{MT}} \right]} > 2,000$	1. Calculated Hedstrom number: $N_{He} = \frac{g_c D^2 \rho \tau_y}{\eta^2}$ Identify its location on a fanning friction factor-Reynolds number $\left(\frac{DV\rho}{\eta}\right)$ plot containing the Hedstrom number grid as a parameter. See reference ⁶² for curve and instructions.
	2. Locate the turbulent-flow friction-factor line on the same plot by $f = 0.079 \left(\frac{\mu}{\eta}\right)^{0.48} (N_{Re})^{-0.25} \left(\frac{\mu}{\eta}\right)^{0.15}$
	3. The intersection of these two curves give the critical Reynolds number $\left(\frac{DV\rho}{\eta}\right)$ for the onset of transition flow.
Where: V_{MT} = minimum transport velocity D = pipe inside diameter ρ = density of slurry η = plastic viscosity g_c = conversion factor τ_y = Bingham Plastic yield stress μ = viscosity defined in reference 62	

2.3.5 Thomas et al., 2004

Thomas et al.⁶³ provides a historical review of stabilized laminar flow at that point in time. In an unpublished report, a homogeneous non-Newtonian slurry at the discharge of a pump with a 25 Pa yield stress containing 2000 μm sand is visually observed 15 diameter lengths downstream of a pump and shown in Figure 2-16, starting at time t = 0. Initially a central core is present, but once the solids start to settle and form a bed, the process accelerates. At 10 seconds, a defined bed is present and it continues to grow as time progresses, to the point where the solids are transported as a sliding bed with clear fluid at the top. The radial velocity profile for this slurry is shown in Figure 2-17, showing the region of the sliding bed and the effect of velocity reducing the bed height for various pipe velocities where sliding beds were present. The same types of flow patterns observed in the Newtonian case are present in the non-Newtonian case, though the regions of flow are different. Thomas et al. makes a statement that even in fine-sand slurries, it can be expected that particles that settle in a laminar flow will move as a sliding bed, typically resulting in a high pressure gradient. He also states that the use of sliding bed transfer for such non-Newtonian slurries still have advantages for relatively short transport distances, hence should not be excluded.

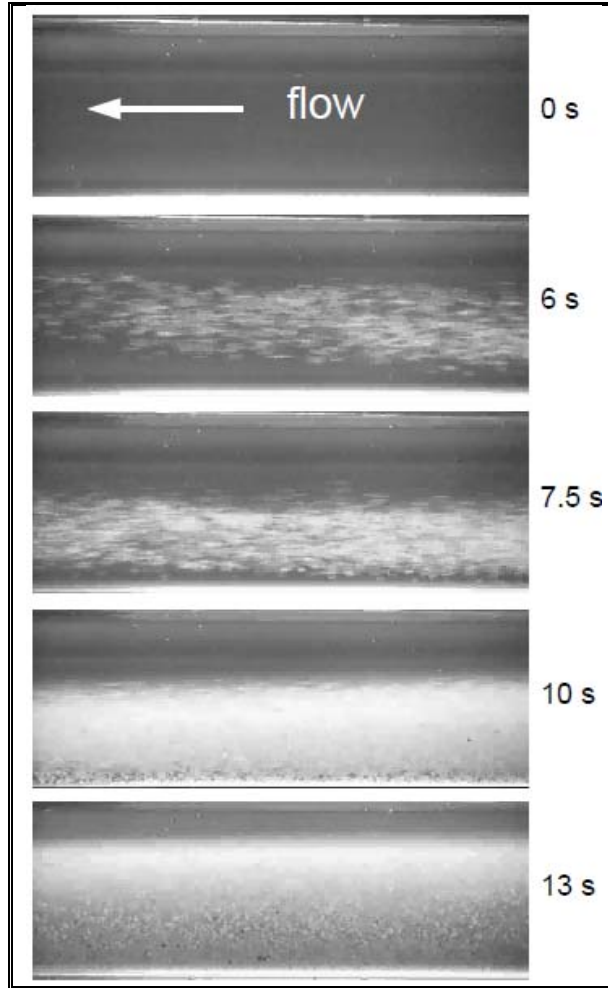


Figure 2-16 Stills Taken from Video of Settling in a non-Newtonian Fluid⁶⁴

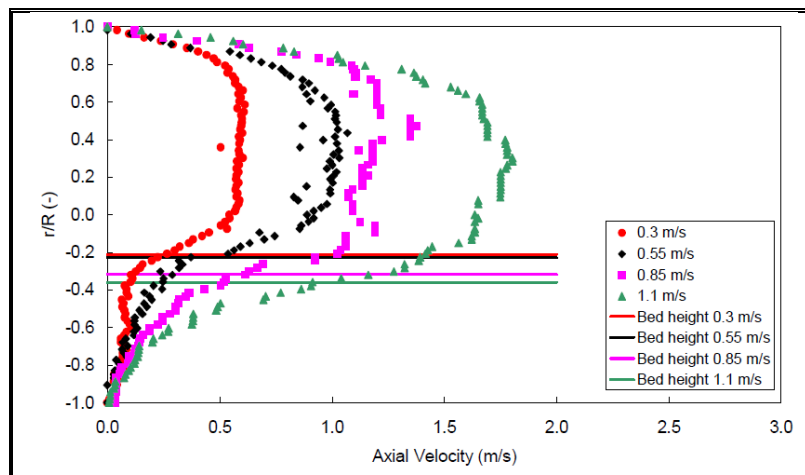


Figure 2-17 Fluid Axial Profile Image Showing a Sliding Bed⁶⁴

2.3.6 Poloski et al., 2009 (development of Stability Map)

Poloski et al.⁴⁹ performed tests to determine a method that can be utilized to determine the critical deposition velocity for non-Newtonian fluids. In this document, the critical deposition velocity is defined as the point where a fixed bed first starts to form for either the Newtonian and non-Newtonian slurries. The Newtonian discussions are in section 2.2.7. The non-Newtonian fluids used in developing the model were kaolin slurries, modeled using either the Bingham Plastic or Casson rheological models. Poloski states the following based on an assessment performed by Wells et al.⁶⁵ of the Hanford Tank Farm insoluble solids. Particles less than 3 μm can be considered fines. The range of sizes spanning 3 to 10, 10 to 50, and 50 to 100 μm can be considered “Low,” “Medium,” and “High” particle sizes, respectively. From the cumulative size distribution, the fines are about 30% of the particles, the “Low” size particles are about 40% of the particles, “Medium” size particles are about 25% of the particles, and “High” size particles are about 5% of the particles by volume.” Coarse particles – soda glass, aluminum oxide and 316L stainless steel particles as described in section 2.2.7 – were added to the kaolin slurries, resulting in total solids ranging from 32.4 wt % to 54.3 wt %. The coarse solids consisted between 20 to 44.5 wt. % of the total slurry, something that is most likely very non-representative of the actual waste mass fraction of such solids. Based on the Bingham Plastic model, the yield stress ranged clustered around 3.2 and 6.5 Pa with corresponding plastic viscosities between 4.3 – 7.3 cP and 7.7 – 12.4 cP respectively for each cluster. Both the Casson yield stress and infinite shear viscosity were lower than the Bingham Plastic properties. The model developed generated a stability map (Figure 2-18) using either the Bingham Plastic or Casson rheologically regressed data, the solids average physical properties of the particles, and that of the fluid. During their testing, they noted a layer of sliding or saltation solids developing prior to reaching the critical velocity but did not provide information on the velocities.

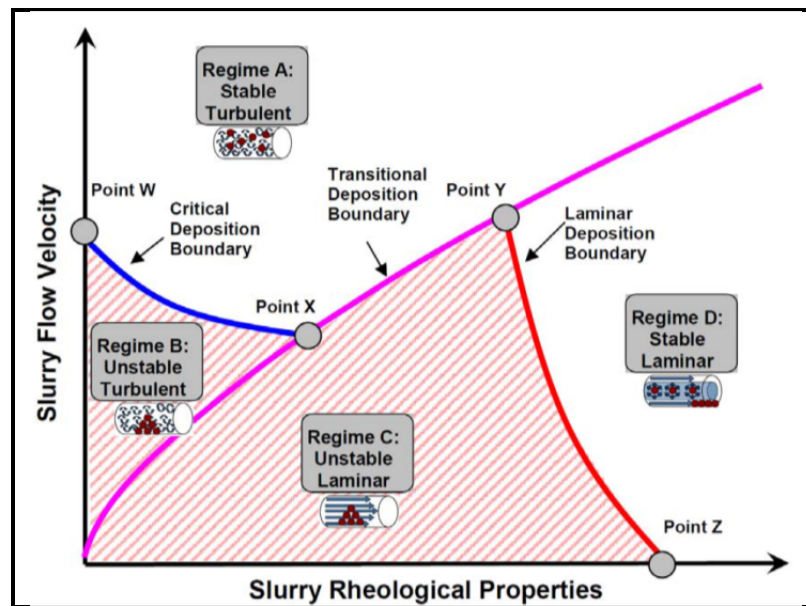


Figure 2-18. Slurry Stability Map⁴⁹

Areas of unstable turbulent and laminar regions were defined in areas where settling could occur in the pipeline when processing at those specific line velocities, as shown in the shaded areas in Figure 2-18. The critical deposition velocity is determined as shown in Table 2-23. The transition deposition velocity (which is the transition between laminar and turbulent flow) is determined as shown in Table 2-24. Finally the laminar deposition velocity (the velocity given the wall shear stress for a given pipe velocity) is determined as shown in

Table 2-25. Poloski also recommends flushing using water at 10 ft/s to remove the solids from the piping.

Table 2-23 Steps to Calculate the Critical Deposition Boundary⁴⁹

Calc. step	Bingham Plastic Fluid	Casson Fluid
(1)	$Ar = \frac{4gd^3(S-1)\rho_f}{3\mu_B^2}(1-\xi)^2 = Ar_\infty(1-\xi)^2$	$Ar = \frac{4gd^3(S-1)\rho_f}{3\mu_C^2}\left(1-\xi^{\frac{1}{2}}\right)^4 = Ar_\infty\left(1-\xi^{\frac{1}{2}}\right)^4$
(2)	$540 < Ar \rightarrow Fr = 1.78Ar_\infty^{-0.019}(1-\xi)^{-0.038}$ $160 < Ar < 540 \rightarrow Fr = 1.19Ar_\infty^{0.045}(1-\xi)^{0.09}$ $80 < Ar < 160 \rightarrow Fr = 0.197Ar_\infty^{0.4}(1-\xi)^{0.8}$ $Ar < 80 \rightarrow Fr = 0.59Ar_\infty^{0.15}(1-\xi)^{0.3}$	$540 < Ar \rightarrow Fr = 1.78Ar_\infty^{-0.019}\left(1-\xi^{\frac{1}{2}}\right)^{-0.076}$ $160 < Ar < 540 \rightarrow Fr = 1.19Ar_\infty^{0.045}\left(1-\xi^{\frac{1}{2}}\right)^{0.18}$ $80 < Ar < 160 \rightarrow Fr = 0.197Ar_\infty^{0.4}\left(1-\xi^{\frac{1}{2}}\right)^{1.6}$ $Ar < 80 \rightarrow Fr = 0.59Ar_\infty^{0.15}\left(1-1-\xi^{\frac{1}{2}}\right)^{0.6}$
(3)	Wall shear stress for Bingham Plastic described in section A.7 and for Casson section A.8 ⁴⁹	
(4)	$V_C = Fr\sqrt{gD(S-1)}$ Where: μ_B = Plastic Viscosity μ_C = Infinite Shear Viscosity ξ = ratio of fluids yield stress (Bingham Plastic or Casson) divided by the wall shear stress	

Table 2-24 Steps to Calculate the Transition Deposition Boundary⁴⁹

Calc. step	Bingham Plastic Fluid	Casson Fluid
(1)	$He = \frac{D^2\rho_f\tau_B}{\mu_B^2}$	$Ca = \frac{D^2\rho_f\tau_C}{\mu_C^2}$
(2)	$Re_t = \frac{DV_t\rho_f}{\mu_B} = 1050\left(1 + \sqrt{1 + \frac{He}{4500}}\right)$	$Re_t = \frac{DV_t\rho_f}{\mu_C} = 1050\left(1 + \left(1 + \frac{Ca}{4500}\right)^{0.4}\right)$
(3)	Solve for V_t	

Table 2-25 Steps to Calculate the Laminar Deposition Boundary⁴⁹

Calc. step	Bingham Plastic Fluid	Casson Fluid
(1)	$\tau_p = \frac{(\rho_s - \rho_f)gd}{6}, \alpha = \frac{\tau_w}{\tau_p}, \xi = \frac{\tau_y}{\alpha\tau_p}$	
(2)	$\tau_{W,B}$ section A.7 ⁴⁹	$\tau_{W,C}$ section A.8 ⁴⁹
(2)	$V = \left(\frac{D}{8}\right)\left(\frac{\alpha\tau_p}{\mu_B}\right)\left(1 - \frac{4}{3}\frac{\tau_B}{\alpha\tau_p} + \frac{1}{3}\left(\frac{\tau_B}{\alpha\tau_p}\right)^4\right)$	$V = \left(\frac{D}{8}\right)\left(\frac{\alpha\tau_p}{\mu_B}\right)\left(1 - \frac{16}{7}\sqrt{\frac{\tau_C}{\alpha\tau_p}} + \frac{4}{3}\frac{\tau_C}{\alpha\tau_p} - \frac{1}{21}\left(\frac{\tau_C}{\alpha\tau_p}\right)^4\right)$

2.3.7 Poloski et al., 2009

Poloski et al.⁶⁶ performed additional tests to cover a much larger range of non-Newtonian properties using two different types of slurries. The simulant slurries were tested, starting with the highest rheology and then diluting with liquid to obtain the lower solids concentrations. The first simulant was a physical simulant where the fines were kaolin and the coarse particle were glass beads having a nominal 150 μm diameter (no distribution provided), each having a density of 2.5 g/cm³. The physical properties (wt % kaolin, wt % glass beads, and Casson and Bingham Plastic rheological properties) of the kaolin slurries are provided in Table 2-26. The second simulant was a precipitated HLW simulant based on the HLW AZ-101 simulant developed by Eibling⁶⁷. Table 2-26 contains the wt % UDS, wt % supernate, and Casson and Bingham Plastic rheological parameters of HLW AZ-101 simulants. Additional supernate, of similar composition to the HLW AZ-101 simulant supernate, was necessary to dilute the AZ-101 sludge to targeted values shown in Table 2-26. There was no information provided about what the average density of the UDS in the HLW AZ-101 slurry. The volumetric particle size distribution for the kaolin and AZ-101 slurries are provided in Table 2-27 and were based on averaging the data from the samples pulled for each concentration. Poloski visually observed deposition velocities (when the solids formed a stationary bed) and the sliding beds (but did not state the width and/or height of the bed) and plotted these velocities on the transition deposition curve as shown in Figure 2-19. These figures, based on Poloski's observations of the two types of slurries, yielded the same type of results. For these data sets, sliding beds were present for the complete range of yield stresses and after approximately 12 Pa yield stress, the yield stress of the fluid was large enough that no observed settling occurred as observed in Figure 2-19. Sliding beds were present prior to reaching the critical velocity. Additionally, for low yield stress (less than 5 Pa), the sliding bed was observed before the deposition velocity was observed, consistent with findings from other researchers^{40,44,63}. This data also shows that increased pressure reading due to deposited beds was not measured until the Casson yield stress fell below 7 Pa. Samples of the sliding bed were not obtained to determine its composition and particle size distribution, which might have provided additional insight of the solids that formed the sliding bed.

Table 2-26 Physical Properties of Slurries Used to Determine Sliding Bed Region⁶⁶

Kaolin and Sand						AZ-101 Simulant					
wt %		Casson		Bingham Plastic		wt %		Casson		Bingham Plastic	
Kaolin	Sand	YS (Pa)	ISV (cP)	YS (Pa)	PV (cP)	UDS	Super-nate	YS (Pa)	ISV (cP)	YS (Pa)	PV (cP)
34.5	16.5	31.0	3.2	36.9	18.2	20.1	3.4	28.0	3.3	33.2	18.7
29.9	14.3	16.6	1.9	19.8	10.9	18.0	3.3	18.6	3.2	22.7	15.5
28.1	13.5	13.1	1.9	15.8	9.6	17.3	3.4	12.8	2.5	15.9	11.5
25.7	12.3	9.8	1.8	12.1	8.3	15.5	3.3	7.5	2.0	9.6	8.1
24.4	11.7	8.8	1.7	11.0	7.8	14.6	3.5	5.1	2.1	6.9	7.3
23.6	11.3	6.7	1.7	8.5	7.0	13.5	3.6	2.6	2.5	4.0	6.6
20.7	9.9	3.7	1.7	5.0	5.7			3.1*	2.3*	4.6	6.6
19.2	9.2	2.6	1.6	3.7	5.0	12.1	3.6	0.9*	2.2*	1.5	5.2
19.0	9.1	1.5	1.6	2.3	4.7						
19.6	9.4	0.3	2.1	0.7	3.9						

* Anti-foam agent used in final two tests due to air entrainment issues.
YS = Yield Stress, ISV = Infinite Shear Viscosity, PV = Plastic Viscosity

Table 2-27 Averaged Volumetric Particle Size Distribution of Slurries Used to Determine Sliding Region⁶⁶

Slurry	Volumetric Particles Size Distribution										
	d ₅	d ₁₀	d ₂₀	d ₃₀	d ₄₀	d ₅₀	d ₆₀	d ₇₀	d ₈₀	d ₉₀	d ₉₅
Kaolin	0.6	1.1	2.3	3.6	5.1	7.1	9.9	14.5	25	105.8	167.0
AZ-101 Sludge	0.4	0.6	1.0	1.4	2.2	3.6	5.4	8.3	14.6	42.1	72.4

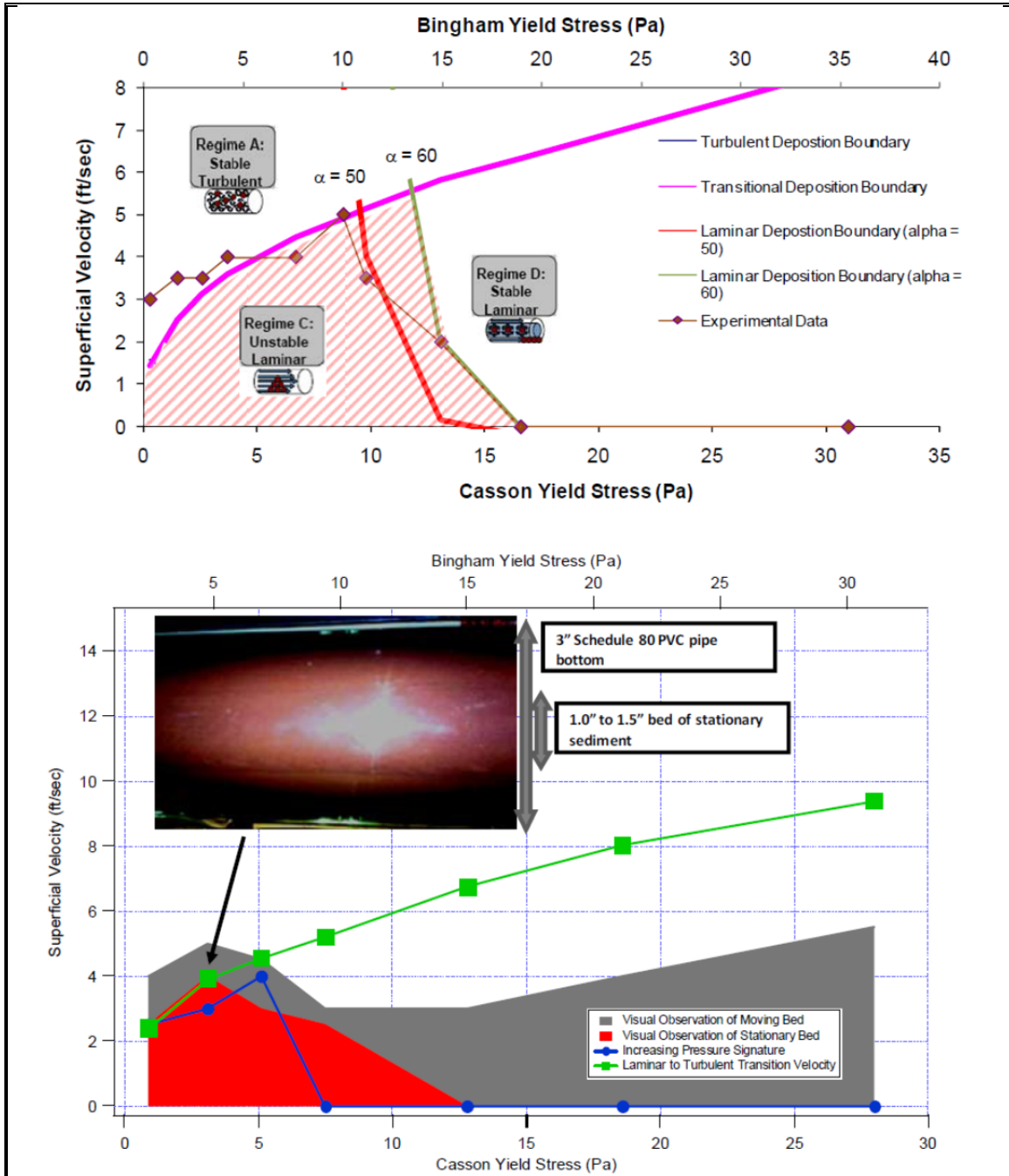


Figure 2-19 Deposition Velocity 150mm Glass Bead + Kaolin Slurry (Top) and AZ-101 HLW Pretreated Simulant (Bottom)⁶⁶

2.3.8 Goosen and Paterson, 2014

Goosen and Paterson⁶⁸ discuss the critical velocity of gold mine tailing slurry, having a solids density of 2.78 g/mL for a wide range of solids volume concentrations that cover both the turbulent and laminar flow regions. The maximum particle size was 300 μm and particle size distribution is shown in Figure 2-20. In this article, Goosen and Paterson used 75 μm as the value to distinguish between the fines and coarse, though they acknowledged 44 μm is also commonly used. For the coarse fraction, they used d_{50} (110 μm) in their assessment. They also obtained rheological measurements of the Bingham Plastic yield stress properties as a function of percent volumetric concentration, Figure 2-21. Given this is not a flocculated material, the volume fraction of solids required to reach 31 vol % is approximately 55 wt %, which is the first point where non-Newtonian characteristics were measured. The free settling concentration of gold tailings was 37.87 vol %.

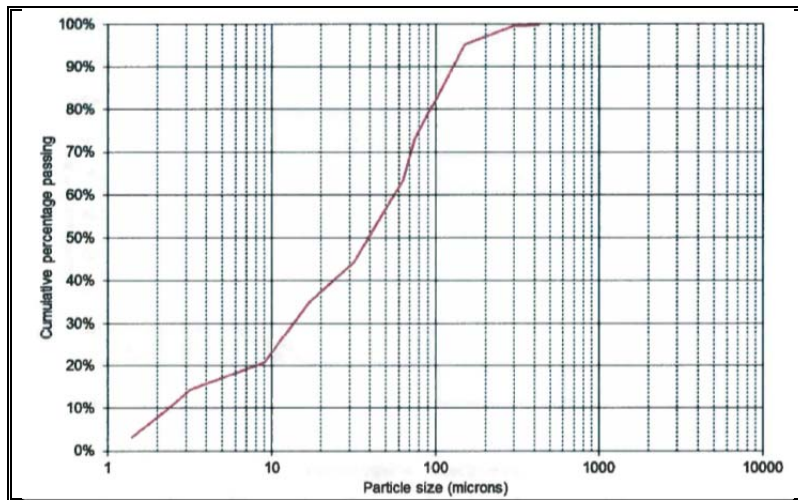


Figure 2-20 Gold Tailing Particle Size Distribution⁶⁸

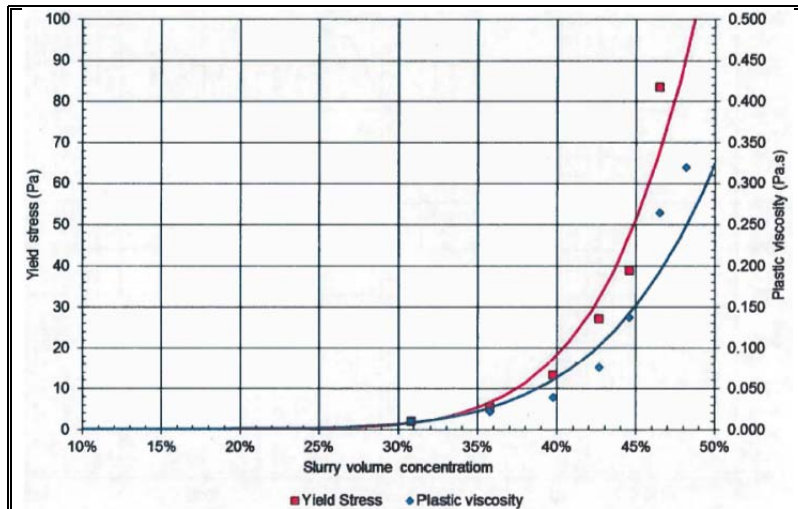


Figure 2-21 Gold Tailing Bingham Plastic Rheological Properties⁶⁸

In their tests, they used 100, 142, and 152 mm pipes and started with a flow rate of 2 m/s, which was above the critical velocity and reduced the velocity until a stationary bed was formed. A typical result for

any given pipe size tested is shown in Figure 2-22 and contains the calculated critical deposition velocity and calculated laminar turbulent transition velocities. Goosen and Paterson⁶⁸ used Sanders et al⁶⁹ and Gillies et al⁷⁰ methods and interpolated between these two methods if necessary. For the case where the fluid behaved like a Bingham Plastic fluid, Goosen and Paterson⁶⁸ used Slatter and Wasp⁷¹ method to determine the laminar/turbulent transition velocity. The point of free settling concentration (also referenced to “freely-settled”) is also provided as reference point of interest, given for all pipe sizes in the study, there was no stationary bed beyond this concentration.

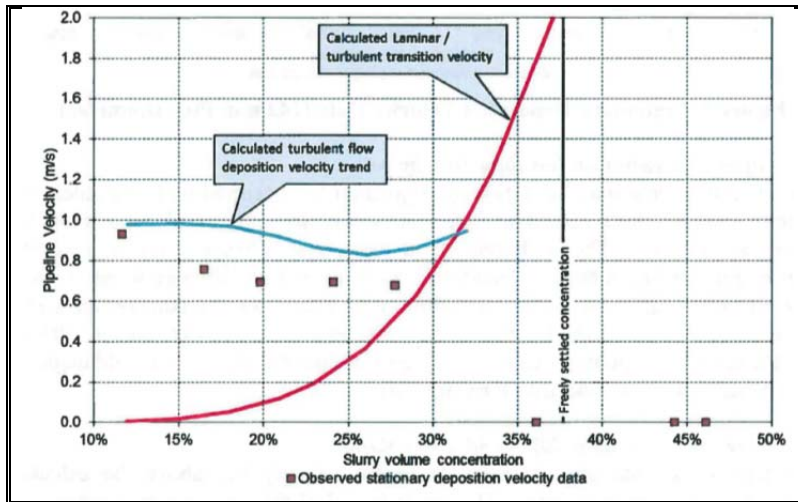


Figure 2-22 Stationary Deposition Velocity Data, 100 mm I.D. Pipe⁶⁸

Goosen and Paterson⁶⁸ determined that the region between turbulent flow and free settling concentration was a region of intermediate concentration where settling could occur and used a two layer model (such models have been extensively used to assess Newtonian slurries as well as non-Newtonian slurries, see references 64, 72, 73, 74, 75 and 76 for other non-Newtonian approaches to utilizing the two layer model). When the Bingham Yield Stress is below 2 Pa, they assessed the slurry to be turbulent, where the yield stress had no effect. The following is a summary of Goosen and Paterson⁶⁸ method/analysis and it is recommended if additional insight is required, the referenced article be reviewed.

1. Perform force-balance analysis between settled bed (A2) and moving layer above (A1), see Figure 2-23.

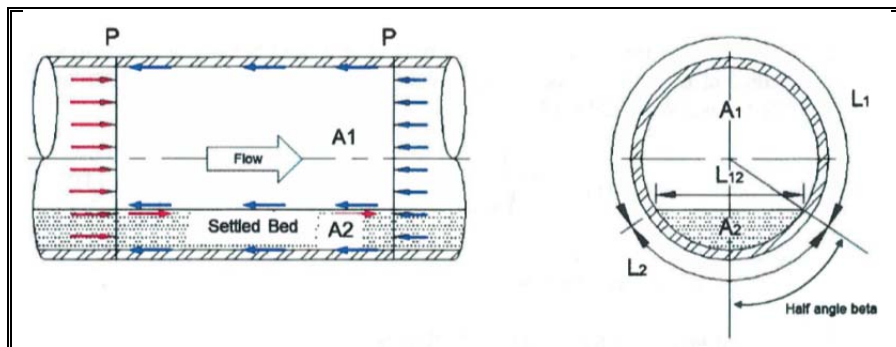


Figure 2-23 Definition Sketch for Force-Balance Analysis⁶⁸

2. Consider pipeline operating at a bulk velocity below the laminar/turbulent transition velocity, Q_m .

3. Since flow is laminar, a settled bed is assumed to have formed. The concentration of the settled bed is assumed to be the “freely-settled” concentration.
4. The bed is **assumed** to be stationary. This may not necessarily be the case.
5. Since bed is stationary, all flow and solids (suspended) occur in layer A1. The depth of the bed is assumed to be established such that there is an equilibrium condition with the flow velocity in the area above the bed.
6. The laminar/turbulent transition velocity is determined using Slatter and Wasp⁷¹.

$$V_{tran} = 26 \sqrt{\frac{\tau_y}{\rho_m}} \quad (12)$$

Where: τ_y = yield stress

ρ_m = slurry density

7. The two layer geometry can now be determined.

$$A_1 = \frac{Q_m}{V_{tran}} \quad (13)$$

$$A_2 = A - A_1 \quad (14)$$

Where: A = cross-sectional area of pipe

A_1 = cross-sectional area of flow

A_2 = cross-sectional area of settled bed

8. Calculate the half-angle β .

$$A_2 = \frac{D^2}{8} (2\beta - \sin 2\beta) \quad (15)$$

9. Calculate the pipe circumference terms.

$$L_1 = D(\pi - \beta) \quad (16)$$

$$L_2 = D\beta \quad (17)$$

$$L_{12} = D \sin 2\beta \quad (18)$$

10. Use Buckingham's equation⁷⁷ to determine the pressure gradient ($\Delta P/\Delta L$) or driving force of the flowing fluid.

a. Use V_{tran} as the flow velocity

b. Determine equivalent diameter of flow area.

$$D_{equ} = \frac{4A_1}{L_1 + L_2} \quad (19)$$

11. The driving force: the wall shear stress (τ_1) on the flowing pipe and the surface shear stress of the bed (τ_{12}) are the same and are related to the pressure gradient.

$$\tau_1 = \tau_{12} = \frac{D_{equ} \Delta P}{4 \Delta L} \quad (20)$$

12. The resisting force: is due to the yield stress at the bed/pipe interface is the maximum value calculated from the yield stress at the free settling concentration ($\tau_{y,Cbree}$) acting over the bed/pipe interface area L_2 .

13. Bed condition (stationary or sliding?)

a. Driving force < maximum resisting force: The bed is stationary

b. Driving force > maximum resisting force: The bed will be sliding

14. Application of the above method:

a. Select a slurry concentration value within the intermediate concentration range.

- b. Start the analysis at a bulk pipeline velocity slightly less than V_{tran} .
- c. Determine the bed condition (sliding or stationary)
- d. Repeat analysis at progressively lower V_{tran} values, down to $0.05 V_{\text{tran}}$ and determine bed conditions.
- e. Repeat analysis for different intermediate slurry concentration.

Goosen and Paterson⁶⁸ made the statement using the above analysis:

“It is found that if the analysis indicates a stationary bed at the top end of the velocity range ($V_m = 0.95V_{\text{tran}}$), where the bed is small (occupying 5% of the pipe area), then it may start to slide at lower velocities. In this case, the initial stationary bed condition is noted as the stationary deposition velocity. Conversely, if the analysis indicates a sliding bed at the top end of the velocity range then it continued to be sliding at lower velocities. In this case the “stationary deposition velocity” is zero.”

This method when applied to the data sets appears to support the analysis, even though two data points contradict the analysis flow sliding or stationary bed. Goosen and Paterson⁶⁸ state this is a novel analysis at predicting the condition of a settled bed under laminar flow condition (stationary or sliding) for mixed regime slurries with non-Newtonian carrier fluid. Review of the data sets also showed that no stationary bed is present if the flow is greater than the laminar/turbulent transition velocity or if the concentration of the slurry is greater than the freely settling concentration, and in this case, the yield stress was approximately 10 Pa for the freely settling concentration. Finally, Goosen and Paterson⁶⁸ stated there is limited data in this mixed regime slurries with non-Newtonian carrier fluid and it would be appropriate to test this analysis/method against bi-modal slurries with distinct carrier fluid and coarse components.

2.3.9 Washington River Protection Solution (WRPS) Data

Over the past five years, Washington River Protection Solution (WRPS) has been performing pipeline transport testing to assess a technology (PulseEcho Sensor) that could be employed to determine the critical velocity (in this case, the deposition velocity) for either Newtonian or non-Newtonian slurries.^{78,79} Two different sets of testing were performed in a 3” diameter schedule 40 stainless steel pipe-loop. The objective of the first set of testing was to determine if the PulseEcho sensor can detect the critical velocity. This testing was performed by Bontha et al.⁷⁸ where the discrete particles included regular and high density glass, $Zr(OH)_4$, $Al(OH)_3$, and alumina. The particle that had the highest density was the high density glass, 4.5 g/cm^3 .⁷⁸ During this testing, they tried to determine where a sliding bed regime occurred and denoted this as Regime III. A review of the simulants where the d_{95} particle is less than $310 \mu\text{m}$ (per ICD-19⁷, this is the maximum size particle to be delivered to WTP), showed the largest velocity offset between Regime III and the critical velocity was 0.2 ft/s and the maximum observed critical velocity was 4.2 ft/s (see Table 6.1)⁷⁸. For the non-Newtonian kaolin based slurry, containing the same maximum particle size, the maximum difference between Regime III and critical velocity was 0.6 ft/s and a maximum observed critical velocity of 4.7 ft/s.⁷⁸ Testing concluded that the PulseEcho might be a viable technology in determining the critical and/or sliding bed condition.

The second set of testing⁷⁹ was designed to assess the potential waste feeds that WRPS might send to WTP. The basis of the simulants used in their testing is provided by Lee⁸⁰ and the components used were gibbsite, sand, ZrO_2 , and stainless steel (Table 2-28) the properties of the supernates are provided in Table 2-27. The components having a diameter greater than 310 micron were the medium and large sand, and stainless steel. There is one other exception, 1588 μm stainless steel particles were used for one test and, given the range of velocities tested, these particles are most likely not transferred down the pipeline based on using O-T equation to determine critical velocity and the fact that for this test the critical velocity was measured at 3.4 ft/s (Table 2-30). A review of Lee’s⁸⁰ document showed a small fraction (less than 2 vol %) of small sand and stainless steel were greater than 310 μm . Based on these exceptions, for the Newtonian fluids, the largest difference between Regime III and the critical velocity was 1.1 ft/s and a

maximum critical velocity of 5 ft/s (Table 2-30). For the non-Newtonian kaolin only slurries, the largest difference between Region III and the critical velocity was 1.6 ft/s and a maximum critical velocity of 5.2 ft/s and there was little difference in the critical velocity for the 3 and 10 Pa slurries. The larger solids used in the non-Newtonian kaolin slurries were the stainless steel and zirconium oxide at a mass fraction of 0.0478 and 0.0116 of the total solids. A video was provided of testing performed by WRPS, but no reference is provided on which test the video shows or the condition of flow; a snap shot of the sliding bed is shown in Figure 2-24, it is obvious the upper section of the pipe is clear and the lower section is much darker, indicating a concentration profile of moving solids. There was no indication for any of these tests that sampling of the sliding or stationary beds was analyzed for composition.

Table 2-28 WRPS Solids Components Used in Typical and High Solids⁸⁰

Component	Typical Solids		High Solids		Density (g/cm ³)	Particle Size (µm)	
	Volume fraction	Mass fraction	Volume fraction	Mass fraction		Medium	Range
Small Gibbsite	0.30	0.27	-	-	2.42	1.3	0.1 - 10.5
Large Gibbsite	0.50	0.44	0.05	0.03	2.42	10	0.8 – 55
Small Sand	-	-	0.47	0.35	2.65	57	20 – 150
Medium Sand	0.13	0.13	-	-	2.65	148	50 - 400
Large Sand	-	-	0.28	0.21	2.65	382	150 – 1020
ZrO ₂	0.05	0.10	0.05	0.08	5.7	6	0.2 – 70
Stainless Steel	0.02	0.06	0.15	0.33	8.0	112	7 - 500
Volume weighted density (g/cm ³)	2.73		3.59				

Table 2-29 Physical Properties of Supernates Used in WRPS Testing at 20°C⁸¹

Liquid	Density (g/mL)	Viscosity (cP)
Low	1.098	1.62
Typical	1.284	3.60
High	1.368	14.6

Table 2-30 WRPS Sliding Bed and Critical Velocity Results⁷⁹

Test Sequence	Target Simulant Properties			Regime III (sliding Bed) (ft/s)	Critical Velocity (ft/s)
	Solids	Liquid	wt % Solids		
46	Typical	Low	9	Direct to V_c	4.7
32	Typical	Typical	9	3.6 → 2.7	2.6
33	Typical	High	9	4.6 → 4.3	4.2
34	Typical	Low	13	5.7 → 5.2	5.0
35	Typical	Typical	13	3.7 → 2.7	2.6
36	Typical	High	13	4.8 → 4.4	4.3
37	High	Low	9	7.1 → 6.9	6.8
38	High	Typical	9	5.4 → 5.2	5.1
39	High	High	9	4.4 → 4.1	4.0
40	High	Low	13	7.6 → 7.1	7.0
41	High	Typical	13	5.6 → 5.5	5.4
41a	High	Typical	13	5.9 → 5.5	5.4
42	High	High	13	4.5 → 4.3	4.2
42a	High	High	13	6.0 → 4.2	4.1
43	non-Newtonian – Kaolin only		3 Pa	6.0 → 5.1	5.0
44	non-Newtonian – Kaolin only		10 Pa	6.8 → 5.3	5.2
45	Typical	Typical	13 (5 wt % spikes)	3.8 → 3.5	3.4



Figure 2-24 Sliding Bed Observed During WRPS Testing⁸⁰

2.3.10 Savannah River Site Data

The Savannah River Site has been transporting HLW sludge in piping to support removal of HLW sludge from storage tanks, pumping of processed sludge in the tank farms, and in the Defense Waste Processing Facility (DWPF). The DWPF processes the HLW sludge it receives from the tank farm and blends it with frit. The frit provides the necessary chemical components when melted with the HLW to produce a waste form acceptable for long term disposal. The particle size specifications for the frit are provided in Table 2-31 and a density of 2.65 g/cm³. The frit is provided by an external vendor containing the chemical components as specified by DWPF. Once the frit is made, it is crushed and sieved to the requirements as stated in Table 2-31. Crushed frit is very angular with sharp edges as shown in Figure 2-25. There is only one data set where frit hardness was measured. Frit #24, having an oxide wt % composition of 12.98

Na₂O, 6.98 Li₂O, 1.00 MgO, 1.08 ZrO₂, and 67.8 SiO₂ had a Vickers hardness* of 457HV/100 with a standard deviation of 20.3HV/100.⁸² The Vicker hardness for 316L stainless steel has been reported between 140-210 HV⁸³. The hardness of frit is much greater than that of 316L stainless.

Table 2-31 Frit Particle Size Specification

Particle Size	Weight Percent
+80 mesh (180µm)	< 2
-80 and +200 mesh (74µm)	remainder
-200 mesh	< 10



Figure 2-25 Shape of Crushed Frit Used at DWPF – Frit 418

Testing was performed by Georgia Iron Works (GIW) in 1979⁸⁴ and 1982⁸⁵ to investigate pressure loss in fitting and piping, flushing requirements, solids deposition, and comparison of laboratory to field rheological measurements. In the 1979 tests, simulated sludge (sand and coal were added to this simulant, but no information is provided by Motyka⁸⁶) was tested, and in the 1982 effort both leached simulant sludge with and without frit and testing, was performed in a 3 inch schedule 40 pipe. The results for sludge only are summarized by Motyka⁸⁶ and the physical properties of the simulants are provided in Table 2-32. For the 1979 tests, sliding beds were observed from 0.5 to 7 ft/s (from the sand and coal) with no plugging observed as low as 1 ft/s. For the 1982 tests, Motyka⁸⁶ summarizes there were no minimum transport velocity (e.g. a settled bed) was observed for either the sludge and sludge/frit slurries. Particle size distributions of the sludges were not provided.

* The Vickers test measures hardness. An indenter (typically made of diamond) can be used on all materials irrespective of their hardness. The Vickers test provides units known as the as the Vickers Pyramid Number (HV) or Diamond Pyramid Hardness (DPH). If the results are provide as HV.AA/BB, AA is the applied force and BB is the duration the pressure is held. If not such designation is provided.

Table 2-32 Physical Properties Tested By GIW 1979 and 1982 Tests⁸⁶

Test	Bingham Plastic Yield Stress (Pa)	Plastic Viscosity (cP)	Slurry Density (g/cm ³)	wt % UDS
Dilute – 1979	3.0	29	1.15	7
Concentrated - 1979	21.9	12	1.25	12
Dilute Sludge – 1982	2.9	16.6	1.23	19
Concentrated Sludge - 1982	20.4	16.1	1.24	26

For DWPF, the design basis for the Slurry Mix Evaporator and Melter Feed is provided in Table 2-33. Lewis⁸⁷ summarized the 1982 GIW tests results concerning DWPF. The physical properties of the slurries tested are provided in Table 2-34. (The DWPF process adds formic acid to sludge during processing. The referenced study uses colloquial terms of “formatted” and “unformatted” sludge to designate sludge before and after this treatment. This author has retained use of those terms for consistency.) The frit was 62% of the solids, by mass. The particle size distribution of the frit is provided in Table 2-35. The sliding bed observations made during these tests are summarized by Lewis⁸⁷ below:

“Visual inspection at the 4" pipe section was somewhat limited by the muddy nature of the slurry. The 40 wt% sludge/frit slurry {sp.gr. = 1.33} showed some evidence of a "moving bed" below 3 ft/sec. ("Moving bed" refers to a high solids region with "settled" appearance but no stationary solids.) At 2 ft/sec this high solids region covered the bottom 1/4 of the pipe. At 1/2 to 1 ft/sec, about 1/3 of the pipe appeared "settled". However, there was no indication of stationary beds. The most dilute sludge/frit slurry (33 wt%, sp.gr. = 1.25) showed less "bedding". Apparently the reduced hindered-settling effect was balanced by the increased turbulence with the thin slurry. (Transition to turbulence was at 4ft/sec.)”

Table 2-33 DWPF Slurry Mix Evaporator (SME) and Melter Feed Tank (MFT) Design Basis⁸⁸

Property	Minimum	Maximum	Units
Design Velocity	3	5	ft/s
Yield Stress	2.5	15	Pa
Plastic Viscosity	10	40	cP
Density	1.2	1.43	g/mL

Table 2-34 1982 GIW Test Slurry Properties⁸⁷

Simulant Run	wt % TS	wt % Soluble	Data From Pipe Loop/Rheometer		
			Density (g/cm ³)	Yield Stress (Pa)	Plastic Viscosity (cP)
Unformatted Sludge 76	33.0	3.4	1.31	56.0	19
Unformatted Sludge 77	28.7	2.8	1.25	22.5	9
Unformatted Sludge 78	20.5	1.8	1.16	4.0	6
Formatted Sludge/Frit 79	55.2	11.5	1.54	54.0	8
Formatted Sludge/Frit 80	48.7	8.9	1.44	22.5	6
Formatted Sludge/Frit 81	40.4	6.5	1.33	10.0	3
Formatted Sludge/Frit 82	33.4	4.8	1.25	4.0	1

Table 2-35 Particle Size Distribution of Frit Used in 1982 GIW Tests⁸⁷

Mesh	+80 (180µm)	+100 (150µm)	+200 (74µm)	-200 (74µm)
Mean wt%	0	21.0	66.2	12.8
Standard Deviation	0	7.1	3.5	8.7

2.4 Erosion

This section reviews literature relating to erosion from particle interaction with the walls of the pipe.

2.4.1 *Wilson et al., 1997, Erosive Mechanism*

Wilson et al.⁸⁹ discusses the major erosive mechanisms which are sliding bed and particle impact. For sliding bed, it involves a bed of contact load particles moving tangentially against a surface as shown in Figure 2-26 producing a stress normal to the surface due to gravity. The erosion rate for sliding bed is dependent on the properties of the particles, wear surface, the normal stress and the relative velocity of the bed. This normal stress can be enhanced in elbows where the centrifugal acceleration exceeds gravity, producing an accelerate wear in the elbow. The other wear mechanism is particle impact, which occurs when individual particles strike the wearing surface at random angles, leading to different types of erosion as shown in Figure 2-26. Removal of material under these conditions occurs through small-scale deformation, cutting, fatigue cracking or combinations of these and is dependent on the properties of the wearing surface and particles. For a given slurry, the erosion rate depends on properties of the wearing surface hardness, ductility, toughness and microstructure. Particle characteristics such as size, shape, and hardness and the concentration of solids near the surfaces are important. In pipe flow, as the level of turbulence increases, particles can also be driven towards the boundary surface.

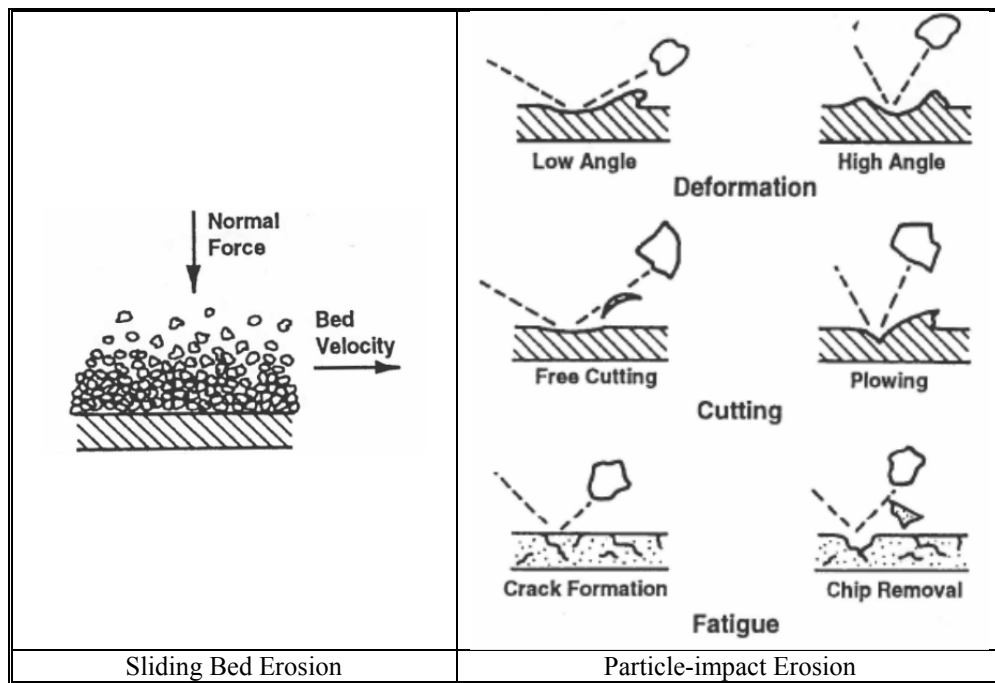


Figure 2-26 Erosive Mechanisms⁸⁹

Wilson et al.⁸⁹ make the following observation concerning low solids concentration (that can impact erosion):

“It is expected that erosion by particle impact will be more effective than sliding abrasion provided that an equal number of particles is involved in each mechanism. The required conditions apply for low solids concentrations, or cases where only a small fraction of the solids moves as contact load. Here the moving contact-load particles coming from upstream will be spaced sufficiently far apart to allow speedy incoming particles to erode the surface by impact.”

2.4.2 Baker and Jacobs, 1979, Sliding Bed Erosion

Baker and Jacobs⁹⁰ provide a guide in the design for slurry transport systems, with experimental results. As part of the experimental results using a 5 volume percent magnetite iron ore in water in a 38 mm diameter mild steel pipe, the wear rate due to sliding bed was reported to be 10 times greater than in conditions where there is no sliding bed. The particle size distribution of the magnetite iron ore is provided in Table 2-36. No information was provided about the density of the magnetite iron ore nor what reference velocity sliding bed erosion is reference to with respect to their pipeline velocity. Baker and Jacobs⁹⁰ notes that it has been observed by many workers that magnetite iron shows rapid increase in wear as the velocity increases. If one assumes a density of approximately 4.5 g/mL for the magnetite iron ore, the wt % of this material in water is approximately 19.2%.

Table 2-36 Magnetic Iron Ore Particle Size Distribution⁹⁰

Particle Size	Volume Percent
+60 mesh (250µm)	20.6
-60 and +240 mesh (63µm)	64.7
-240 mesh	14.7

2.4.3 Wu et al., 2011, Visual Means

Wu et al.⁹¹ provide a methodology to assess areas of erosion in process equipment using a paint modeling technique. Visual paint patterns (layers) were used to illustrate potential erosion damage and provides an insight into the underlying fluid dynamics process involved with erosion. Wu et al.⁹¹ applied this technique to horizontal piping. A sand water slurry flowing at 4 m/s in 50 mm diameter pipe produced the erosion patterns shown in Figure 2-27, showing significantly more wear at the bottom of the pipe. The critical velocity was calculated to be 0.82 m/s. The sand concentration and particle size were not provided. Wu et al.⁹¹ goes on to suggest stratification of solids had occurred, with the possible formation of a sliding bed of solids or increased solids concentration towards the pipe bottom, resulting in the increased wear. The mechanisms due to bed or particulate erosion are different, but the paint technique has a limitation in differentiating which mechanism is controlling, in other words, the erosion mechanism observed in Figure 2-27 cannot be determined using this method. This paint technique is low cost and could be used to assess regions of most erosion to support more detailed testing.

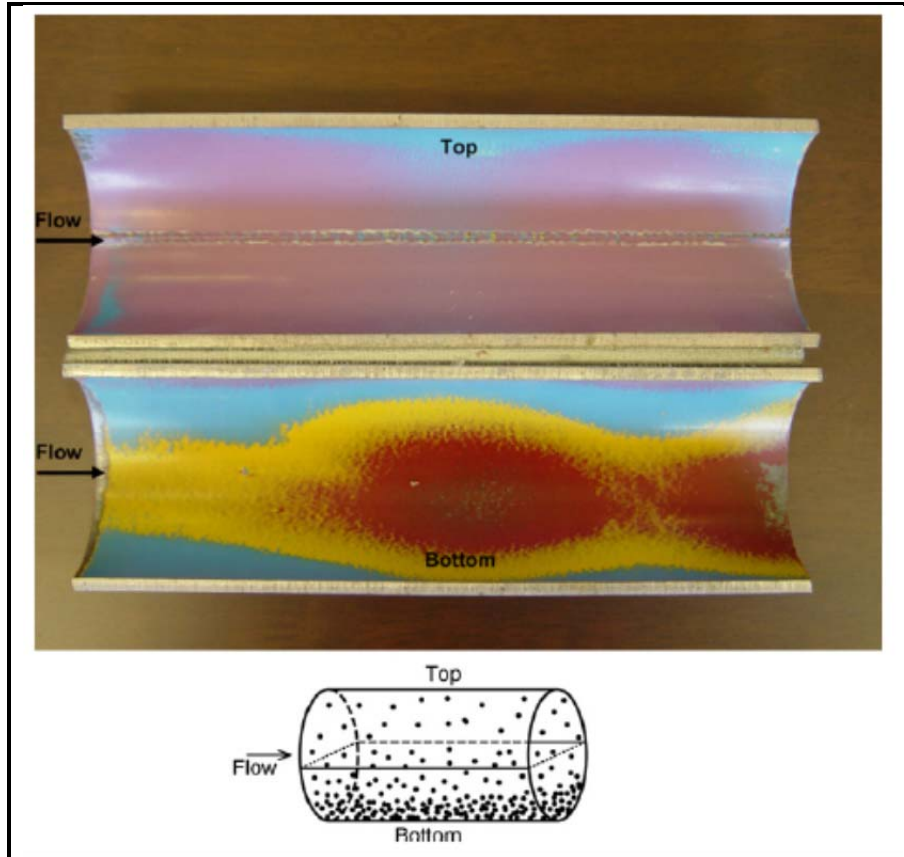


Figure 2-27 Flow Erosion Pattern in Horizontal Pipe⁹¹

2.4.4 Savannah River Site – Experience

At the Savannah River Site (SRS), erosion issues have been a concern since the introduction of frit, a crushed glass that contains sharp and angular particles, and is blended with the processed HLW slurry. This stream is an issue related to DWPF. Sharp and angular particles typically result in higher wear rates.⁹² The physical properties of the frit are provided in section 2.3.10 and a nominal blend of sludge to frit on a mass basis is 35 to 65 percent, indicating a large fraction being frit. The first indication of erosion due to frit was noticed in 1981⁹³ during testing, where pumps and valves were exhibiting substantial wear after only 20 hours of operations processing a 40-50 wt % solids mixture of sludge and frit. Subsequent testing using stainless steel flow loops was performed. In one of the erosion test loops⁹³, it was run for 200 hours using -200 mesh (74 μm) frit and “formatted” sludge (i.e. sludge processed with formic acid) in 1” pipe and elbows (10-20 ft/s) and 2” pipe and elbows (3-5 ft/s) showed no significant erosion wear. Additional testing using a 1” pipe with 35 wt % -100 mesh (150 μm) and “formatted” sludge for 200 hours at 8 ft/s, 37 wt % -200 mesh (74 μm) and “formatted” sludge for 200 hours at 8 ft/s, and 41 wt % -200 mesh (74 μm) and “formatted” sludge for 200 hours at 8 ft/s showed no erosion wear. Graf⁹³ recommends using a wear rate of < 10 mils per year for fluid velocities less than 8 ft/s for straight section of pipe from these sets of tests.

In 2006, Jenkins⁹⁴ summarized an assessment of the slurry systems associated with 10 years of DWPF operations for wear. In his summary, he states that erosion loss occurs at 4 mils per year in straight pipe and 40 mils per year at elbows, for the DWPF slurry process lines that handle frit. Localized erosion due high exposure to frit were noted at tight radius bends. Jenkins also states that there is little concern about

erosion/corrosion in the tank farm slurry transfer piping and that of DWPF where frit is not used and wear by waste has not been observed. The estimated erosion rate of 0.4 mils per year for horizontal piping containing only sludge was estimated by Zapp⁹⁵ in 1994. Sliding bed erosion to date has not been identified.

3.0 Discussion and Conclusion

This discussion is broken in two sections, for Newtonian and non-Newtonian slurries.

3.1 Newtonian Slurries

The review of the literature is summarized as follows.

- Most of the researchers defined the critical velocity, deposition velocity, and critical deposition velocity as the point where a static layer of solids form at the bottom of the pipe. No consistency in terminology usage among researchers.
- Correlations to determine the regime of sliding beds were very limited.
- Correlations to define the various regimes of flow, stationary, sliding or saltation, heterogeneous, and homogeneous have a lot of uncertainty.
- Multi-component and varying density solids showed that the particles with the highest terminal velocities controlled the critical velocity. Little research followed this conclusion.
- The impact of small particles generally reduced the critical velocity; hence if the small particles are not considered, the calculated critical velocity is conservative using the WTP design procedure 24590-WTP-GPG-M-0058. In some cases, the addition of small particles had no effect in reducing the critical velocity.
- A distribution of small particles was more effective in reducing the critical velocity than a narrow range of small particles.
- Testing performed by PNNL on critical velocity stated that the WTP correlation is conservative given their test data, but also stated that the O-T equation should be used as stated by the author rather than using a modified O-T equation that has not been vetted.
- Sliding beds are present prior to the formation of stationary beds. The solids profile as flow decreased from a homogeneous suspension, to heterogeneous, to saltation, to sliding, show an increase of solids concentration in the lower section of the piping.
- Velocity and solids concentration profiles are present for all conditions of flow (settled, sliding bed, heterogeneous flow), other than pseudo-homogeneous flow conditions. Test conditions provided in Wu et al. using paint to determine areas of erosion, stipulate that a solids profile could be present for highly turbulent conditions.
- Erosion rates could be greater in the lower section of piping due to solids concentration profiles being larger.
- Sliding bed erosion rate is higher than particulate impact erosion rate due to turbulence. The case provided (section 2.4.2) is very bounding compared to WTP solids, given the large and very abrasive nature of the material processed in the case study.
- Wear in SRS HLW transfer lines (excluding DWPF HLW+Frit) is almost non-existent, even though the frit is much more abrasive than the 316L stainless steel. An early estimate of 0.4 mils per year was predicted and is much larger than measured.

Based on 24590-WTP-RPT-PE-12-005 (section 2.1.2), processing the waste (dissolution) from the tank farm drastically reduced the weighted mean particle size for all the HLW waste streams. This indicates that these larger crystalline particles are in the incoming HLW waste streams (FRP14) and are less dense (less than 2.7 g/cm³), given the increase in density of the leached HLW waste (UFP07 & FEP19). The

maximum particle size per ICD-19 (section 2.1.5) that will be transported to WTP will be 310 μm . The case of sliding bed not being present is sufficiently captured in both the WTP safety margin assessment (section 2.1.5) and from the testing performed by WRPS (section 2.3.9). In the WRPS testing, the typical solids results showed that there were no sliding beds present at 6 ft/s and if the components were sieved to less than 310 μm and the larger and the more dense stainless particles to a more representative particle size distribution, the values reported in the WRPS testing for the Newtonian slurries would result in lower velocities for all cases.

3.2 non-Newtonian Slurries

The review of the literature is summarized below.

- Operating at or above the critical transition velocity, the transition between laminar and turbulent flow, settled beds are not present in the flocculated systems. This was observed in kaolin slurries, TiO_2 slurries and SRS HLW simulated slurries.
- Operating at or above the critical transition velocity where discrete particles are added (or present) to flocculated systems can result in settled beds. This behavior was observed in testing performed by Poloski et al⁶⁶ and Thomas⁵⁸. This was not observed in the SRS HLW + Frit simulated slurry where the discrete particles are larger and in a larger concentration than tested by Poloski et al⁶⁶. The particles used by Thomas⁵⁸ were larger than the SRS Frit.
- Sliding beds were observed when operating below the critical transition velocity. This was observed in kaolin only slurries, TiO_2 slurries, SRS HLW and SRS HLW + Frit simulated slurries and simulants tested by Poloski et al⁶⁶. Poloski et al⁶⁶ observed sliding beds above the critical transition velocity when the Bingham Plastic yield stress was below 5 Pa and the sliding bed velocities were all below 6 ft/s for 3 inch pipe. The method developed by Poloski et al⁶⁶ does not have uncertainty associated with their predictions.
- Referenced documents do not provide sufficient information on sliding beds with high density particles as noted in the processed HLW waste in Table 2-5. Thomas⁶¹ (section 2.3.4) analyzed high density ThO_2 slurries having non-Newtonian properties, but did not provide any figures to show when sliding bed occurs such as that with the kaolin, though he stated such did occur. Thomas⁶¹ states that the sliding beds were due to particles of near colloidal dimensions sticking together to form loose and irregular clumps of flocculated particles. Densities of the HLW simulants processed by both SRNL and PNNL were not quantified.
- The AZ-101 HLW simulant tested by Poloski et al⁶⁶ did not show any signs of sliding beds at a transfer velocity of 6 ft/s for any rheological condition. The deposition velocity curve associated with this simulant indicated that as the yield stress increased, sliding beds were observed at higher velocities, consistent with Thomas⁶¹.
- WRPS testing using kaolin slurries indicated sliding beds were present above 6 ft/s.⁷⁹ This data has not been reconciled with any of the non-Newtonian models presented in this document.
- In the SRS tests where the simulant HLW sludge contained a large fraction of FRIT, settled beds were not observed, even down to 0.5 ft/s. Sliding beds were first observed at 3 ft/s. This data has not been assessed using the PNNL non-Newtonian methodology proposed by Poloski et al⁶⁶ as an independent data set to substantiate the PNNL method.
- Goosen and Paterson⁶⁸ used a two-layer model approach in analyzing a gold mine tailing slurry in the laminar region of non-Newtonian flow for both sliding and settled beds. Unlike flocculated solids, the solids concentration to reach non-Newtonian properties required was 55 wt%, even though 65% of the solids were smaller than 75 μm . This method also requires a freely settled solids bed concentration be measured, which is used in their model as the concentration of the settled/sliding bed. For the gold tailings, the fluid was assessed as Newtonian slurry up to a Bingham Plastic yield stress of 2 Pa. This method (two-layer model) might be applicable to existing DOE slurry data.

- The critical transition velocity for a 1200 kg/m³ slurry for Bingham Plastic yield stresses and plastic viscosities were calculated using the equation from Table 2-24 and the results are provided in Table 3-1. The shaded areas are where the transition velocities are greater the 6 ft/s. There is insufficient data from Poloski et al.^{66,49} tests to determine if a sliding bed would be present for the higher yield stress/plastic viscosity combinations. The testing performed by Thomas⁶¹, using only kaolin, showed that the critical transition velocity and sliding bed were about 1 ft/s apart, but this difference gets larger when reaching a specific yield stress, indicating no sliding bed. The sliding bed defined by Thomas was when a filament (not wide or much mass) of sliding solids was observed.

Table 3-1 Critical Transition Velocity for Bingham Plastic Fluid

		Plastic Viscosity (cP)									
		3	6	9	12	15	18	21	24	27	30
Bingham Plastic Yield Stress (Pa)	3	2.68	2.80	2.92	3.05	3.18	3.31	3.46	3.60	3.75	3.90
	6	3.74	3.86	3.98	4.10	4.23	4.35	4.49	4.62	4.76	4.90
	9	4.56	4.67	4.79	4.91	5.03	5.16	5.29	5.42	5.55	5.69
	12	5.25	5.36	5.48	5.60	5.72	5.84	5.97	6.10	6.23	6.36
	15	5.85	5.97	6.08	6.20	6.32	6.44	6.57	6.69	6.82	6.95
	18	6.40	6.51	6.63	6.75	6.87	6.99	7.11	7.24	7.36	7.49
	21	6.90	7.02	7.13	7.25	7.37	7.49	7.61	7.73	7.86	7.99
	24	7.37	7.49	7.60	7.72	7.84	7.96	8.08	8.20	8.32	8.45
	27	7.81	7.93	8.04	8.16	8.28	8.39	8.52	8.64	8.76	8.89
	30	8.23	8.34	8.46	8.57	8.69	8.81	8.93	9.05	9.18	9.30

- Solids concentration profiles such as observed in Newtonian slurries can be present in non-Newtonian slurries.
- After operating for 10 years, the erosion rate for DWPF HLW + Frit slurry lines only showed a 4 mil per year wear rate.

Based on 24590-WTP-RPT-PE-12-005 (section 2.1.2) after processing the sludge through UFP-02, the weighted max particle size (d95) for the discrete particle was at most 12 μm and the weighted mean particle size between 1-2 μm. Testing performed using the AZ-101 simulant by Poloski et al.⁶⁶ had a d95 of 72 μm and d80 of 14 μm. Plugging will not occur in the WTP 3 inch slurry transfer lines at 6 ft/s. Ten years of operating experience at SRS-DWPF has shown that wear rates for piping is around 4 mils per year for HLW slurries containing 65 wt % frit and there was no observed or reported sliding bed wear. Given the small particle size distribution of the expected WTP processed HLW streams, if a sliding bed is present, it most likely will be small, but the actual size of the bed cannot be predicted using Poloski et al.^{66,49} method but can potentially be calculated using Goosen and Paterson⁶⁸ method. Goosen and Paterson⁶⁸ method has not been properly assessed with multiple non-Newtonian slurries, hence its ability to determine sliding bed and the size of the bed is uncertain and not quantified.

4.0 Recommendations

For the case of Newtonian based slurries that will be processed in the WTP-PT facility, it is not expected that sliding beds of solids will be present given the constrains provided by the applicable interface control document (ICD-19), the safety margin in the WTP design for Newtonian slurries, the projected HLW streams that will be processed (Wilkins²²), the transport velocity of 6 ft/s in the PT facility, and testing performed by WRPS and PNNL. This finding is for systems where centrifugal pumps are utilized to transfer or recirculate waste in a 3 inch transfer line.

For the non-Newtonian case, there is insufficient data available to determine if sliding beds will cause more erosion compared to turbulent flow and the mechanism of sliding bed erosion is different than that experienced in turbulent flow. Experience at SRS processing only HLW slurries in the tank farm showed essentially no erosion over a 10 year span. Processing HLW slurries containing large and abrasive frit in DWPF showed an erosion rate of 4 mils per year over a 10 year span without any observation of erosion due to sliding bed. Testing with non-Newtonian slurries show that a sliding bed can be present below the critical transition velocity and such conditions could exist in WTP for the higher combinations of yield stress and plastic viscosity given a 6 ft/s flowrate in 3 inch pipe. For a 30 Pa, 30 cP Bingham plastic fluid, the transition velocity in a 3 inch pipe is 9.3 ft/s. Observations of the sliding beds could be due to the flocculation of colloidal particles, at high non-Newtonian conditions. Literature does not provide sufficient information on the size (depth) of the sliding bed for non-Newtonian slurries. The following recommendations are provided to assess for sliding bed erosion.

- 1: Perform a technical review of characterized Tank Farm and processed (Al-dissolution/washing) Hanford HLW waste where mass fraction versus Bingham Plastic rheological and physical properties have been ascertained in the regions shown in Table 3-1. Characterization of the solids speciation is also a requirement, such as chemical composition, density, hardness, and particle size distribution. Assess this data to determine if a sliding bed could be present for pipeline velocity of 6 ft/s using the methods specified by Poloski et al^{66,49} and Goosen and Paterson⁶⁸ to assess for sliding bed. An additional assessment should also determine the fraction of HLW streams that could have a sliding bed based on using a process model (such as G2) and existing characterization data. Based on the latter assessment, if the fraction of non-Newtonian HLW for sliding beds is reasonably low, Recommendation 2 below should be reassessed to determine if it necessary to performed for the non-Newtonian sliding bed erosion testing. Such a reassessment for instance could include evaluating the average hardness of the calculated sliding bed materials as compared to the piping material in reaching this determination.
- 2: Perform pipe loop testing to determine the size (height/width) of the sliding bed, composition of the sliding bed, and erosion at steady state conditions and potentially the erosion rate for start/stop conditions. Elbow and vertical piping should also be assessed if testing is required and captured in this testing. If start/stop testing is to be performed, an assessment of WTP-PT operations should be performed to determine the fraction of operating time stop/start activities occur for HLW vessels. If start/stop operations are a small percentage of the overall transfer operations, then such testing may not be necessary. Flushing activities should be consistent with WTP protocol to verify flushing methodology is adequate. Both Poloski et al.⁶⁶ and Goosen and Paterson⁶⁸ (two-layer model) methods should be used to assess the collected data.
- 3: Assess RFD operations for systems in WTP-PT that are utilized in transporting HLW. Assessment is to review how the RFD will be operated; flowrate, number of cycles per nominal transfer and flushing capabilities. Assessment should include open literature on the operation and erosion issues related to RFD operations. Issues raised in this review should determine if additional testing is required to assess the overall issue of erosion due to a cyclic pumping system given the streams it will process.
- 4: UFP-VSL-00002A/B is the primary HLW processing vessels in PT. These vessels utilize a 10 inch transfer line for crossflow filter activities. There is insufficient data to determine if this transfer line has been properly assessed for both Newtonian and non-Newtonian operations, including flushing in maintaining the line for long term operations. An independent assessment of this transfer system is recommended.

5.0 References

- ¹ Winokur, P. S., Defense Nuclear Facilities Safety Board, Letter to Mr. David Huizenga, August 8, 2012
- ² Huizenga, D., Department of Energy – Environmental Management, Letter to The Honorable Peter S. Winokur, April, 28, 2018
- ³ Inter-entity Work Order M0SRV00097 Amendment 5, “Statement of Work for DOE National Laboratories to Support DOE’s Full Scale Vessels Testing Program,” 28 July 2014
- ⁴ Hall, M.N., “Design Guide: Minimum Flow Velocity for Slurry Lines”, 24590-WTP-GPG-M-0058, Rev. 0, November 2006
- ⁵ Hall, M.N., “Design Guide: Pipe Sizing for Lines with Liquids Containing Solids – Bingham Plastic Model”, 24590-WTP-GPG-M-016, Rev. 3, August 2012
- ⁶ Hall, M.N., “Design Guide: Pipe Sizing for Lines with Liquids Containing Solids – Power Law Fluids”, 24590-WTP-GPG-M-039, Rev. 2, June 2007
- ⁷ Taki, B.D., “ICD 19 – Interface Control Document for Waste Feed”, 24590-WTP-ICD-MG-01-019, Rev. 7, September 2014
- ⁸ “Waste Transfer, Dilution, and Flushing Requirements”, TFC-ENG-STD-26, WRPS, Rev. B, June 2014
- ⁹ Mauss, J., “Standardized High Solids Vessel Design (SHSVD) Selection”, 24590-PTF-ES-ENG-14.001, Rev. 0, May, 2014
- ¹⁰ Sen, U., “Mechanical Data Sheet: Centrifugal Pump, API-610-Slurry, UFP-PMP-00042A/43A”, 24590-PTF-MPD-UFP-00024, July 16, 2009
- ¹¹ Xu, C., and Yu, H., “Prediction of the pumping capacity for reverse-flow diverter pumps”, Chemical Engineering Research and Design, Vol. 92, 2014
- ¹² Vatankhah, A. R., “Analytical Solutions for Bingham Plastic fluids in Laminar regime”, Journal of Petroleum Science and Engineering, Vol. 78, 2011
- ¹³ Swamee, P.K. and Aggarwal, N., “Explicit Equations for Laminar Flow of Bingham Plastic Fluids”, Journal of Petroleum Science and Engineering, Vol. 76, 2011
- ¹⁴ Wilson, K.C., and Thomas, A.D., “Analytical Model of Laminar-Turbulent Transition for Bingham Plastics”, The Canadian Journal of Chemical Engineering, Volume 84, October 2006
- ¹⁵ Gan, Y., “Continuum Mechanics – Progress in Fundamentals and Engineering Applications”, Chapter 3, InTech, March 2012
- ¹⁶ Miedema, S.A. and Ramsdell, R.C., “An Analysis of the Hydrostatic Approach of Wilson for the Friction of a Sliding Bed”, Power Point Presentation
- ¹⁷ Jewett, J.R., Reynolds, D.A., Estey, S.D., Jensen, L., Kirch, N.W., and Onishi, Y., “Values of Particle Size, Particle Density, And Slurry Viscosity to Use in Waste Feed Delivery Transfer System Analysis”, RPP-9805, Rev. 0, January 2002
- ¹⁸ Ashley, G, Edwards, R. , Myler, C., Brunson, G., Holton, L., and Alexander, D., “Technology Steering Group – Issue Closure Record – Closure EFRT Issue M1 – Plugging in Process Piping”, CNN214961, February 24, 2009
- ¹⁹ Burke, R., “Issue Response Plan for Implementation of External Flowsheet Review Team (EFRT) Recommendations – M1, Plugging in Process Piping”, 24590-WTP-PL-ENG-06-0010, Rev. 2, November 27, 2007
- ²⁰ Gebhardt, M., Clossey, K., “Process Inputs Basis of Design (PIBOD)”, 24590-WTP-DB-PET-09-001, Rev. 1, June 2, 2011
- ²¹ Wells, B.E., Knight, M.A., Buck, E.C., Daniel, R.C., Meyer, P.A., Tingey, J.M., Callaway, W.S., Johnson, M.E., Washenfelder, D.J., Thomson, S.L., Cooley, S.K., Mahoney, L.A., Poloski, A.P., Cooke, G.A., Thien, M.G., Davis, J.J., Smith, G.L., and Onishi, Y., “Estimate of Hanford Waste Insoluble Solid Particle Size and Density Distribution”, WTP-RPT-153, Rev. 0, February 2007
- ²² Wilkins, N., and Gimpel, R., “River Protection Project – Waste Treatment Plant: Waste Mineralogy and Particle Physical Property Characterization”, 24590-WTP-RPT-PE-12-005, Rev. 0, September 2013
- ²³ McCullough, M. G., “Contract No. DE-AC27-01RV14136 – Description of How the Design and Safety Margin Will be Applied to the Hanford Tank Waste Treatment and Immobilization Plant (WTP) Design with Respect to the Current Particle Size Basis”, CNN 229195, April 2014
- ²⁴ Newitt, D.M., Richardson, J.F., Abbott, M., and Turtle, R.B., “Hydraulic Conveying of Solids in Horizontal Pipes”, Trans. Institution of Chemical Engineers., Vol. 33, 1955
- ²⁵ Durand, R. “Basic Relationships of the Transportation of Solids in Pipes-Experimental Research”, Proceedings, Minnesota International Hydraulics Convention, September, 1953

- ²⁶ Sasic, M and P. Marjanovic, "On the Methods for Calculation of Hydraulic Transport and Their Reliability in Practice", 5th International Conference on Hydraulic Transport of Solids in Pipes, 1978, Paper A5
- ²⁷ Miedema, S. A., "An Overview of Theories Describing Head Losses in Slurry Transport – A Tribute to Some of the Early Researchers", Journal of Dredging, Volume 14, No. 1 March 2014
- ²⁸ Carleton, A. J. and Cheng, D. C-H, "Pipeline design for industrial slurries", Chemical Engineer, April 25, 1977
- ²⁹ Weast, R. C., "CRC Handbook of Chemistry and Physics", 66th edition, CRC Press, 1985
- ³⁰ Carleton, A. J. and Cheng, D. C-H, Proceedings, 3rd International Conference on Hydraulic Transport of Solids in Pipes, 1974, Paper E5
- ³¹ Turian, R. M., Hsu, F. L., and Ma, W., "Estimation of the critical velocity in pipeline flow of slurries", Powder Technology, Vol. 51, 1987
- ³² Oroskar, A. R. and Turian, R. M., "The Critical Velocity in Pipeline Flow of Slurries", AIChE Journal, Vol. 26, No. 4, July 1980
- ³³ Oroskar, A. R., "Flow of Slurries in Horizontal Pipeline", Master of Science in Chemical Engineering, B. Tech., Indian Institute of Technology, Bombay, 1977
- ³⁴ Cho, K. T., Bae, K. S., and Lee, C. S., "Minimum Transport Velocity of Bidispersed Slurries with Different Sizes and Densities", Journal of the Korean Institute of Chemical Engineers, Vol. 25, April 1987
- ³⁵ Bae, K. S., Lee, H., Park, C. G., and Lee, C. S., "Empirical Correlations for the Minimum Transport Velocity of Multi dispersed Slurries in Horizontal Pipes", Korean Journal of Chemical Engineering", Vol. 8, 1991
- ³⁶ Parzonka, W., Kenchington, J. M., and Charels, M. E., "Hydrotransport of Solids In Horizontal Pipes: Effects of Solids Concentration and Particle Size on the Deposit Velocity", The Canadian Journal of Chemical Engineering, Vol. 59, 1981
- ³⁷ Durand, R. and Condolios, E., "Deuxiemes Journees de l'hydraulique", Society Hydraulics de France, Grenoble (1952)
- ³⁸ Hisamitsu, N., Shoji, Y., and Kosugi, S., "Effect of Added Fine Particles on Flow Properties of Settling Slurries", 5th International Conference on the Hydraulics Transport of Solids in Pipe, Paper D3, 1978
- ³⁹ Warren, T., "Flow of Fine Particle Suspensions in Horizontal Pipeline", Masters of Science in Chemical Engineering, Texas Tech University, 1981
- ⁴⁰ Cairns, R. C. and Turner, K. S., "Study of Small Particles Suspensions for L.M.F.R. – Part III. Correlations of Horizontal Settling Velocity", Australian Atom Energy Commission, E17, February, 1958
- ⁴¹ Cairns, R. C. and Turner, K. S., "Study of Small Particles Suspensions for L.M.F.R. – Part V. The Effects of Concentration, Pipe Diameter, and Solid Density on the Horizontal Settling Velocity", Australian Atom Energy Commission, E34, September, 1958
- ⁴² Abraham, B. M., Fltow, H. E., and Carlson, R. D., "UO₂-NaK Slurry Studies in Loops to 600°C", Nuclear Science and Engineering, Vol. 2, 1957
- ⁴³ Thomas, A. D., "Predicting the Deposit Velocity For Horizontal Turbulent Pipe Flow of Slurries", International Journal Multiphase Flow, Vol. 5, 1979
- ⁴⁴ Pinto, T. C. S., Junior, D. M., Slatter, P. T., and Filho, L.S. L., "Modelling the critical velocity for heterogeneous flow of mineral slurries", International Journal of Multiphase Flow, Vol. 65, 2014
- ⁴⁵ Durand, R., "The hydraulic transportation of coal and other materials in pipe", International Conference of National Coal Board, London, 1952
- ⁴⁶ Wasp, E. J., Slatter, P.T., and Gandhi, R. L., "Solid-Liquid Flow Slurry Pipeline Transportation", Series on Bulk Material Handling, 1st Ed., Vol. 1, Trans Tech Publications, 1977
- ⁴⁷ Schiller, R. E., and Herbich, P. E., "Sediment Transport in Pipes", Handbook of Dredging, McGraw-Hill, New York, 1991
- ⁴⁸ Wilson, K.C. and Judge, D.G., "New Techniques for the scale-up of pilot-plant results to coal slurry pipelines", Proceeding International Symposium on Freight Pipelines, University of Pennsylvania, 1977
- ⁴⁹ Poloski, A. P., Nigl, F., Adkins, H. E., Minette, M. J., Abrefah, J., Toth, J. J., Casella, A. M., Tingey, J. M., Hohimer, R. E., Yokuda, S. T., "Deposition Velocities of Newtonian and non-Newtonian Slurries in Pipelines", PNNL-17639, March 2009
- ⁵⁰ Wilson, K. C., Addie, G. R. , and Clift, R., "Slurry Transport Using Centrifugal Pumps", Elsevier Applied Science, 1992
- ⁵¹ Shook, C. A. and Roco, M. C., "Slurry Flow – Principle and Practice", Series in Chemical Engineering, Butterworth-Heinemann, 1991
- ⁵² Aude, T. C., Cowper, N. T., Thompson, T. L., and Wasp, E. J., "Slurry Piping Systems: Trends, Design Methods, Guidelines, Chemical Engineering, June 28, 1971

- ⁵³ McKetta, J. J., "Pipeline Design, Slurry Systems", Encyclopedia of chemical Processing and Design", Volume 36, 1991
- ⁵⁴ Abulnaga, B., "Slurry Systems Handbook", McGraw-Hill, 2002
- ⁵⁵ Wasp, E. J., Kenny, J. P., Gandhi, R. L., "Solid-Liquid Slurry Pipeline Transportation", Series on Bulk Materials Handling, Vol. 1, No. 4, 1st edition, Trans Tech Publication, 1977
- ⁵⁶ Verkerk, C. G., "Some Practical Aspects of Correlating Empirical Equations to Experimental Data in Slurry Pipeline Transport", Bulk Solids Handling, Volume 5, Number 4, August 1985
- ⁵⁷ Crowe, C. R., "Multiphase flow handbook", CRC, Taylor and Francis, 2006
- ⁵⁸ Thomas, A. D., "Coarse Particles in a Heavy Medium – Turbulent Pressure Drop Reduction and Deposition Under Laminar Flow", 5th International Conference on Hydraulic Transport of Solids in Pipes, 1978, Paper D5
- ⁵⁹ Shah, S. N. and Lord, D. L., "Critical Velocity Correlations for Slurry Transport with non-Newtonian Fluids", AIChE Journal, Vol. 37, No. 6, June 1991
- ⁶⁰ Song, T. and Chiew, Y.-M., "Settling Characteristics of Sediments in Moving Bingham Fluid", Journal of Hydraulic Engineering, September 1997
- ⁶¹ Thomas, D.G., "Transport Characteristics of Suspensions: II. Minimum Transport Velocity for Flocculated Suspensions in Horizontal Pipes", AIChE, Vol. 7, September 1961
- ⁶² Thomas, D.G., "Hedstrom Plot for the Calculation of Laminar Flow Pressure Drop for Bingham Plastic Materials With Hedstrom Numbers from 0 to 10¹⁵", Oak Ridge National Laboratory, CF-57-6-111, June 1957
- ⁶³ Thomas, A.D., Pullum, L., and Wilson, K. C., "Stabilised laminar slurry flow: review, trends, and prognosis", Hydrotransport 16, April 2004
- ⁶⁴ Pullman, L., Graham, L., Rudman, M., and Hamilton, R., "High Concentration Suspension Pumping", Minerals Engineering, Vol. 19, 2006
- ⁶⁵ Wells, B.E., Knight, M.A., Buck, E.C., Daniel, R.C., Cooley, S.A., Mahoney, L.A., Meyer, P.A., Poloski, A.P., Tingey, J.M., Callaway III, W.S., Cooke, G.A., Johnson, M.E., Thien, M.G., Washenfelder, D.J., Davis, J.J., Hall, M.N., Smith, G., Thomson, S. L., and Onishi, Y., "Estimate of Hanford Waste Insoluble Solid Particle Size and Density Distribution," PNWD-3824, Rev. 0, PNNL, 2007
- ⁶⁶ Poloski, A. P., Adkins, H.E., Bonebrake, M.L, Chun, J., Casella, A.M., Denslow, K.M., Johnson, M.D., Luna, M.L., MacFarlan, P.J., Tingey, J.M., and Toth, J.J., Deposition Velocities of Non-Newtonian Slurries in Pipelines: Complex Simulant Testing, PNNL-18316, Rev.0, July 2009
- ⁶⁷ Eibling, R.E. Schumacher, R. F., and Hansen, E.K., "Development of Simulants to Support Mixing Tests for High level Waste and Low Activity Waste", WRSC-TR-2003-00220, Rev. 0, SRNL, December 2003
- ⁶⁸ Goosen, P. and Paterson, A., "Trends in stationary deposition velocity with varying slurry concentration covering the turbulent and laminar flow regimes", 19th International Conference on Hydrotransport, 2014
- ⁶⁹ Sanders, R.S., Sun., R., Gillies, R.G., McKibben, M.J., Litzenberger, C., and Shook, C.A., "Deposition Velocities for Particles of Intermediate Size in Turbulent Flow", 16th International Conference on Hydrotransport, Vol. II, 2004
- ⁷⁰ Gillies, R. G., Schaan, J., Sumner, R.J., McKibben, M.J., and Shook, C.A., "Deposition Velocities for Newtonian Slurries in Turbulent Flow", Canadian Journal of Chemical Engineering, Vol. 78, 2000
- ⁷¹ Slatter, P.T. and Wasp, E.J., "the Laminar/Turbulent Transition in Large Pipes", 10th International Conference on Transport and Sedimentation of Solid Particles, 2000
- ⁷² Lazarus, J., "Mixed-Regime Slurries in Pipelines. I: Mechanistic Model", Journal of Hydraulic Engineering, November 1989j
- ⁷³ Gillies, R.G., Shook, C.A., and Wilson, K.C., "An Improved Two Layer Model for Horizontal Slurry Pipeline Flow", The Canadian Journal of Chemical Engineering, February 1991
- ⁷⁴ Rojas, M.R. and Saex, A.E., "Two-layer Model for Horizontal Pipe Flow of Newtonian and non-Newtonian Settling Dense Slurries", Industrial & Engineering Chemistry Research", May, 2012
- ⁷⁵ Maciejewski, W., Oxenford, J., and Shook, C.A., "Transport of Coarse Rock with sand and Clay Slurries", Hydrotransport 12, BHR, 1993
- ⁷⁶ Pullman, L., Graham, L.J.W., and Slatter, P., "A non-Newtonian Two-Layer model and its Application to High Density Hydrotransport", Hydrotransport 16, April 2004
- ⁷⁷ Hanks, R.W. and Pratt, D.R., "On the Flow of Bingham Plastic Slurries in Pipes and Between Parallel Plates", Society of Petroleum Engineers Journal", December 1967
- ⁷⁸ Bontha, J.R., Adkins, H.E., Denslow, K.M., Jenks, J.J., Burns, C.A., Schonewill, P.P., Morgen, G.P., Greenwood, M.S., Blanchard, J., Peters, T.J., MacFarlan, P.J., Baer E.B., and Wilcox, W.A., "Test Loop Demonstration and Evaluation of Slurry Transfer Line Critical Velocity Measurement Instruments", PNNL-19441, Rev. 0, July 2010
- ⁷⁹ Denslow, K.M., Bontha, J.R., Adkins, H.E., Jenks, J.J., and Hopkins, D.F., "Hanford Tank Farms Waste Feed Flow Loop Phase VI: PulseEcho System Performane Evaluation", PNNL-22029, Rev. 0, November 2012

-
- ⁸⁰ Lee, K.P., Well, B.E., Gauglitz, P.A., and Sexton, R.A., "Waste Feed Delivery Mixing and Sampling Program Simulant Definition for Tank Farm", RPP-PLAN-51625, Rev. 0, March 2012
- ⁸¹ Lee, K.P., "One System Waste Feed Delivery Mixing and Sampling Program System Performance Test Plan", RPP-PLAN-52623, Rev. 0, August 2012
- ⁸² WSRC-NB-90-932, NQA-1, "1984 Corning Engineering Laboratory Services Laboratory Analysis Report #11988-003", 1984
- ⁸³ Brandes, E.A. and Brook, G.B., "Smithells Metals Reference Book", 7th edition, Butterworth-Heinemann, 1992
- ⁸⁴ Carsten, M.R., "Slurry Tests in 3-inch Diameter Pipe", for the E. I. Dupont Company, the GIW Hydraulic Laboratory, Grovetown, Georgia, November 1979
- ⁸⁵ Carsten, M.R., "Flow Characteristics of Simulated Slurries", for the E. I. Dupont Company, the GIW Hydraulic Laboratory, Grovetown, Georgia, DPST-82-955, September 1982
- ⁸⁶ Motyka, T., "Slurry Pipeline Tests in Support of the In-Tank Sludge Processing Program", DPST-83-266, January 1983
- ⁸⁷ Lewis, D.P., "Hydraulic Testing of Simulated DWPF Waste Slurries at the Georgia Iron Works Hydraulic Laboratory: Summary Report", DPST-82-954, December 1982
- ⁸⁸ "Technical Data Summary For the Defense Waste Processing Facility, Part 10"; DPSTD-80-38-2; Savannah River Site: Aiken, SC, 1982
- ⁸⁹ Wilson, K.C., Addie, G.R., Sellgren, A., Clift, R., "Slurry Transport Using Centrifugal Pumps", 2nd edition, Blackie Academic & Professional, 1997
- ⁹⁰ Baker, P.J. and Jacobs, B.E.A., "A Guide to Slurry Pipeline Systems", BHRA Fluid Engineering, 1979
- ⁹¹ Wu, J., Graham, L.J.W, Lester, D., Wong, C.Y., Kilpatrick, T., Smith, S., and Nguyen, B., "An effective modeling tool for studying erosion", Wear, Vol. 270, 2011
- ⁹² Hutchins, I.M., "Wear By Particulates", Chemical Engineering Science, Vol. 42, 1987
- ⁹³ Graf, P. L., "Erosion Wear By Frit Slurries", DPST-82-545, May 1982
- ⁹⁴ Jenkins, C. F., "DWPF Jumpers – Assessment After 10 Years Service", SRNL-MTS-2006-00031, February 2006
- ⁹⁵ Zapp P.E., "Potential for Erosion Corrosion of Stainless Steel Components in the Late Wash Facility", SRT-MTS-94-2051, December 1994.